

ISSN 2074-272X

**науково-практичний
журнал**

2018/5



ЕІЕ **Електротехніка і Електромеханіка**

Electrical Engineering

& Electromechanics



Присвячується 100-річчю НАН України

Електротехніка. Визначні події. Славетні імена

Електричні машини та апарати

Електротехнічні комплекси та системи.

Силова електроніка

Теоретична електротехніка та електрофізика

Техніка сильних електричних та магнітних полів.

Кабельна техніка

Електричні станції, мережі і системи

Безпека електрообладнання

З 2015 р. журнал індексується у міжнародній

наукометричній базі Web of Science

Core Collection: Emerging Sources

Citation Index



«ELECTRICAL ENGINEERING & ELECTROMECHANICS»

SCIENTIFIC & PRACTICAL JOURNAL

Journal was founded in 2002

Founders:

National Technical University «Kharkiv Polytechnic Institute» (Kharkiv, Ukraine)

State Institution «Institute of Technical Problems of Magnetism of the NAS of Ukraine» (Kharkiv, Ukraine)

INTERNATIONAL EDITORIAL BOARD

Klymenko B.V.	Editor-in-Chief , Professor, National Technical University "Kharkiv Polytechnic Institute" (NTU "KhPI"), Ukraine
Sokol Ye.I.	Deputy Editor , Professor, Corresponding member of NAS of Ukraine, Rector of NTU "KhPI", Ukraine
Rozov V.Yu.	Deputy Editor , Professor, Corresponding member of NAS of Ukraine, Director of State Institution "Institute of Technical Problems of Magnetism of the NAS of Ukraine" (SI "ITPM NASU"), Kharkiv, Ukraine
Batygin Yu.V.	Professor, Kharkiv National Automobile and Highway University, Ukraine
Bíró O.	Professor, Institute for Fundamentals and Theory in Electrical Engineering, Graz, Austria
Bolyukh V.F.	Professor, NTU "KhPI", Ukraine
Colak I.	Professor, Nisantasi University, Istanbul, Turkey
Doležel I.	Professor, University of West Bohemia, Pilsen, Czech Republic
Féliachi M.	Professor, Technological Institute of Saint-Nazaire, University of Nantes, France
Gurevich V.I.	Ph.D., Honorable Professor, Central Electrical Laboratory of Israel Electric Corporation, Haifa, Israel
Ida N.	Professor, The University of Akron, Ohio, USA
Kildishev A.V.	Associate Research Professor, Purdue University, USA
Kuznetsov B.I.	Professor, SI "ITPM NASU", Ukraine
Kyrylenko O.V.	Professor, Member of NAS of Ukraine, Institute of Electrodynamics of NAS of Ukraine (IED of NASU), Kyiv, Ukraine
Nacke B.	Professor, Gottfried Wilhelm Leibniz Universität, Institute of Electrotechnology, Hannover, Germany
Podoltsev A.D.	Professor, IED of NASU, Kyiv, Ukraine
Rainin V.E.	Professor, Moscow Power Engineering Institute, Russia
Rezynkina M.M.	Professor, NTU "KhPI", Ukraine
Shkolnik A.A.	Ph.D., Central Electrical Laboratory of Israel Electric Corporation, member of CIGRE (SC A2 - Transformers), Haifa, Israel
Trichet D.	Professor, Institut de Recherche en Energie Electrique de Nantes Atlantique, Nantes, France
Yatchev I.	Professor, Technical University of Sofia, Sofia, Bulgaria
Yufarov V.B.	Professor, National Science Center "Kharkiv Institute of Physics and Technology", Ukraine
Zagirnyak M.V.	Professor, Member of NAES of Ukraine, rector of Kremenchuk M.Ostrohradskyi National University, Ukraine
Zgraja J.	Professor, Institute of Applied Computer Science, Lodz University of Technology, Poland

ISSUE 5/2018

TABLE OF CONTENTS

Electrical Engineering. Great Events. Famous Names

Baranov M.I., Rozov V.Yu., Sokol E.I. To the 100th anniversary of the National Academy of Sciences of Ukraine – the cradle of domestic science and technology.....	3
Zolotaryov V.M. Plant «Yuzhicable works»: milestones of the road (75th anniversary of the plant «Yuzhicable works») ...	12

Electrical Machines and Apparatus

Bolyukh V.F., Kashanskij Yu.A., Kocherga A.I., Schukin I.S. Investigation of linear pulse electromechanical converter of induction type with double armature intended for destroying information on SSD storage device	17
Vaskovskiy Yu.M., Poda M.V., Koshikar I.V. Electric generator in the recuperation system of the energy from mechanical oscillations in vehicles.....	24
Shevchenko V.V., Minko A.N., Strokous A.V. Analysis of electromagnetic vibration forces in the elements of the turbogenerator stator fastening to the case in non-nominal operation modes	29

Electrotechnical Complexes and Systems. Power Electronics

Kuznetsov B.I., Nikitina T.B., Kolomiets V.V., Bovdvi I.V., Voloshko A.V., Vinichenko E.V. Synthesis of robust active shielding systems of magnetic field generated by group of high-voltage power lines.....	34
--	----

Theoretical Electrical Engineering and Electrophysics

Suprunovska N.I., Shcherba M.A. Method for voltage control in charge circuit of electric discharge installations with two capacitors under non-zero initial conditions	39
---	----

High Electric and Magnetic Field Engineering. Cable Engineering

Baranov M.I., Buriakovskiy S.G., Rudakov S.V. The metrology support in Ukraine of tests of objects of energy, aviation and space-rocket engineering on resistibility to action of pulses of current (voltage) of artificial lightning and commutation pulses of voltage	44
Brzhezytskyi V.O., Vendychanskyi R.V., Trotsenko Ye.O., Haran Ya.O., Desyatov O.M., Khominich V.I. Characteristics of specialized single-phase high voltage doubler rectifier	54

Power Stations, Grids and Systems

Dehghani M., Montazeri Z., Ehsanifar A., Seifi A.R., Ebadi M.J., Grechko O.M. Planning of energy carriers based on final energy consumption using dynamic programming and particle swarm optimization	62
--	----

Electrical Safety

Glebov O.Yu., Koliushko D.G., Koliushko G.M., Eremeeva E.P. On the issue of design of grounding systems of 330(220) kV substations to ensure the electromagnetic compatibility of secondary circuits	72
---	----

Editorial office address: Dept. of Electrical Apparatus, NTU «KhPI», Kyrpychova Str., 2, Kharkiv, 61002, Ukraine
phones: +380 57 7076281, +380 67 3594696, **e-mail:** a.m.grechko@gmail.com (**Grechko O.M.**)

ISSN (print) 2074-272X
ISSN (online) 2309-3404

© National Technical University «Kharkiv Polytechnic Institute», 2018
© State Institution «Institute of Technical Problems of Magnetism of the NAS of Ukraine», 2018

Printed 22 October 2018. Format 60 x 90 1/8. Paper – offset. Laser printing. Edition 200 copies.
Printed by Printing house «Madrid Ltd» (11, Maksymilianivska Str., Kharkiv, 61024, Ukraine)

M.I. Baranov, V.Yu. Rozov, E.I. Sokol

TO THE 100TH ANNIVERSARY OF THE NATIONAL ACADEMY OF SCIENCES OF UKRAINE – THE CRADLE OF DOMESTIC SCIENCE AND TECHNOLOGY

Purpose. Preparation of short scientifically-historical essay about creation and development of the National Academy of Sciences (NAS) of Ukraine. **Methodology.** Known scientific methods of collection, analysis and analytical treatment of scientific and technical information, touching creation and development of NAS of Ukraine and resulted in scientific monographs, journals and internet-reports. **Results.** A short scientifically-historical essay is presented about creation and development of NAS of Ukraine. The main scientific achievements of NAS of Ukraine in various fields of science are presented. It is pointed that a large scientifically-organizational contribution to these achievements brought by present President of NAS of Ukraine, Academician B.Ye. Paton, his 100th Birthday (27 November, 2018) coincides surprising appearance with the 100th anniversary of NAS of Ukraine. An important role of NAS of Ukraine in the development of society and international scientific and technical cooperation was noted. The results of scientific research, achieved over the past few years by the Institute of Technical Problems of Magnetism of the NAS of Ukraine (Kharkiv), as well as by the Institute of Ionosphere of the NAS and Departments of education and science (DES) of Ukraine (Kharkiv) are briefly presented. The research cooperation in the field of electrical engineering of NTU «KhPI» with scientific institutions of the NAS of Ukraine is highlighted. **Originality.** Certain systematization is executed of known from scientific journals and other mass of scientific and technical materials, touching the results of activity of research workers of institutes of NAS of Ukraine in the last few years. **Practical value.** Scientific popularization and deepening for the students of higher school, engineer-technical and scientific workers, working in the different sectors of economy of country, scientific and technical knowledge in an area of physical-technical and mathematical sciences, chemical and biological sciences, and also social and humanitarian sciences, extending their scientific range of interests and further development of scientific and technical progress in society. References 28, figures 10.

Key words: National academy of Sciences of Ukraine, history of creation and development of Academy.

Приведен краткий научно-исторический очерк о создании, развитии и структуре Национальной академии наук (НАН) Украины. Отмечена важная роль НАН Украины в развитии общества и международном научно-техническом сотрудничестве. Приведены основные научные достижения ученых НАНУ в различных областях науки, а также кратко изложены результаты научных исследований, достигнутые за последние несколько лет Институтом технических проблем магнетизма НАН Украины и Институтом ионосферы НАН и МОН Украины (г. Харьков). Освещено сотрудничество ученых-электротехников НТУ «ХПИ» с научными учреждениями НАН Украины. Библ. 28, рис. 10.

Ключевые слова: Национальная академия наук Украины, история создания и развития.



«...Without scientific schools there will be no science. Without science there will be no technology.»

(From the lecture of the outstanding scientist of our time the President of the National Academy of Sciences of Ukraine B.Ye. Paton, 2012)

Introduction. Modern generations of humanity will soon become a witness to the unique Ukrainian socio-scientific phenomenon: at the end of November 2018, the National Academy of Sciences (NAS) of Ukraine and its current President, Academician B.Ye. Paton celebrate their 100th Anniversaries. This event is symbolic both in its form and in its content. Beginning not only since 1962, when Academician Boris Yevgenovich Paton headed the Academy of Sciences of the Ukrainian SSR (since 1994, the NAS of Ukraine), and throughout all his life this prominent scientist of the modern day was, as they say, «a foot in the foot» with the development of domestic science and technology. Therefore, many years of scientific and organizational activity of Academician B.Ye. Paton as the President of the National Academy of Sciences of Ukraine should be considered as an integral part of the fruitful work of the head of the headquarter of Ukrainian science and technology. Without this important work, it would be impossible to coordinate and direct the multifaceted

activities of the numerous scientific and technical community of the state in the necessary direction.

Humanity at a certain stage of its long-term development has objectively come to the important conclusion that without new scientific and technological ideas and techniques, progress in society becomes impossible. In order to get these ideas and methods, in society we must actively pursue both fundamental and applied scientific research. These studies require highly skilled scientific and technical personnel of a different profile, for which preparation special institutions of society must comply. New methods can be practically implemented in society only with the help of new technology. Therefore, without new technology with higher technical characteristics it is fundamentally impossible to ensure industrial progress of society. In this connection, in a progressive society, a symbiosis of science and technology is needed. To achieve this symbiosis, an appropriate coordinating body becomes necessary. In our opinion, the Academy of Sciences of our state became a similar governing body in Ukraine.

The goal of the paper is drawing up a short scientific and historical essay on the creation and development of the National Academy of Sciences of Ukraine and the achievements of its scientists, as well as the fruitful cooperation of the NAS of Ukraine and the NTU «KhPI» of the Ministry of Education and Science of Ukraine.

1. Brief history of the creation of the National Academy of Sciences of Ukraine. The NAS of Ukraine as the Ukrainian Academy of Sciences (UAS) was founded on November 27, 1918 by the Hetman P.P. Skoropadsky government, and prominent domestic scientist-geochemist, Academician V.I. Vernadsky (Fig. 1) was a founding member and the first President of the UAS [2].

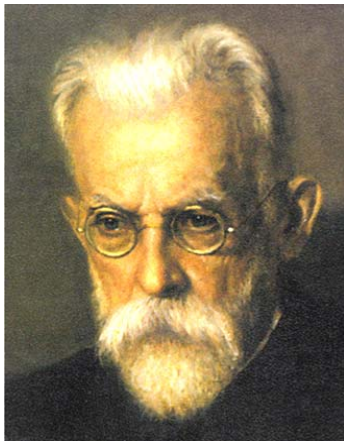


Fig. 1. The first President of the UAS, prominent domestic scientist-geochemist Academician V.I. Vernadsky (12.03.1863 – 06.01.1945)

During the long history as the Presidents of the Academy were elected [2]: M.P. Vasilenko (1921-1922), O.I. Levitsky (1922), V.I. Lipsky (1922-1928), D.K. Zabolotny (1928-1929), O.O. Bogomolets (1930-1946), and O.V. Palladin (1946-1962). Since 1962 the Academy is headed by B.Ye. Paton (Fig. 2).



Fig. 2. The current President of the National Academy of Sciences of Ukraine, outstanding scientist in the field of electric welding of materials, Academician of NAS of Ukraine B.Ye. Paton (born on November 27, 1918)

The name of the Academy was changed four times [1]. In 1918-1921 it was named as the Ukrainian Academy of Sciences (UAS). From 1921 to 1936 as the All-Ukrainian Academy of Sciences (AUAS). In the period 1936-1991 as the Academy of Sciences of the Ukrainian SSR (AS of the Ukrainian SSR). From 1991 to 1993 as the Academy of Sciences of Ukraine (AS of Ukraine), and since 1994 as the National Academy of Sciences of Ukraine (NAS of Ukraine) [1]. The UAS was the oldest of the republican Academies during the

existence of the USSR. In the first year of its activities (until 1920), it consisted of only three scientific Departments: for history and philology, for physics and mathematics, and for social sciences, which covered 3 Institutes, 15 commissions and the National Library [1]. For comparison, we note that now the National Academy of Sciences of Ukraine has 3 sections, 14 branches, about 170 Institutes and other scientific institutions, which employs about 16 thousand researchers [2].

Many scientific schools have been formed at the NAS of Ukraine. Their founders were [2]: prominent mathematicians D.O. Grave, M.M. Krylov, M.M. Bogolyubov, Yu.O. Mitropolsky; mechanics S.P. Tymoshenko, O.M. Dinnik, M.O. Lavrentyev, G.S. Pisarenko; physicists K.D. Sinelnikov, A.K. Walter, L.V. Shubnikov, V.E. Lashkaryov, O.I. Akhiezer, O.S. Davydov, A.F. Prihotko, O.Ya. Usikov; power engineers V.M. Khrushchev, G.F. Proscura; astronomers O.Ya. Orlov, M.P. Barabashov, Ye.P. Fedorov, S.Ya. Braude; geologist P.A. Tutkovsky; material scientist I.M. Frantsevich, V.I. Trefilov; chemists L.V. Pisarzhevsky, O.I. Brodsky, A.V. Dumansky, V.I. Atroshchenko; medical doctors D.K. Zabolotny, O.O. Bogomolets, V.P. Filatov, M.G. Kholodny, I.I. Shmalgauzen, M.M. Amosov. There are the world-famous Ukrainian electric welding schools of Ye.O. Paton and B.Ye. Paton [3] and cybernetics school of V.M. Glushkov, economic and humanitarian schools that were headed by [2] economists M.V. Ptukha and K.G. Woblii; historians M.S. Grushevsky and D.I. Yavornytsky; lawyer V.M. Koretsky; philosopher V.I. Shinkaruk; orientalist A.Yu. Krymsky; linguistics L.A. Bulakhovsky, V.M. Rusanivsky; literary critics S.O. Efremov and O.I. Biletsky.

Note that Academician B. Ye. Paton is the only head of the state Academy of Sciences in the world, who is its contemporary (the day of foundation of the Academy of Sciences of Ukraine and the day of his birth surprisingly coincide – November 27, 1918) [3]. Personal communication with this person-statesman leaves many years unforgettable impression (Fig. 3).



Fig. 3. Meeting of scientists of the NTU «KhPI» with the President of the National Academy of Sciences of Ukraine, Academician B.Ye. Paton after the award of the State Prizes of Ukraine in the field of science and technology for 2006 (Kyiv, Mariinsky Palace, February 2007)

2. Structure, management and basic functions of the National Academy of Sciences of Ukraine. According to the current legislation, the National

Academy of Sciences of Ukraine is the highest state-owned scientific institution in Ukraine [4]. The self-government of the Academy is to independently determine the subjects of research and the forms of their organization and conduct, the formation of structure, the solution of scientific and organizational, economic and personnel issues, the implementation of international scientific relations, election and collegiality of management [4]. The Academy unites true members (Academicians), Corresponding Members and foreign members, all scientists of its institutions. It organizes and implements fundamental and applied scientific research on the most important problems of the natural, technical, social and human sciences [4]. The highest authority of the National Academy of Sciences of Ukraine is its General Meeting, consisting of true members (Academicians) and Corresponding members. In the period between sessions of the General Meeting, the Presidium of the National Academy of Sciences of Ukraine conducts the Academy's work, which is elected by the General Meeting for a term of 5 years. The Presidium of the National Academy of Sciences of Ukraine currently employs 32 people, including [4]: the President, five Deputy Presidents, Chief Scientific Secretary, 14 Academics-secretaries of Departments and 11 other members. As of 01.01.2018, the National Academy of Sciences has 177 true members (Academicians), 352 Corresponding Members and 98 foreign members, and the total number of employees at the National Academy of Sciences of Ukraine at that time amounted to 29870 people, including 15529 research workers. Among them, 2362 Doctors of Sciences and 6807 Candidates of Sciences [4].

The National Academy of Sciences of Ukraine has 3 sections (physical, technical and mathematical sciences; chemical and biological sciences; social sciences and humanities), which combine 14 Departments of science [4]: mathematics; informatics; mechanics; physics and astronomy; earth sciences; physical and technical problems of materials science; physical and technical problems of energy; nuclear physics and energy; chemistry; biochemistry, physiology and molecular biology; general biology; economy; history, philosophy and law; literature, language and art studies. There are 5 regional research centers in the Academy with double subordination to the Ministry of Education and Science of Ukraine [4]: Donetsk (Pokrovsk city), Western (Lviv city), Southern (Odessa city), Northeast (Kharkiv city), Prydniprovsky (Dnipro city), as well as the Center for Evaluation of Scientific Institutions and the Development of Regions (Kyiv city). The Departments of the National Academy of Sciences of Ukraine include relevant research institutes and other scientific institutions (observatories, botanical gardens, arboreturns, preserves, libraries, museums, etc.), which are the main link in the structure of the Academy.

Scientists of NAS of Ukraine are active participants in international programs supported by such foreign and international foundations and organizations as [4]: European Commission, STCU, NATO, UNESCO, DFG, CRDF, etc. The grants of these organizations, obtained on a competitive basis, annually

support implementation of about 300 research, coordination and supporting scientific exchanges scientific and technical projects. It should be noted that in accordance with the Association Agreement with the EU, relations with the research centers of the EU countries and European Commission organizations are expanding, in particular regarding participation in EU programs on research and innovation «Horizon 2020», Euratom, as well as fruitful interaction on an ongoing basis with Joint Research Center of the European Commission (JRC) [4, 5]. The National Academy of Sciences of Ukraine conducts independent scientific evaluation of strategic, forecast and program documents (doctrines, concepts, strategies, etc.) as well as state-level materials on the instructions of the President of Ukraine, the Verkhovna Rada of Ukraine, the Cabinet of Ministers of Ukraine and/or on its own initiative, develops proposals on the principles of state scientific and scientific and technical policy, forecasts, information and analytical materials, suggestions, recommendations on socio-political, socio-economic, scientific and technical, innovation and human development of state, carries out scientific and technical examination of numerous draft of laws.

3. Main scientific achievements of the National Academy of Sciences of Ukraine. On May 18, 2017, the President of Ukraine signed the Decree No. 136/2017 on the 100th Anniversary of the National Academy of Sciences of Ukraine, scheduled for November 2018. What results does the Academy meet with its anniversary?

NAS of Ukraine is one of the prominent scientific centers of the world, which enriched the national and world science with valuable discoveries and inventions. Thus, the Academy's physicists in the 20th century carried out a number of important scientific studies in the field of theoretical and experimental physics, as well as in the study of the physical properties of semiconductors (for example, germanium diodes and triodes) [1, 4]. The fundamental scientific works of physicists of the Ukrainian Institute of Physics and Technology (UFTI, Kharkiv, now the NSC «KhPTI») are widely known from that period: by Academicians O.I. Leipunsky and A.K. Walter in the field of physics of the atomic nucleus and powerful accelerators of charged particles, as well as by Academician K.D. Sinelnikov in the field of vacuum physics, vacuum metallurgy and high-temperature plasma [6]. In 1965, this Institute built the largest linear electron accelerator in Europe for energy up to 2000 MeV [6]. In addition, Kharkiv scientists during this period built the world's largest radio telescope type UTR-2 (Fig. 4), which is located near the village Grakovo (Kharkiv region) [7]. The UTR-2 radio telescope has a T-shaped arrangement of antennas with a total area of 150,000 m². It is today one of the most powerful scientific and technical research tools in the world to investigate the Universe. It should be noted that with the help of the UTR-2 radio telescope, which now belongs to the Institute RIAN of the NAS of Ukraine, an atlas of the back of the Moon was created. This merit belongs to the native of the Kharkiv region, the famous Soviet scientist-astronomer, Academician of the Academy of Sciences of the Ukrainian SSR, Professor of the Kharkiv State University M.P. Barabashov [7].



Fig. 4. General view of the object of national heritage of Ukraine «Radio telescope UTR-2 with the system of interferometers URAN» of the Radio Astronomical Institute of the National Academy of Sciences of Ukraine (Grakovo village, Kharkiv region)

Works by Academicians M.M. Krylov and M.M. Bogolyubov and their students are an outstanding contribution to the study of approximate methods of mathematical analysis and the theory of dynamical systems. These well-known in the world Ukrainian mathematicians have created a substantially new section in the field of mathematical physics – nonlinear mechanics. A significant contribution to domestic and world science is the research work by Academician G.F. Proscura on aerohydrodynamics and by Academician M.O. Lavrentiev on the geometric theory of functions of complex variable and its practical application for solving urgent modern technical problems of hydrodynamics and aerodynamics.

At the Institute of Electrical Engineering of the Academy of Sciences of the USSR (now Institute of Electrodynamics of the National Academy of Sciences of Ukraine, Kyiv) for the first time in the USSR a small electronic computer was created. In many technical branches, the Academy of Sciences of the USSR came out first in the USSR (for example, in powder metallurgy and electric welding). Scientists-chemists of the Academy of Sciences of the USSR were the first in the USSR to receive «heavy water» for the needs of nuclear physics and energy, as well as the corresponding isotopes of hydrogen and oxygen for a complex of promising experimental nuclear-physical studies [1, 4, 8]. The materials science Institutes of the Academy successfully developed the technological processes that enabled the new branches of development of the economy. Significant scientific results were obtained at the Institutes of chemical technology, biochemistry, physiology and theoretical medicine, general biology.

The multifaceted and powerful contribution to the development of world science and our state of the National Academy of Sciences of Ukraine does today. Modern achievements of the Academy's scientists in 2017 which are indicated in the final annual report of the President of the National Academy of Sciences of Ukraine, Academician B.Ye. Paton [9] confirm that the NAS of Ukraine continues to perform its statutory duties in a worthy manner. Thus, in the difficult labor conditions of 2017, with significant underfunding of the Academy, scientists of the National Academy of Sciences of Ukraine received the following significant fundamental and applied results in various fields of science [9], including:

- new solutions of the Mathisson-Papapetrou equations have been obtained, which have revealed previously unknown features of the motion of fast particles with their own rotation moment around the black Schwarzschild hole in the Sitter space model;
- new highly effective combinations of cybernetic algorithms are developed, which enable the specialists to parallelize the process of solving complex discrete optimization problems of large dimension;
- a fundamentally new method of transporting drugs in human blood has been developed, the essence of which is to bind specially modified molecules of medicinal preparations with lipoprotein particles of plasma of human blood;
- two extremely important breakthrough discoveries in the field of extragalactic astronomy and cosmology have been made (this is the opening of two galaxies, one of which is the galaxy with the smallest content of chemical elements heavier than the helium, and the other is a galaxy whose radiation is so powerful that it can ionize neutral intergalactic environment in the era of reionization of the Universe);
- new functional nanomaterials were created based on the integration of important functional characteristics of graphene, graphene oxides, inorganic semiconductors with the properties of conjugated electrical conductive polymers;
- new unknown previously condensed pyrimidine derivatives have been obtained that effectively suppress the harmful human papillomavirus;
- a number of compounds effective against pathogens of multi-resistant tuberculosis have been discovered and studied by biochemists;
- it has been proven that acetylcholine receptors play an important role in activating regulatory β -lymphocytes, suppressing the synthesis of antibodies and activating the processes of regeneration of the liver;
- biologists studied the molecular-genetic properties of the five enterobacterium viruses, which are considered as promising agents of phagetherapy of burns of fruit plants;
- a new concept of the organization of protected areas of polyfunctional type with various flexible protection regimes, which provides introduction of ecosystem principle instead of territorial, is grounded;
- a three-dimensional computer model of the Moho (or Mohorovičić) surface is built on super-supercomputers SKIT intended to accurately locate and evaluate stocks of ultra-deep oil and gas deposits, which are often expensive to exploration through traditional drilling;
- an effective information technology of the classification of the ground cover has been developed under the research program of the NAS of Ukraine «Aerospace Observations for Sustainable Development and Security», which enables to receive scores of areas for the scale of the whole country and is a key component of the integrated assessment of the development of a «smart city» in the context of comfort and security of residence in it;
- scientists in the field of mechanics together with specialists of the State Enterprise «M.K. Yangel Design

Office «Pivdenne» developed a special module for the removal of the third stage of the carrier rocket, which, among other things, is proposed to be used to remove from the orbit of the third stage of the carrier rocket «Cyclone-4M» and spacecrafts that worked out the term of their active existence;

- material scientists have created an automated broad-spectrum complex that allows specialists to remotely control the quality of structures of metal and composite materials in real-time;

- thermophysics scientists have developed a multi-stage technology and installation for the production of insulating ultra-fine basalt fiber, which is important for the further creation of a new environmentally safe, durable and fire-proof thermal insulation for civil engineering;

- chemical scientists have proposed highly effective methods for the processing of plant waste and sediments of the Bortnitskaya Aeration Station;

- biochemists of the country tested a new hemostatic agent, intended for use by patients with congenital pathologies of hemostasis, in particular hemophilia;

- a technology is developed for obtaining a recombinant creatinine deaminase – a sensory element of the sensor for creatinine, which serves as a biomarker for renal insufficiency and an indicator of the efficiency of the hemodialysis process;

- a highly effective innovative technology for restoring speech of post-stroke patients is developed, the feature of which is the personified activation of the patient's body reserves;

- the first National biodiversity information network (UkrBIN) was developed in our country;

- economists have created an information and analytical system for forecasting the development of domestic energy;

- nuclear scientists, energy specialists and nuclear safety experts substantiated the term and showed the possibility of prolonging the safe operation of the nuclear reactor of power unit No. 2 of the South-Ukrainian NPP for at least 20 years in the over-project period, that is, until 2048, and the nuclear reactor of power unit No. 4 of the Rivne NPP at least until 2026;

- the RODOS system developed by the domestic scientists, which is intended to predict and support the decision-making on reacting to radiation accidents at Ukrainian nuclear power plants, has proved its efficiency;

- the process of introduction into the industrial production of the drug «Metovitan», which performs energy-stimulating, cardioprotective and hepatoprotective functions, and prevents the aging of the body, is completed;

- with the participation of cybernetics, networks for group work of domestic robotized ground and air combat systems were developed;

- scientists accomplished a large complex of works on the creation of: import substitution elements, including a semiconductor element base for the maintenance of high-precision weapons; technologies for prolonging the life of aviation and armored vehicles; materials of heat-resistant composites for combustion chambers of gas turbine

engines; components of solid rocket fuel; technology of laser and arc welding of thin-walled elements of a steering wheel and nozzle of guided missiles and for underwater welding of shells of warships in extreme conditions; technologies of strengthening and processing of smoothbore and threaded channels of different caliber trunks; technologies of creation of composite transparent and layered structures from ceramics and alloys of light metals for the protection of light-armored machinery; technologies of coating creation that minimize the visibility of vehicles in microwave, RF and IR bands of electromagnetic waves.

4. Kharkiv Academic science. Kharkivites are proud of the fact that their city is now the second in the country after Kyiv on the strength of Academic science. Thus, in Kharkov there are 13 research Institutes of the National Academy of Sciences of Ukraine, which represent 3 Sections and 6 Departments of the National Academy of Sciences of Ukraine. They are the B.I. Verkin Physical-Technical Institute of Low Temperatures (PTINT), the O.Ya. Usikov Institute of Radiophysics and Electronics (IRE), the Radio Astronomy Institute (RIAN), the Institute of Ionosphere of the National Academy of Sciences and the Ministry of Education and Science of Ukraine (IION), which are members of the Department of Physics and Astronomy. The members of the Department of Nuclear Physics and Energy are the National Science Center «Kharkiv Physical-Technical Institute» (NSC «KhPTI», former UFTI) and the Institute of Electrophysics and Radiation Technologies (IERT). The members of the Department of Physical and Technical Problems of Materials Science are the Research and Technological Complex «Institute of Single Crystals» (RTC «ISC»), the Institute of Single Crystals (ISC), the Institute of Scintillation Materials (ISMA). The Department of Biology, Physiology and Molecular Biology is represented by the Institute of Problems of Cryobiology and Cryomedicine (IPCC), and the Department of Economics by the Research Center for Industrial Development Problems (RC «IDP»).

Close to the readers of the Journal «Electrical Engineering and Electromechanics» the technical sciences in Kharkiv are represented by the A.M. Podgorny Institute of Mechanical Engineering Problems (IPMach) and the Institute of Technical Problems of Magnetism (ITPM), which are part of the well-known for us Department of Physical and Technical Problems of Power Engineering (DPTPE) of the National Academy of Sciences of Ukraine.

Academic Institutes have a powerful and unique scientific and experimental base. So, in Kharkiv there are 6 scientific objects that make up the National heritage of Ukraine [10]. These are such objects as «Nuclear and Physical Installations» of the NSC «KhPTI»; «Complex for physical research at ultralow temperatures» of the PTINT; «Cryomagnetic radio spectroscopic complex of millimeter wavelength range» of the IRE; «Radio telescope UTR-2 with the system of URAN interferometers» of the RIAN (Fig. 4),

«Ionospheric probe» of the IION (Fig. 5); «Hydrodynamic stands» of the IPMach, and the «Magnetodynamic complex» of the ITMP.

Institute of Ionosphere of the National Academy of Sciences and Ministry of Education and Science of Ukraine. It is close to the NTU «KhPI» on the history and territorial location. It was founded in 1991 on the basis of the Department of Radio Electronics of the NTU «KhPI». This institute has a unique ionospheric observatory, the ionospheric probe of which is the object of the national heritage of Ukraine [11]. The general view of this unique object – the incoherent scattering (IS) radar with an parabolic antenna type NDA-100, whose diameter is equal to 100 m, is presented in Fig. 5 [12].



Fig. 5. Object of national heritage of Ukraine «Ionospheric probe» of the Institute of Ionosphere of the National Academy of Science and Ministry of Education and Science of Ukraine (Zmiev city, Kharkiv region)

Since 1996, in this observatory of the Institute of Ionosphere, in conjunction with the Haystack Observatory of the Massachusetts Institute of Technology and the Arecibo Observatory of the Cornell University (USA), regular studies of the height-time dependence of the relative concentration of light ions by the method of incoherent scattering were conducted in accordance with the International Geophysical Calendar, which made it possible to detect in the ionosphere of the Earth longitudinal and latitudinal variations in the concentration of hydrogen ions [12]. These studies are important for the safety of flights in near-Earth orbits of satellites of various applications and other spacecrafts, forecasting the state of radio communications and weather [11, 12].

Institute of Technical Problems of Magnetism of the National Academy of Sciences of Ukraine. ITPM is the only one Academic research institution in the city of Kharkiv working in the field of electrical engineering. The institution was founded in 1970 [13] and functioned until 1991 as the Kharkiv branch of the All-Union Research Institute of Electromechanics – the main organization in the USSR for the development of «low-magnetic» ship electrical equipment. In 1992, this institution as a legal entity in the status of a separate Department of Magnetism of the Institute of Electrodynamics became a member of the National Academy of Sciences of Ukraine, which in 2005 was transformed into the Scientific and Technical Center for Magnetism of Technical Objects (STC MTO of the NAS

of Ukraine) with the rights of a research Institute. In 2010, the institution celebrated its 40th anniversary (Fig. 6).



Fig. 6. Scientific presentation by the Corresponding Member of the NASU V.Yu. Rozov which is devoted to the 40th anniversary of the founding of the STC MTO of the NAS of Ukraine (Kharkiv, 2010)

In 2013, this institution was renamed the Institute of Technical Problems of Magnetism (ITPM) of the National Academy of Sciences of Ukraine. ITMP of the NAS of Ukraine is the only research institution in Ukraine and the world that performs theoretical and experimental scientific researches of static and low frequency (with frequency 0-5000 Hz) magnetic field created by various technical objects (ships, vehicles, orbital spacecrafts, trunk pipelines, electrical engineering, building constructions, etc.). Investigations are carried out according to the following approved scientific directions: the theory of magnetism of technical objects; definition of magnetic characteristics of technical objects; control of the magnetic field of technical objects; reduction of electromagnetic effects of objects of electric power to the person and the environment. The results of the research of the ITPM in these directions correspond to the international standards of high level due to the unique scientific staff of the Institute, an integrated approach to solving the scientific problems of magnetism of various technical objects, as well as the widespread use of the powerful and unique experimental base of the Institute – its «Magnetodynamic complex» in carrying out both fundamental, as well as applied research (Fig. 7).

For the period of work in the NAS of Ukraine, the specialists of the ITPM on the basis of generalization of features of various classes of technical objects (ships, armored vehicles, pipelines, spacecrafts and electric power equipment) as sources of magnetic field, formed a new scientific direction – «magnetism of technical objects» which is aimed at studying the totality of magnetic properties of technical objects and phenomena associated with the interaction of technical objects and the environment through a magnetic field. In the framework of this direction, fundamentally new scientific achievements of the world level, which have been introduced into the defense and space domestic industries, fuel and energy complex and medical ecology, have been obtained.



Fig. 7. A unique magnetometric stand of the object of the national heritage of Ukraine «Magnetodynamic complex «of the Institute of Technical Problems of Magnetism of the National Academy of Sciences of Ukraine (Kharkiv)

Among the most important applied results of the ITMM, it is possible to note the creation and introduction in the Magnetodynamic complex of the Institute of industrial technology of a high-precision measurement of the magnetic characteristics of spacecrafts developed by the State Enterprise «Design Office «Pivdenne» [14]. The developed technology became an integral part of the technology of the creation of domestic spacecrafts and allowed to provide high-quality magnetic control of spacecrafts of types «Microsatellite», «EgiptSat-1», «Sich-2» (Fig. 8), «Microsat», «Sich-2-1» and the development of a number of advanced spacecrafts in terms of their magnetic characteristics.



Fig. 8. Determination of the magnetic characteristics of the flying sample of the spacecraft «Sich-2» at the magnetometric stand of the Institute of Technical Problems of Magnetism of the National Academy of Sciences of Ukraine (Kharkiv, 2010)

The industrial practical technology of demagnetization of welding joints of large diameter pipes has been developed and introduced on main pipelines of Ukraine and other countries (see Fig. 9) as an important practical result of the research activity of the ITPM of the National Academy of Sciences of Ukraine. This allows to significantly improve the quality of electric welding during repair work by eliminating the phenomenon of «magnetic blast» of the arc [15]. Approximately 80 demagnetizing devices have been currently introduced. Developed over the past five years at the ITPM methods and means for the determination and normalization of the magnetic field of industrial frequency in residential buildings and workplaces of power engineering objects, as well as technogenic hypogeomagnetic field have Important social significance. A number of important and

relevant developments have been completed in this direction, among which the following can be noted:



Fig. 9. Repair works on the main gas pipeline DU 1200×12 mm «Urengoy-Pomari-Uzhgorod» using the technology of demagnetization of welding joints developed at the ITPM of the National Academy of Sciences of Ukraine (Ternopil, 2017)

1. A new method for modeling and calculating the magnetic field of a three-phase power transmission line, which, unlike the known ones, allows to use the purely effective values of the magnetic flux density, which are subject to both normalization and measurement by standard devices is developed [16, 17]. This approach greatly simplifies both the experimental check (verification) of the calculation of the level of the magnetic field, and its sanitary-hygienic assessment. The results of the work formed the scientific basis of the new normative document of the Ministry of Energy and Coal COV-H EE 20.179:2008 «Calculation of electric and magnetic fields of transmission lines. Methodology» (as amended), which was put into effect by the order of the Ministry of Energy and Coal of 01.07.2016 No. 423.

2. A new method for reducing the magnetic field of high-voltage transmission lines is proposed – a method of vector compensation of the magnetic field that does not require additional alienation of land plots and allows, by an optimal spatial distribution of split phase wires of the transmission line, to reduce orderly the level of their magnetic field [18]. Recommendations on the implementation of this method have been transferred for implementation to the energy sector of Ukraine (State Enterprise «NEC Ukrenergo»).

3. A new method for the synthesis of active screening systems of technogenic magnetic field of industrial frequency, developed by high-voltage overhead lines in nearby residential buildings [19, 20], was developed and experimentally grounded. The implementation of the proposed method, which is carried out in a closed structure, forms the scientific basis of the latest domestic technology of reducing the magnetic field of the industrial frequency to a safe level in residential premises. This technology has significant economic advantages over the well-known foreign technologies of active screening of the magnetic field of overhead lines that are widely used in the world.

4. The theoretical basis for the construction of new systems of contour screening of the magnetic field of high-voltage cable lines, which, in comparison with the best world models, has 30 % fewer elements with high screening efficiency (up to 10 units) is developed [21-23].

The research results formed the scientific basis of the first domestic technology for the design of environmentally friendly cable lines with voltage up to 330 kV, developed by order of the State Enterprise «NEC Ukrenergo» and implemented in the normative document of the Ministry of Energy and Coal COY-H MEB 40.1-37471933-49:2011 «Design of cable lines with voltage up to 330 kV. Instruction» (new edition), which was put into effect in 2017 by the order of the Ministry of Energy and Coal of January 26, 2017 No. 82.

5. The mechanism of biotrophic attenuation of the natural static geomagnetic field in the premises of modern residential buildings, which was caused by the magnetization of their steel structural elements, was for the first time investigated. Recommendations on the design of «magnetically clean» residential and public buildings, which have no negative influence on the population, including the use of the construction of residential buildings of special low-magnetic steel with a relative magnetic permeability of not more than 70 units instead of standard rolled steel with magnetic permeability of about 300 units are developed [24-26].

In recent years, the ITPM cooperation with NTU «KhPI» has been growing. For example, in 2014, the third in Ukraine doctoral Specialized Scientific Council D 64.050.17 in defense of Theses in the specialty 05.09.05 «Theoretical Electrical Engineering» was jointly created and ensured functioning. Since 2014, the joint publication of the scientific and practical Journal «Electrical Engineering and Electromechanics» (Certificate KB No. 2121-10821PR of 07.10.2014) has been started, which in 2017, due to the growth of its scientific level, is included in the leading world scientometric base Web of Science, and is still the only one in the NTU «KhPI» scientific journal of the highest level. In 2017, the joint training in the postgraduate course of the NTU «KhPI» of specialists of the third (educational and scientific) level of higher education of the Doctor of Philosophy in the specialty 141 «Power Engineering, Electrical Engineering and Electromechanics» was started, which is carried out under the joint scientific guidance of the scientists of the NTU «KhPI» and the ITPM of the NASU. For more than 10 years together with the NTU «KhPI» an annual International Symposium «Problems of Electric Power Engineering, Electrical Engineering and Electromechanics (SIEMA)» is held. Traditional collaboration between the ITPM of the NASU and the NTU «KhPI» is expanding under the agreements on scientific and technical cooperation. Joint research is conducted with Departments of Engineering Electrophysics, Automated Electromechanical Systems, Electrical Apparatus, Theoretical Fundamentals of Electrical Engineering of the NTU «KhPI», internship of lecturers, lectures for students and their pre-diploma practice.

5. Cooperation of the NTU «KhPI» with the Institute of Electrodynamics of the National Academy of Sciences of Ukraine. Proceeding from the professional interests of the main readers of the Journal «Electrical Engineering and Electromechanics» – experts in the field of electrical engineering, the closest to them are the Institutes of the Department of physical and technical problems of energy of the National Academy of Sciences of Ukraine of the electrical engineering, including the Institute of Electrodynamics of the NAS of Ukraine (Kyiv).

The staff members of the NTU «KhPI» are first of all connected with the IED of the NAS of Ukraine by the joint conduction of the International Scientific and Technical Conference «Power Electronics and Energy Efficiency» (CEE), which since 1993 and at this time, together with the IED, is held by the Department of Industrial and Biomedical Electronics of the NTU «KhPI». During this time, due to the scale, high scientific and organizational level of the CEE Conference, it became a powerful catalyst for the scientific and technical «forces» of the NTU «KhPI» and the IED on solving energy saving problems by using power and information electronics, a real «forge» of joint training of highly skilled personnel [27 , 28]. Managers of the work of the Conference are: from the IED Academicians of of NAS of Ukraine B.S. Stogniy, A.K. Shidlovsky, O.V. Kirilenko and from the NTU «KhPI» Corresponding Member of the National Academy of Sciences of Ukraine Ye.I. Sokol Fig. 10).



Fig. 10. Participants of the CEE'2010 Conference: Professor B.V. Klepikov, Academician O.V. Kirilenko, Academician B.S. Stogniy, Corresponding Member Ye.I. Sokol (Alushta, 2010)

Successful cooperation of such scientific institutions of the National Academy of Sciences of Ukraine of the electrical engineering profile as the Institute of Electrodynamics and the Institute of Technical Problems of Magnetism with NTU «KhPI» confirms the prospect of deeper integration in our state of University and Academic science.

Conclusions. The 100th anniversary the National Academy of Sciences of Ukraine marks by new outstanding scientific achievements, which confirm that without science in the modern society technical progress is unthinkable. In order for Ukraine to become one of the high-tech countries of the world in the future, domestic science and, first of all, the technical one should become one of the priority directions of development at the state level. The level of its state financial support should be consistent with the indicators adopted in the leading countries of the world – at least 1.7 % of GDP.

The joint scientific potential of the National Academy of Sciences of Ukraine and the University science still allows to raise the technological level of our country to the world one. However, for the practical realization of this high-purpose scientific and technological task of state importance, the consolidation of society and the unwavering will of the country's leadership in its achievement are necessary. We very much hope that in the next 100 years the National Academy of Sciences of Ukraine will enter, experiencing the necessary support of the state.

REFERENCES

1. Available at: https://en.wikipedia.org/wiki/National_Academy_of_Sciences_of_Ukraine (accessed 12 June 2017).
2. Available at: <http://www.nas.gov.ua/EN/About/Pages/history.aspx> (accessed 08 September 2017).
3. Available at: https://en.wikipedia.org/wiki/Borys_Paton (accessed 22 April 2018).
4. Available at: <http://www.nas.gov.ua/EN/About/Pages/default.aspx> (accessed 02 May 2018).
5. Available at: <http://files.nas.gov.ua/text/infNASU/nasudovidnyk2016.pdf> (accessed 26 October 2017).
6. Baranov M.I. *Antologija vydajushhijhsja dostizhenij v nauke i tehnikе: Monografija v 3-h tomah. Tom 3* [An anthology of the distinguished achievements in science and technique: Monograph in 3 volumes. Volume 3]. Kharkiv, PhPB Panov A.N. Publ., 2016. 415 p. (Rus).
7. Available at: <https://all-ukraine.com.ua/ru/object.html?id=2864> (accessed 13 July 2017). (Rus).
8. Malicjkyj B.A., Ghrachev O.O., Kubaljsjkyj O.N., Kornilov V.A., Rybachuk V.P., Khorjevin V.I., Videnina N.G., Gholovashhenko L.R., Ovcharova L.P. *Nacionaljna akademija nauk Ukrainy: statystychnyj i naukometrychnyj analiz efektyvnosti naukovogho potencijalu* [National academy of sciences of Ukraine: statistical and scientific-metrical analysis of efficiency of scientific potential]. Kyiv, Phoenix Publ., 2016. 228 p. (Ukr).
9. Available at: <http://files.nas.gov.ua/text/report/2017ua.pdf> (accessed 13 April 2018). (Ukr).
10. Available at: <http://www1.nas.gov.ua/infrastructures/NationalProperty/Pages/default.aspx>. (Ukr).
11. Available at: https://ru.wikipedia.org/wiki/Институт_ионосферы_НАН_и_МОУ_Украины (accessed 28 February 2018). (Rus).
12. Available at: https://ua.igotoworld.com/ru/poi_object/66097_institute-of-ionosphere.htm (accessed 15 June 2017). (Rus).
13. Rozov V.Yu. To the 40th anniversary of the Science and Technology Center of Magnetism of Technical Objects of the NAS of Ukraine. *Technical electrodynamics*, 2010, no.3, pp. 74-80. (Rus).
14. Rozov V.Yu., Getman A.V., Petrov S.V., Erisov A.V., Melanchenko A.H., Horoshilov V.S., Shmidt I.R. Magnetism of spacecraft. *Technical electrodynamics. Thematic issue «Problems of modern electrical engineering»*, 2010, chapter 2, pp. 144-147. (Rus).
15. Volokhov S.A., Dobrodeiev P.N., Mamin G.I. Integrated demagnetization of pipes at arc welding. *Technical electrodynamics*, 2012, no.4, pp. 19-24. (Rus).
16. Rozov V.Yu., Reutskyi S.Yu., Pelevin D.Ye., Yakovenko V.N. The research of magnetic field of high-voltage ac transmissions lines. *Technical Electrodynamics*, 2012, no.1, pp. 3-9. (Rus).
17. Rozov V.Yu., Reutskyi S.Yu., Piliugina O.Yu. The method of calculation of the magnetic field of three-phase power lines. *Technical electrodynamics*, 2014, no.5, pp. 11-13. (Rus).
18. Rozov V.Yu., Reutskyi S.Yu., Pelevin D.Ye., Piliugina O.Yu. The magnetic field of power transmission lines and the methods of its mitigation to a safe level. *Technical electrodynamics*, 2013, no.2, pp. 3-9. (Rus).
19. Kuznetsov B.I., Nikitina T.B., Voloshko A.V., Bovdyj I.V., Vinichenko E.V., Kobilyanskiy B.B. Synthesis of an active shielding system of the magnetic field of power lines based on multiobjective optimization. *Electrical engineering & electromechanics*, 2016, no.6, pp. 26-30. (Rus). doi: **10.20998/2074-272X.2016.6.05**.
20. Rozov V.Yu., Grinchenko V.S., Pelevin D.Ye., Chunikhin K.V. Simulation of electromagnetic field in residential buildings located near overhead lines. *Technical electrodynamics*, 2016, no.3, pp. 6-8. (Rus). doi: **10.15407/techned2016.03.006**.
21. Rozov V.Yu., Kvytsynskyi A.A., Dobrodeiev P.N., Grinchenko V.S., Erisov A.V., Tkachenko A.O. Study of the magnetic field of three phase lines of single core power cables with two-end bonding of their shields. *Electrical Engineering & Electromechanics*, 2015, no. 4, pp. 56-61 (Rus). doi: **10.20998/2074-272X.2015.4.11**.
22. Rozov V.Yu., Dobrodeiev P.N., A.A. Kvytsynskyi A.A. Double-circuit passive shielding of the magnetic field of high-voltage cable lines in junction zones. *Technical electrodynamics*, 2017, no.1, pp. 23-28. (Rus). doi: **10.15407/techned2017.01.023**.
23. Rozov V.Yu., Tkachenko O.O., Yerisov A.V., Grinchenko V.S. Analytical calculation of magnetic field of three-phase cable lines with two-point bonded shields. *Technical electrodynamics*, 2017, no.2, pp. 13-18. (Rus). doi: **10.15407/techned2017.02.013**.
24. Rozov V.Yu., Zavalnyi A.V., Zolotov S.M., Gretsikh S.V. The normalization methods of the static geomagnetic field inside houses. *Electrical Engineering & Electromechanics*, 2015, no.2, pp. 35-40 (Rus). doi: **10.20998/2074-272X.2015.2.07**.
25. Rozov V.Yu., Levina S.V. Modeling of the static geomagnetic field indoor dwelling houses. *Technical electrodynamics*, 2014, no.4, pp. 8-10. (Rus).
26. Rozov V.Yu., Reutskyi S.Yu., Levina S.V. The study of the effect of weakening of static geomagnetic field by steel columns. *Technical electrodynamics*, 2014, no.1, pp. 12-19. (Rus).
27. Sokol Ye.I., Kipenskii A.V., Krivosheev S.Yu. Educational and methodical work and research activities of the Department of Industrial and Biomedical Electronics of the National Technical University «KhPI». On the occasion of the 55-th anniversary of the foundation. *Bulletin of NTU «KhPI». Series: New solutions in modern technologies*, 2018, no.26(1302), vol.1, pp. 3-12. (Rus).
28. Dolbnja V.T., Sokol Ye.I., Krivosheev S.Yu. *Kafedra promyshlennoj i biomedicinskoj elektroniki NTU «KhPI». Istoriya. Dostizheniya. Perspektivy* [Department of Industrial and Biomedical Electronics NTU «KhPI» History. Achievements. Prospects]. Kharkiv, Golden Pages Publ., 2013. 224 p. (Rus).

Received 20.07.2018

M.I. Baranov¹, Doctor of Technical Science, Professor,
V.Yu. Rozov², Doctor of Technical Science, Corresponding
member of NAS of Ukraine,
E.I. Sokol³, Doctor of Technical Science, Professor,
Corresponding Member of the National Academy of Science of Ukraine,

¹ Scientific-&-Research Planning-&-Design Institute
«Molnija»,
National Technical University «Kharkiv Polytechnic Institute»,
47, Shevchenko Str., Kharkiv, 61013, Ukraine,
phone +380 57 7076841, e-mail: baranovmi@kpi.kharkov.ua

² State Institution «Institute of Technical Problems
of Magnetism of the NAS of Ukraine»,
19, Industrialna Str., Kharkiv, 61106, Ukraine,
phone +380 57 991190, e-mail: Rozov@nas.gov.ua

³ National Technical University «Kharkiv Polytechnic Institute»,
2, Kyrpychova Str., Kharkiv, 61002, Ukraine,
phone +380 57 7001564, e-mail: omsroot@kpi.kharkov.ua

How to cite this article:

Baranov M.I., Rozov V.Yu., Sokol E.I. To the 100th anniversary of the National Academy of Sciences of Ukraine – the cradle of domestic science and technology. *Electrical engineering & electromechanics*, 2018, no.5, pp. 3-11. doi: **10.20998/2074-272X.2018.5.01**.

V.M. Zolotaryov

PLANT «YUZHicable WORKS»: MILESTONES OF THE ROAD (75TH ANNIVERSARY OF THE PLANT «YUZHicable WORKS»)

With the history of the creation and development of the Plant «Yuzhicable works», the formation of the national cable industry is connected. The enterprise is the flagship of the industry. Its production potential and the range of products demonstrate the unique capabilities of this production. Such a plant has become thanks to a systematic approach to the technical re-equipment of existing facilities, which has been going on here for the last decades. Modern technological equipment, new workshops and sites ensure the production of competitive products that are in demand both in Ukraine and abroad. References 5.

Key words: history of the plant «Yuzhicable works», cable, cable products.



С историей создания и развития завода «Южicable» связано становление отечественной кабельной промышленности. Предприятие – флагман отрасли. Его производственный потенциал и номенклатура выпускаемой продукции свидетельствуют об уникальных возможностях этого производства. Таким завод стал благодаря системному подходу к техническому перевооружению существующих мощностей, который здесь длится на протяжении последних десятилетий. Современное технологическое оборудование, новые цеха и участки обеспечивают изготовление конкурентоспособной продукции, пользующейся спросом как в Украине, так и за границей. Библ. 5.

Ключевые слова: история завода «Южicable», кабель, кабельная продукция.

Today the Plant «Yuzhicable works» is the leader of the Ukrainian cable industry. It recycles 40 % of the total volume of non-ferrous metals used in the domestic cable industry [1]. It is one of the ten largest producers of cable products in the CIS, it is the leading among the machine-building enterprises of Kharkiv in the production of marketable products [2]. Annually, the plant sells cable products worth more than USD 60 million.

«Yuzhicable works» did not begin immediately the modern, dynamically developing plant. This was preceded by 75 years of painstaking work of many generations of plant's workers, who built the first workshops, mastered the production of cables and wires necessary for the front and victory.

Looking at the modern look of the production buildings of the Kharkiv plant «Yuzhicable works», it is hard to believe that in those distant military and postwar years everything began on the abandoned outskirts of the city, where even before the Second World War, the foundation of the shops of enterprise No. 332 of the radio engineering industry – branch of the Kharkiv electromechanical plant was laid.

To create a large enterprise in Kharkiv, which received No. 804, the All-Union Administration «Glavcable» was appointed group of managers – plant Director G.A. Zybin, Chief Engineer V.I. Yuzefov and two experienced, qualified engineers N.V. Kudryavtsev and N.N. Garnier.

The new enterprise produced trial products on March 7, 1944. These several tens kilograms of winding and enamel wires were the first prototype production, so necessary for the front and the industrial enterprises that are being restored in Ukraine. People rejoiced at this event as something extraordinary.

By early 1946 the plant already had 286 units of various equipment. In addition to the three main workshops, they also commissioned own lacquer section, a spinneret. No matter how difficult it was, they also created a central plant laboratory for input control of raw materials and testing of finished products.

Considering the special importance of the plant's products for the construction of enterprises and housing in the country, on May 9, 1951, the Council of Ministers of the USSR revised and approved a new technical passport of the plant, after which the construction gained acceleration. Almost immediately the construction of the building No. 2 began – the winding wires workshop as well as the building No. 4 – the power cable workshop.

In 1954, their construction was completed. The equipment, mainly imported, came on schedule and was immediately mounted on production sites.

In the Soviet period, all the efforts of the labor collective were directed towards the fulfillment of the state plan. Export of goods was a significant part of the commodity output. Quality of cables with the brand «Yuzhicable works» was especially appreciated in many countries of the world.

About 20 % of the total output was exported to Cuba, Argentina, Vietnam, Mongolia, India, Iran, Iraq, Syria, Egypt, Romania, Angola, South Africa and many other countries. For example, enamel wires were shipped to Vietnam in large quantities, and power cables to India. In 1956 – 1959 in the Bhilai (State of Madhyapradesh, India), the USSR built a metallurgical plant. Almost all power cables used at this facility were branded with the «Yuzhicable works».

In this period, the enterprise management paid special attention to the development of the power cable workshop as a promising direction. This workshop was one of the first in the country where they installed a unique domestic hydraulic press for the application of aluminum shells П-958, mounted new, instead of old, paper insulation machines ИЖ-32Э and torsion-isolating machines, extrusion presses for applying plastic shells to power cables «Anduard-150» and «Anduard-200» and booking machines. This equipment made it possible to significantly increase labor productivity.

© V.M. Zolotaryov

In 1978, the consumer goods workshop was put into operation, which by that time was advanced in terms of technical equipment and production organization. It replaced a small section of consumer goods in the workshop of signal-blocking cables. Thanks to this, the plant was able to establish the manufacture of extension cords, various connectors, adapters, switches, which differed in high quality and reliability, which were in high demand not only among Kharkovites.

In the same year, the plant built wastewater treatment plants, such necessary for the purification of industrial wastewater. The enterprise became one of the first in Kharkiv, which put into operation such an environmental protection facility.

The crisis of the 80s and 90s brought certain adjustments to the plans for the technical development of the plant. They became a kind of exam, which the collective had to take. The destroyed planned system of supplying raw materials and materials, selling finished products forced the team to seek their own ways of solving the emerging problems. It was necessary not only to independently develop and mount the necessary equipment, but also to create new cable designs, which consumers so much need. For example, at that time the specialists of the plant successfully mastered the production of wires for water and oil submersible pumps.

In an effort to preserve the enterprise, in the early 90s the labor collective transferred to lease relations, and then, in 1995, initiated a change in the form of economic activity - the repurchase of the enterprise as an integral property complex.

In September 1995, a meeting took place, at which workers of the plant decided to create a closed joint-stock Company «Yuzhcable works».

The plant's incorporation by the labor collective gave a powerful impetus to the development of its production potential. The initiative, the indifference to what is happening, the conscientiousness, diligence of each worker, multiplied by common goals, soon yielded positive results. The enterprise overcame the crisis and began to develop rapidly. At that time, the strategy and tactics for the technical re-equipment of cable production was developed.

The first in the framework of this plan we put into operation an aluminum press ПЮ-741, which simplified the process of manufacturing conductive cores of power cables, and a high-performance drawing-string «Synchron».

Soon, without any outside investment, the plant was able to purchase from the well-known Austrian firm MAG two enamel aggregates. These new units are technically advanced, much more productive, environmentally safer than the equipment that was dismantled at the plant several years ago. Thus, the plant has restored this production already at a completely different, modern level.

It is necessary to emphasize that all services and divisions, all specialists of the Company, have been engaged in technical re-equipment and continue to be actively engaged from design to installation and commissioning. Since 2003, the plant almost every year

put into operation new production – a new workshop or site, new equipment [3].

It was this year that a large-scale project was successfully implemented to organize the production of power cables with XLPE insulation for voltage up to 110 kV at a cost of USD 9.4 million. In its framework, a new workshop with an area of 5000 m² was built on the territory of the plant.

High-tech equipment was purchased and put into operation:

- universal torsion machine of DRUM TWISTER type from Company «Pourtier» (France);
- inclined line of continuous vulcanization from the Company «Troester» (Germany);
- machine for twisting conductor cores of cables from the firm «Cortinovis» (Italy);
- extrusion line for the application of shells from the Company «Troester» (Germany);
- test equipment from firms «Hipotronics» (USA) and «Haefely» (Switzerland);
- torsion machine from the firm «Cortinovis» (Italy), where for the first time in the CIS the industrial production of sealed conductor wires with a section of up to 800 mm² with longitudinal sealing against the spread of moisture by waterblasting threads was mastered. This technology has significantly increased reliability and improved performance of power cables for medium and high voltage.

The implementation of this project in 2003 made it possible to refuse from importing expensive cables from world-famous manufacturers such as «Nexans», «Prysmian», and «Telefonika» to Ukraine.

At that time, some CIS cable plants were just beginning to work in this direction, and we already had a ready-made production facility for the production of cables with a voltage of up to 110 kV and a cross-section of the core up to 800 mm². Cables of these brands today are the most in demand in the world, reliable in operation and more simple for installation and maintenance [4, 5].

Just in time for development and implementation in mass production since 2003 of medium and high voltage domestic cables (6-110 kV), in 2007 the State Prize of Ukraine in the field of science and technology was awarded to the general Director of the Plant «Yuzhcable works», Candidate of Technical Sciences V.M. Zolotaryov, Candidates of Technical Sciences, Chief Engineer V.P. Karpushenko and leading specialists of the company – Yu.A. Antonets, L.G. Vasilets and A.F. Krivenko. This became a recognition of the merits of the plant's staff members in ensuring the energy security of the national economy.

In 2004, the team implemented a second investment project to create the production of fiber-optic communication cables. Equipment was purchased from the company «Nextrom» (Finland-Switzerland) was purchased. This is an optical fiber color line, an optical module manufacturing line, an SZ-twist line, an extrusion line for cable shielding, a cable rewind line and a test equipment set. Separate units of the lines were additionally equipped with the equipment from the

Companies «Weber & Schör» (USA), «Medek & Schörner» (Austria), «Sikora» (Germany) and other leading firms. The equipment also included a torsion machine from the firm «Proton & Products» (UK) for applying wire armor to the cable.

According to the technical specifications developed by the plant, the production of a wide range of fiber-optic cables began, which fully met the various needs of consumers.

The design capacity of the new workshop was 8,000 kilometers of fiber optic cable per year.

In 2006, a workshop was put in operation to produce self-supporting and protected wires of the CIII type. These wires are designed for transmission and distribution of electrical energy in overhead lines, as well as for branches to entrances to houses and outbuildings.

The use of the equipment of leading European companies in this workshop allowed to raise the quality of produced self-supporting insulated wires to the requirements of international Standards. In particular, the manufacture of a core with the use of a high-strength aluminum alloy has been mastered. It replaced the traditional designs of such wires, reinforced with steel wire. Such alloy is used in CIII, which are exported to the countries of near and far abroad.

With the increase in the nomenclature of manufactured cable products, it became necessary to organize modern insulating materials production at the plant. For this purpose, a scientific and technical center was created, whose workers, together with specialists of the central plant laboratory, develop materials for insulation, filling and shells, including special formulations.

In parallel with such research work, preparations were made for placing in the enterprise production of processing polymeric materials and working off formulations of individual materials for use in the drawing and signal-blocking cables workshops, as well as power cables. The creation of a new workshop with a complex technological cycle took the plant several years. The painstaking work of engineering services in this direction was crowned with success. Today the Plant «Yuzhcable works» has a workshop for processing polymeric materials, analogues of which are not available at other cable plants. Here work is carried out, starting from research and laboratory works and finishing with the industrial manufacture of finished products.

For this purpose we installed:

- line from the firm «Repkon» (Turkey) for the production of insulating and hose compositions of PVC plastic;
- multifunctional equipment from the firm «Ermafa» (Germany) for the manufacture of compositions of polyolefins (including silanol-crosslinked, light stabilized, fireproof). The line is equipped with computerized control of the technological process, including systems for formulating, transporting and dispensing ingredients of polymer compositions, maintaining process parameters, degassing of volatile products;
- equipment for the production of highly filled PVC and halogen-free polyolefin compositions from the firm

«X-Compound» (Switzerland). With the putting in operation of this equipment, the plant was able to fully provide its own production with highly-filled and halogen-free compounds.

Equipment of the workshop for processing polymeric materials with progressive equipment made it possible to use silanes here. This allowed the workshop to reach a whole new level in its development. After all, such high-tech industries are few in the CIS countries. They require not only sufficient investment, but also qualified personnel capable of mastering advanced technologies and further working on particularly complex equipment.

Economic analysis indicates that the prices of polyolefin compositions developed at the plant are 5 to 20 % lower than those of other manufacturers of similar products. This makes it possible to reduce the cost of the «Yuzhcable works» products as a whole and, thus, to receive certain preferences when selling it.

In addition to the production of insulating materials, the plant also organized the production of round anoxic billet from cathode copper by the method of ascending casting from the leading European firm «Upcast» (Finland), which allows to produce up to 10,000 tons of billets per year with a diameter of 8 to 20 mm.

This technology, which has almost 50 years of history, has proved to be a good choice for many manufacturers of cables and wires for various applications. Currently, there are more than 130 plants for the production of oxygen-free copper rod in the world using the method of continuous ascending casting.

This site is able to ensure a 100 % transition of the main workshops of the plant to the use of copper of its own production. The plant's capacity can flexibly vary according to needs.

In 2008, the «Yuzhcable works» successfully implemented one of its most ambitious projects: a new plant equipped with high-tech equipment was built by the plant workers to produce power cables with XLPE insulation for a voltage of 6 to 330 kV inclusive.

The construction of a new production was a natural result of the reaction of plant specialists to the world development trends of both domestic and global power systems. Every year the demand for high and ultra high voltage power cables is increasing. This is due to the implementation of major projects in energy, metallurgy, mining and the construction of megacities. The laying of such cable lines makes it possible to replace overhead power lines, which saves energy and ensures the reliability of its transmission.

Cables with XLPE insulation have long been widely used in the power systems of economically developed countries. For example, in the USA 85 % of power cables have polyethylene insulation, in Finland, France, Sweden, Germany and Japan only cables with polyethylene insulation are used. A number of power systems in Russia, Ukraine and other CIS countries also use such cables.

At the new site, the specialists of the plant installed:

- line of superimposition of screen elements on cables of the «DRUM TWISTER» type produced by the firm «Pourtier» (France);

- two lines of rough drawing of copper and aluminum wires from the firm «Niehoff» (Germany);
- line for rewinding and laying armored pouches made of steel tapes from the firm «Pourtier» (France);
- inclined line of continuous vulcanization from the firm «Maillefer» (Finland);
- machine for twisting conductors of aluminum and copper from the firm «Ceeco-Bartell» (USA);
- line of application of the outer shell from the firm «Maillefer» (Finland);
- test equipment, including two modular reactors, each providing a test voltage of 250 kV, from the firms «Hipotronics» (USA) and «Haefely» (Switzerland).

Specialists of the plant chose an energy-saving test technology with increased voltage based on a series resonance using a test facility from these companies. Today, in Ukraine only the «Yuzhcable works» has such a powerful facility. It also carries out tests to measure the level of partial discharges in each construction length of the cables, determine the tangent of the dielectric loss angle in insulation, the electrical resistance of the core and insulation.

To organize such a complex production, the plant built a new building with an area of 12000 m². This is the only such a high-tech and science-intensive production in the CIS with a capacity of 2000 kilometers of cable per year, taking into account the specialization of the workshop for the production of high and extra high voltage cables.

The volume of capital investments since the beginning of construction of a new workshop was USD 20 million.

In September 2010, the plant manufactured and tested 8.6 kilometers of XLPE insulated power cable for voltage of 330 kV for Berezovskaya TPP (Republic of Belarus). Such cable in the CIS countries was first manufactured at the «Yuzhcable works».

And in the beginning of 2011 all work on laying, installation and commissioning of the first in Belarus cable line for 330 kV has been completed.

This year, the «Yuzhcable works» has already produced and supplied 9.5 kilometers of power cable with XLPE insulation with an aluminum conductor of cross-section of 2000 mm² for 220 kV for the substation Kremenskaya, in the Lugansk region. As a result of military operations in the region, main and distribution power networks were damaged. The commissioning of this substation with the cable system from the «Yuzhcable works» will allow to synchronize the power supply system of the north of Donbass with the United Power System of Ukraine, which previously operated with a lower generation of the Lugansk TPP. The commissioning of the substation will enable the Severodonetsk Company «Azot» and the Lisichansk refinery to operate at full capacity.

Ultrahigh-voltage cables have successfully passed tests at the European testing center of the company «KEMA» (Netherlands), the plant received international quality certificates.

To work for consumers, take into account their wishes and needs – this is the rule that our Company is guided by in its activities.

For example, in Ukraine, the demand for winding wires has increased. To meet this demand, the plant bought a modern, high-performance two-way machine from the firm «Newtech» (Italy). In the shortest time, we assembled it, carried out commissioning and commissioned the production of wires with fiberglass insulation. The wires made on this machine have higher performance and reliability.

The «Yuzhcable works» takes an active part in the national program on import substitution. Increasing the range of cables produced, the Company thereby provides an opportunity for consumers in the Ukrainian market to choose between similar imported and domestic products, which sometimes are much better in quality than foreign ones and competitive in price.

It was within this program that the plant purchased new equipment for manufacturing low-voltage fire-proof cables and flexible household wires:

- from the firm «Niehoff» (Germany) 8-creek drawing machine MMN 121 for drawing copper wire in the range of diameters of 0.20 – 1.13 mm and three double-twisting machines D631 and D1001 for the production of high-quality flexible conductors of cross-section of 0.5 – 35 mm²;
- from the firm «Rosendahl» (Austria) two universal lines designed for insulating conductors with a cross-section of 0.50 – 35 mm² and for their twisting by the «SZ-twist» method with the simultaneous application of the inner and outer shells.

The plant received the certificates of the Institute for Testing and Certification VDE (Germany), Institute Innogy SE Eurotest (Germany) and the Research Institute of Energy IEn (Poland). Due to the huge work on adaptation of cables and wires with the brand «Yuzhcable works» to foreign Standards and requirements, the Company now exports its products to the CIS countries, the European Union, and also to the countries of Southeast Asia and the Middle East.

Our plant continued its active participation in the national import substitution program. It was decided to expand the range of products produced by manufacturing special-purpose cables that are in demand at nuclear power facilities, transport engineering enterprises, and also used in critical fire alarm and fire fighting systems.

During 2015-2016 the plant concluded contracts with leading foreign Companies for the supply of special technological equipment:

- line for the production of copper wire coated with tin by electrolytic tinning;
- two high-speed tape winding machines for applying insulation from glass-mica belts to conductive wires. Their introduction into production allows the enterprise, first of all, to master the production of fire-resistant control cables of small cross-sections with current-conducting wires of non-welded and tinned copper, and also of thermocouple alloys;
- two braiding machines and one cane machine for making copper and copper tin-plated wire screens.

The regulatory documentation for the manufacture of special-purpose cables by the plant's employees was developed, agreed upon and approved. Jointly with the representatives of the State Nuclear Security Center, the State Enterprise NAEC «Energoatom» and representatives of the three NPPs of Ukraine, the acceptance tests of the experimental lots of new products were successfully carried out. And these are control cables and small ones that have a number of technical advantages in terms of noise immunity, fire safety and corrosion resistance in comparison with traditionally used cables.

Taking into account the wishes of consumers and the rapid development of solar energy in the country, the specialists of the enterprise developed the design and in a short time mastered the production of cables for photovoltaic systems (solar power stations). These are single-core cables with flexible copper tin-plated cores. The insulation and shell of these cables are made of halogen-free cross-linked material.

The total amount of investments into the production of the plant in recent years has amounted to more than UAH 3 billion.

The implementation of projects for the technical re-equipment of production was largely made possible thanks to many years of close business cooperation between the plant specialists and the NTU «KhPI», in particular, with the Department for Electrical Insulation and Cable Technology, as well as with the staff of the Institute of Electrodynamics of the National Academy of Sciences of Ukraine.

Today the enterprise produces about 25 thousand markings of various cables, wires and cords. The «Yuzhcable works» is a recognized brand. The Company is well known in the countries of near and far abroad. The plant has a stable credit and financial history. The «Yuzhcable works» is one of the main participants of the International Associations «Electrocable» and «Intercable», which includes companies – world leaders in the manufacture of cables and wires, high-tech equipment, producers of raw materials for the cable industry.

How to cite this article:

Zolotaryov V.M. Plant «Yuzhcable works»: milestones of the road (75th anniversary of the plant «Yuzhcable works»). *Electrical engineering & electromechanics*, 2018, no.5, pp. 12-16. doi: 10.20998/2074-272X.2018.5.02.

The basis for the stable development of the «Yuzhcable works» is a successfully operating quality management system in accordance with the requirements of ISO 9001 and the environmental management system in accordance with the requirements of ISO 14001, which have been recertified according to the new version of the 2015 Standards.

The main wealth of the plant is its labor collective. The 75-year history of the plant shows that the plant's team has always successfully solved and will continue to solve the problems arising before it, achieving the set goals.

REFERENCES

1. Zolotaryov V.M., Zhernovnykov V.M., Karpushenko V.P., Kryvenko A.F., Kudryavtseva R.I. *Zavodu «Yuzhkabel'» 60: Stranitsy istorii trudovogo kollektiva* [Yuzhcable works 60: history pages of the labor collective]. Kharkiv, Maydan Publ., 2003. (Rus).
2. Zolotaryov V.M. The seventy years history of plant «Yuzhcable». *Electrical engineering & electromechanics*, 2013, no.4, pp. 4-9. doi: 10.20998/2074-272X.2013.4.01.
3. Zolotaryov V.M., Shcherba M.A., Guryn A.G., Suprunovska N.I., Chopov E.Yu., Oboznyi A.A. *Elektrotekhnologicheskii kompleks proizvodstva kabel'nykh sistem na napriazhenie do 400 kV* [Electrotechnological complex of production of cable systems for voltage up to 400 kV]. Kyiv, Pro Format Publ., 2017. 594 p. (Rus).
4. Zolotaryov V.M. Private Joint-stock company Yuzhcable works – 70 years. *Cables and wires*, 2013, no.4, pp. 34-35. (Rus).
5. Antonets Yu.A. Power cables with XLPE insulation for voltage 20 kV for distribution networks of electric power systems. *Electrical networks and systems*, 2016, no.4-5, pp. 37-41. (Rus).

Received 10.08.2018

V.M. Zolotaryov, Doctor of Technical Science, Professor,
Private Joint-stock company Yuzhcable works,
7, Avtogenskaya Str., Kharkiv, 61099, Ukraine,
phone +380 57 7545248,
e-mail: zavod@yuzhcable.com.ua

V.F. Bolyukh, Yu.A. Kashanskij, A.I. Kocherga, I.S. Schukin

INVESTIGATION OF LINEAR PULSE ELECTROMECHANICAL CONVERTER OF INDUCTION TYPE WITH DOUBLE ARMATURE INTENDED FOR DESTROYING INFORMATION ON SSD STORAGE DEVICE

Purpose. The goal of the paper is to determine the influence of the linear pulse electromechanical converter (LPEC) parameters with a double armature on its electrical, power and temperature indices and experimental verification of the proposed design for an information destruction device in a flat SSD storage device. **Methodology.** Using the mathematical model that takes into account interrelated electrical, magnetic, thermal and mechanical processes, the influence of geometric parameters on the electrodynamic characteristics and the indices of the induction type LPEC with a double armature spanning the inductor from opposite sides is investigated. **Results.** It is shown that the currents in the inductor and armature change in accordance with the oscillation-damping law practically in antiphase. The maximum value of the current density in the inductor is 215.8 A/mm^2 , and in each of the identical parts of the double armature it is 299.7 A/mm^2 . The maximum value of electrodynamic forces (EDF) acting in opposite directions on the front and rear of the double armature is 11.99 kN , and the value of the EDF pulse is $4.59 \text{ N}\cdot\text{s}$. **Originality.** It is established that with axial removal of the rear part of the armature from the inductor, the maximum current densities in the inductor decrease, in the front part of the armature increase, and in the rear part of the armature decrease. The maximum value and the pulse of the EDF between the armature parts decrease. With an increase in the number of turns in the inductor and a decrease in the thickness of the copper bus, all the basic indicators of the LPEC increase. With an increase in the number of turns of the inductor from 26 to 56, the maximum EDF value acting between the parts of the armature increases almost 3 times, and the magnitude of the EDF pulse is 3.3 times. With an increase in the width of the copper bus and the width of the inductor, the main indicators of the LPEC decrease. With an increase in the width of the inductor from 10 mm to 20 mm, the maximum EDF between the armature parts decreases by 1.3 times, and the value of the EDF pulse decreases by 1.2 times. **Practical value.** Based on the conducted studies, an induction-type LPEC model with a double armature was designed and tested experimentally, designed to destroy information located on a solid-state digital SSD storage device. References 14, figures 9.

Key words: linear pulse electromechanical converter of induction type, double armature, electrodynamic processes, digital SSD storage device, experimental sample.

При помощи математической модели, учитывающей взаимосвязанные электрические, магнитные, тепловые и механические процессы исследовано влияние геометрических параметров на электродинамические характеристики и показатели линейного импульсного электромеханического преобразователя (ЛИЭП) индукционного типа с двойным якорем, охватывающим индуктор с противоположных сторон. При аксиальном удалении задней части якоря от индуктора максимальные плотности токов в индукторе уменьшается, в передней части якоря увеличивается, а в задней части якоря уменьшается. Максимальная величина и импульс электродинамических усилий (ЭДУ) между частями якоря уменьшаются. При увеличении числа витков индуктора и уменьшении толщины медной шины происходит увеличение всех основных показателей ЛИЭП. При увеличении числа витков индуктора от 26 до 56 максимальная величина ЭДУ, действующая между частями якоря, возрастает практически в 3 раза, а величина импульса ЭДУ в 3,3 раза. При увеличении ширины медной шины и ширины индуктора происходит уменьшение основных показателей ЛИЭП. При увеличении ширины индуктора от 10 мм до 20 мм максимальная величина ЭДУ между частями якоря уменьшается в 1,3 раза, а величина импульса ЭДУ уменьшается в 1,2 раза. На основании проведенных исследований был разработан и экспериментально испытан образец ЛИЭП индукционного типа с двойным якорем, предназначенный для уничтожения информации, размещенной на цифровом SSD накопителе. Библ. 14, рис. 9.

Ключевые слова: линейный импульсный электромеханический преобразователь индукционного типа, двойной якорь, электродинамические процессы, цифровой SSD накопитель, экспериментальный образец.

Introduction. Linear pulse electromechanical converters (LPECs) of induction type are widely used to create shock-mechanical pulses [1-4]. Such converters are used in many branches of science and technology as shock-power devices. In construction, electromagnetic hammers and perforators are used; in the mining industry – devices to beat the butt and vibrators; in geological prospecting – vibroseismic sources; in mechanical engineering – hammers with a large range of impact energy and devices for electrodynamic treatment of welded joints; in the chemical and medical-biological industry – vibromixers, metering devices, etc. LPECs are used in test complexes for testing critical equipment for shock loads, in magnetic-pulse devices for pressing

ceramics powders, for cleaning containers from sticking loose materials [4-6]. One of the promising areas is the use of LPECs to destroy information on digital storage devices at unauthorized access [7]. Such LPECs should have a high speed and short working cycle, limited by mass and dimensions, autonomy and develop high shock- mechanical loads. The problem acquires an increased complexity in the destruction of information distributed over the surface of a flat solid state SSD storage device [8].

The most promising for solving this problem is the inductive type LPEC, in which the electrically conductive armature interacts electroodynamically with the stationary

inductor [4, 9, 10]. When a multiturn inductor is excited from a capacitive energy storage (CES) device, eddy currents are induced in the electrically conducting armature. As a result of this, the electrodynamic forces (EDFs) of repulsion act on the armature, causing its axial movement together with the impact actuator (striker) relative to the inductor.

However, with a rapid change in electromagnetic, mechanical and thermal parameters, the power indices of the induction-type LPEC of traditional design are not high enough [4]. One of the ways to increase these indicators is the development of new LPEC designs. Since in the traditional LPEC design, only one side of the inductor interacts inductively with an armature, a significant part of the magnetic field from the opposite side of the inductor is scattered into the surrounding space, adversely affecting closely located electronic and biological objects, and is not used to create additional EDFs.

Let us consider the design of the LPEC of a coaxial configuration, containing a fixed inductor 1 and a double armature, enclosing the inductor from opposite sides [8] (Fig. 1).

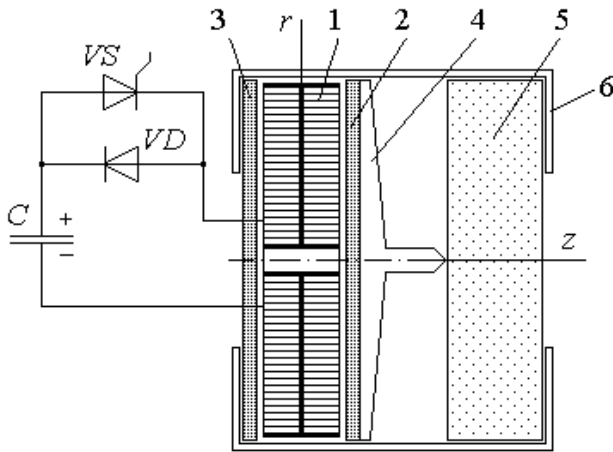


Fig. 1. LPEC with double armature: 1 – inductor; 2 – FPA; 3 – BPA; 4 – striker; 5 – object of action; 6 – fixing clips

The front part of the armature (FPA) 2 and the back part of the armature (BPA) 3 are made in the form of coaxially mounted disks covering the inductor from opposite sides. A striker 4 is connected to the FPA 2, directed towards the object of action 5. The BPA 3 and the object of action 5 on the outer surface are covered by fixing clips 6. Note that the outer electrically conductive screen can play the role of one of the parts of this armature [11].

When a signal is applied to the thyristor VS , the current excites a stationary inductor from the CES C , and due to the emerging magnetic field, eddy currents are induced in each of the parts of the double armature. As a consequence, oppositely directed EDFs of repulsion act on both sides of the double armature on the inductor side, which leads to the total force action of the striker on the object of action. Due to the use of the VD diode, the excitation of the inductor is carried out by a multi-polar

pulse, at which the oscillating-damped character of the current variation is realized.

However, this raises the question of the influence of the parameters of the inductor and the location of the parts of the double armature on the power parameters of the LPEC.

The goal of the paper is determination of ways to increase the power characteristics of a linear pulse electromechanical converter of induction type with a double armature, designed to destroy information in a flat solid state SSD storage device.

Mathematical model. We consider a mathematical model that describes the electromechanical processes of LPEC using the lumped parameters of the active elements – the inductor and the movable parts of the double armature. Electrical processes can be described by a system of equations:

$$i_1 R_1(T_1) + L_1 \frac{di_1}{dt} + \frac{1}{C} \int i_1 dt + \sum_{n=2,3} \left(M_{1n}(z) \frac{di_n}{dt} + i_n e_m \right); \quad (1)$$

$$\frac{1}{C} \int_0^t i_1 dt = U_0; \quad (2)$$

$$i_n R_n(T_n) + L_n \frac{di_n}{dt} + M_{1n}(z) \frac{di_1}{dt} + M_{nm}(z) \frac{di_m}{dt} + i_1 e_3 + i_m e_1 = 0; \quad (3)$$

where $p = 1, 2, 3$ are the indexes of the inductor, FPA and BPA, respectively; $m = 5 - n$; $n = 2, 3$; $e_1 = (v_{12}(t) + v_{13}(t)) \frac{dM_{23}}{dz}$; $e_2 = v_{13}(t) \frac{dM_{13}}{dz}$; $e_3 = v_{12}(t) \frac{dM_{12}}{dz}$; $R_p(T_p)$, L_p , i_p , T_p are the resistance, inductance, current and temperature of the p -th active element, respectively; $M_{12}(z)$, $M_{13}(z)$, $M_{23}(z)$ are the mutual inductances between the corresponding p -th active elements; $v_{13}(t)$, $v_{12}(t)$ are the oppositely directed speeds of the BPA and the FPA relative to the inductor along the z axis, respectively.

The solution of equations (1) – (3) for currents in active elements is presented in [12].

Electrodynamics processes can be described by a system of equations:

$$i_1 \frac{dM_{1n}}{dz} = i_n \frac{dM_{nm}}{dz} + (m_n + m_e) \frac{dv_{1n}}{dt} + K_T v_{1n}(t) + 0.125 \pi \gamma_a \beta_a D_{2\max}^2 v_{1n}^2(t) + K_P \Delta z_{1n}(t), \quad (4)$$

where $\Delta z_{13}(t)$, $\Delta z_{12}(t)$ are the oppositely directed movements of the BPA and the FPA relative to the inductor along the z axis; m_2 , m_3 , m_e are the masses of the FPA, the BPA and the striker, respectively; K_T is the coefficient of dynamic friction; γ_a is the density of medium of displacement; β_a is the aerodynamic resistance coefficient; $D_{ex\ m}$ is the maximum armature diameter; K_P is the coefficient of rigidity of the object of action.

The displacements of the BPA and the FPA relative to the inductor can be represented in the form of recurrence relations:

$$\Delta z_{1n}(t_{k+1}) = \Delta z_{1n}(t_k) + v_{1n}(t_k)\Delta t + \frac{\Delta t^2}{2(m_n + m_e)} \times$$

$$\times \left[\left(i_1(t_k) \frac{dM_{1n}}{dz} - i_2(t_k) \frac{dM_{nm}}{dz} \right) i_n(t_k) - K_T v_{1n}(t_k) - \right. \quad (5)$$

$$\left. - 0.125 \cdot \pi \cdot \beta_a \gamma_a D_{exn}^2 v_{1n}^2(t_k) - K_p \Delta z_{1n}(t_k) \right].$$

A method for calculating the interrelated electric, magnetic, thermal, and electrodynamic processes with allowance for various nonlinear dependences is described in [12].

As indicators of LPIEC with a double armature we will use:

- the amplitude of the axial EDF f_{z23m} acting on the fixing clips from the oppositely directed forces on the front and back parts of the double armature $f_{z23m} = f_{z2m} - f_{z3m}$, where f_{z2m} , f_{z3m} are the amplitudes of the EDFs acting on the FPA and the BPA, respectively;
- the value of the EDF pulse $F_{z23m} = F_{z2m} - F_{z3m}$ acting on the fixing clips from oppositely directed forces on the front and back parts of the double armature, where F_{z2m} , F_{z3m} are the amplitudes of the EDF pulses acting on the FPA and the BPA, respectively; impulse $F_z = \int f_z(t) dt$;
- maximum values of current densities in the inductor j_{1m} , FPA j_{2m} , and BPA j_{3m} ;
- rise of the temperatures of the inductor $\theta_1 = T_1 - T_0$, FPA $\theta_2 = T_2 - T_0$, and BPA $\theta_3 = T_3 - T_0$, where T_1 , T_2 , T_3 are the temperature of the inductor, FPA and BPA, respectively; T_0 is the ambient temperature.

The main parameters of the LPEC. Let us consider the LPEC of a coaxial configuration in which both parts of the double armature are identical and are made in the form of a flat disc of technical copper, one of whose sides faces the inductor.

The LPEC has the following initial parameters:

Inductor: outer diameter $D_{ex1}=100$ mm, inner diameter $D_{in1}=10$ mm, height $H_1 = 10$ mm, section of copper bus $a \times b = 1.8 \times 4.8$ mm², the number of turns of the bus $N_1 = 46$ pcs. The inductor is made in the form of a double-layer winding with external electrical terminals.

Parts of the armature: outer diameter $D_{ex2,3}=100$ mm, inner diameter $D_{in2,3}=10$ mm, height $H_{2,3}=3$ mm.

CES: capacitance $C=500$ μ F, voltage $U_0=1$ kV.

The striker has a mass $m_e=0.45$ kg; coefficient of rigidity of the object of action $K_p=3 \cdot 10^7$ N/m. Such stiffness is characteristic for the object of action like the digital SSD storage device when the sharpened striker is acts on it.

Let us consider an excitation circuit that provides a vibrationally damped character of the change in the excitation current of the inductor, at which the highest electrodynamic indices of the LPEC are realized (Fig. 1) [13].

Electrodynamic characteristics and indicators of LPEC with a double armature. Let us consider the influence of geometric parameters on the electromechanical processes of a LPEC of induction type with a double armature. Fig. 2 shows the current densities

in the inductor j_1 and in both parts of the armature $j_2=j_3$, the value of f_{z23} and the impulse F_{z23} of EDF acting between the front and back parts of the double armature for the LPEC with the initial parameters.

In this LPEC, the currents in the inductor and armature change in an oscillatory-damped law almost in antiphase. The maximum value of the current density in the inductor is $j_{1m}=215.8$ A/mm², and in each of the identical parts of the double armature – $j_{2m}=j_{3m}=299.7$ A/mm². EDFs have the form of damped polar pulses, the repetition frequency of which is almost 2 times higher than the oscillation frequency of the inductor current. The maximum value of the EDF acting in opposite directions on the front and back of the double armature is $f_{z23m}=11.99$ kN. And the magnitude of the EDF impulse between the parts of the double armature is $F_{z23}=4.59$ N·s. At the end of the action of the current pulses, the inductor's temperature rise is $\theta_1=0.4$ °C, and the temperature rise of the armature parts is $\theta_2 = \theta_3 = 0.17$ °C.

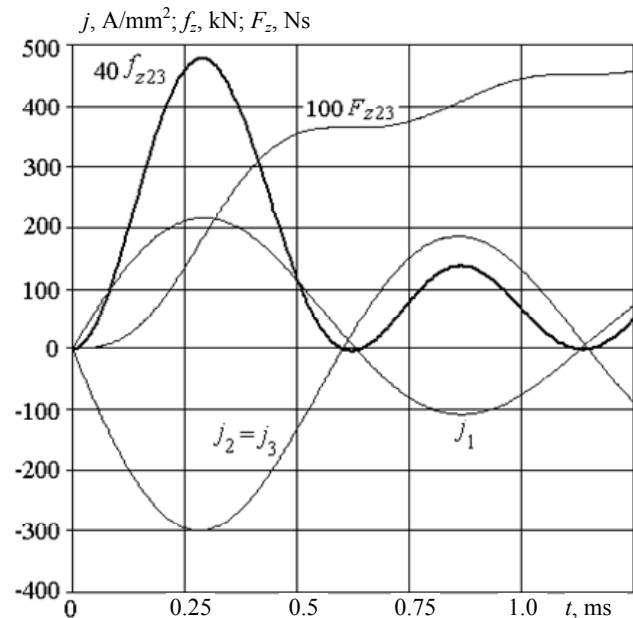


Fig. 2. Electrodynamic indicators of the LPEC with initial parameters

With the axial removal of the BPA from the inductor by a distance $\Delta z_{13}=6$ mm, the following changes are observed (Fig. 3). The current in the FPA by the end of the first half-period is somewhat ahead of the inductor current, while the current in the BPA is almost in antiphase with it. In comparison with the LPEC with the initial parameters, in this case the maximum current density in the inductor j_{1m} decreases by 1.06 times, in the FPA j_{2m} increases by 1.05 times, and in the BPA j_{3m} decreases by 1.92 times. As a result, the maximum EDF value acting on the FPA f_{2m} increases by 1.07 times, on the BPA f_{3m} decreases by 4.55 times, which leads to a reduction of the total forces f_{z23m} by 1.55 times.

The EDF impulse F_{z2} acting on the FPA increases by 1.05 times, on the BPA F_{z3} decreases by 4.73 times, which leads to a decrease in the total EDF impulse between the armature parts F_{z23} by 1.58 times.

For a given LPEC, the temperature rise of the inductor θ_1 decreases by 1.33 times, of the FPA θ_2 increases by 1.075 times, and of the BPA θ_3 decreases by 4 times.

Fig. 4 shows the dependence of the electrodynamic parameters of the LPEC with a double armature upon removal of the BPA from the inductor. When removing the BPA from the inductor by a distance of 8 mm, the maximum current density in the inductor decreases by 1.07 times, in the FPA increases by 1.1 times, in the BPA decreases by 2.91 times.

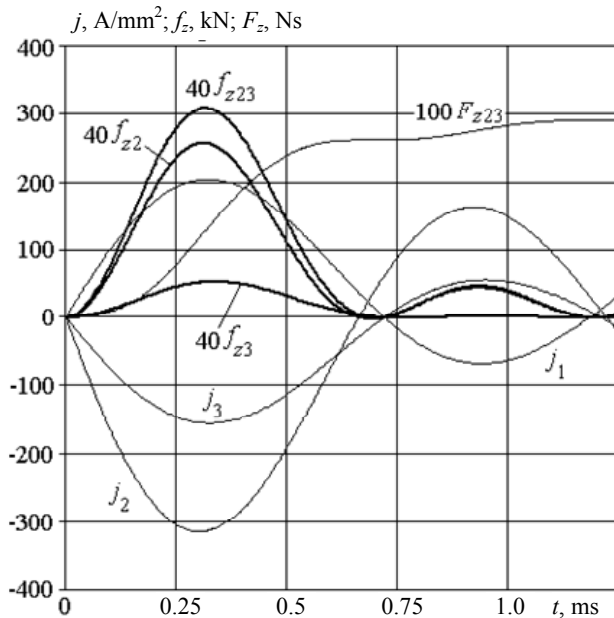


Fig. 3. Electrodynamic indicators of the LPEC, in which the BPA is removed by a distance $\Delta z_{13} = 6$ mm from the inductor

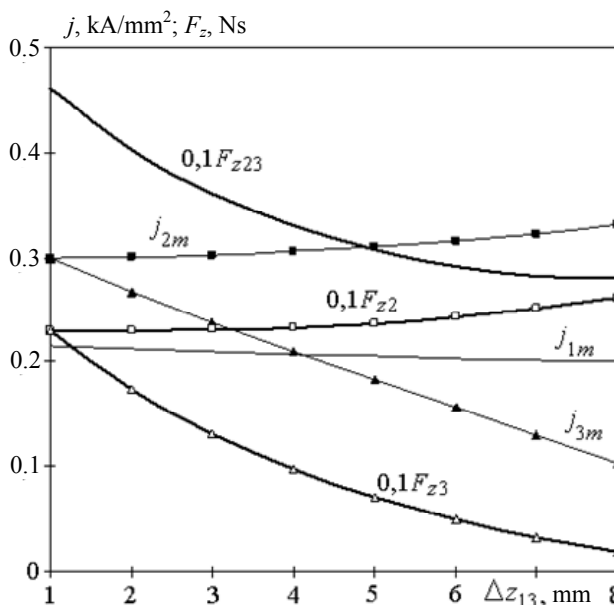


Fig. 4. Dependence of electrodynamic indicators of the LPEC on the removal of the BPA from the inductor by a distance Δz_{13}

The maximum value of the EDF f_{2m} acting on the FPA increases by 1.17 times, on the FHM f_{3m} decreases by 13.12 times, which leads to a reduction of the total forces f_{23m} by 1.62 times. The impulse of the EDF F_{z2} acting on the FPA increases by 1.14 times, on the BPA

F_{z3} it decreases by 12.1 times, which leads to a decrease in the total EDF impulse F_{z23} by 1.64 times.

In this case, the temperature rise of the inductor θ_1 decreases by 1.16 times, of the FPA θ_2 increases by 1.18 times, and on the BPA θ_3 decreases by 6.63 times.

Let us consider the effect of the geometric parameters of the inductor on the indicators of LPEC with a double armature. One such indicator is the thickness of the copper bus b , which affects the number of turns of the inductor N_1 . If the bus has a section $a \times b = 6.8 \times 2.6$ mm², then the inductor has $N_1 = 26$ turns. If the bus has a section $a \times b = 6.8 \times 1.4$ mm², then the inductor has $N_1 = 56$ turns. With an increase in the number of turns of the inductor N_1 , and therefore with a decrease in the thickness of the copper bus b , all the main indicators of the LPEC increase (Fig. 5). With an increase in the number of turns of the inductor from 26 to 56, the maximum current density in the inductor j_{1m} increases by 1.5 times, and in both parts of the armature $j_{1m} = j_{3m}$ in 1.73 times.

This leads to the fact that the maximum EDF value f_{23m} acting between the armature parts increases almost 3 times, and the value of the EDF impulse F_{z23} by 3.3 times. However, in this case, the temperature rise in the inductor θ_1 increases by 2.82 times, and for both parts of the armature $\theta_2 = \theta_3$ by 3.37 times at the end of the working cycle.

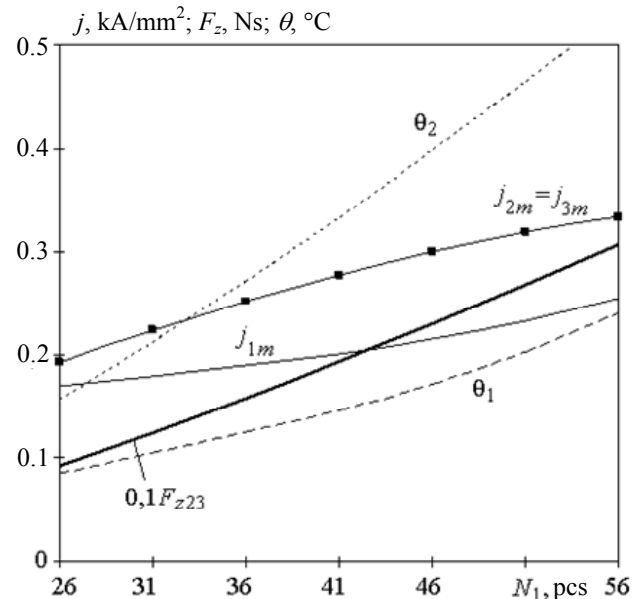


Fig. 5. Dependence of electrodynamic and thermal indicators of the LPEC on the number of turns of the inductor N_1

With an increase in the width of the copper bus, and hence the width of the inductor, the main indicators of the LPEC decrease (Fig. 6). With an increase in the width of the copper bus a from 4.8 mm to 9.8 mm, and hence the width of the inductor H_1 from 10 mm to 20 mm, the following regularities can be noted. The maximum current density in the inductor j_{1m} decreases significantly (more than 2 times), and the maximum current densities in both parts of the armature $j_{2m} = j_{3m}$ decrease insignificantly (by 1.1 times). The maximum value of EDF f_{23m} between the armature parts decreases by 1.3 times, and the value of the EDF impulse F_{z23} decreases by 1.2 times. In this case, the rise of the

temperatures of the inductor θ_1 decreases significantly (almost 4 times), and the temperature rise of the armature $\theta_2 = \theta_3$ decreases insignificantly (by 1.1 times).

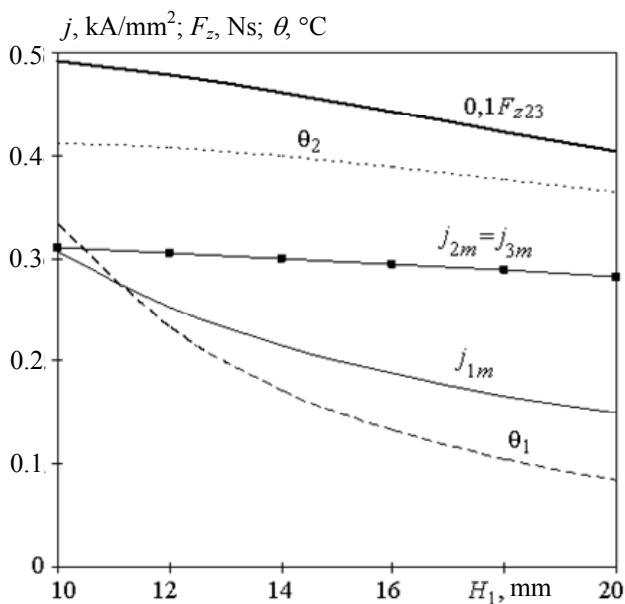


Fig. 6. Dependence of electrodynamic and thermal indicators of the LPEC on the width of the inductor H_1

Design and sample of LPEC for destroying information on the SSD storage device. Based on the conducted research, the design of the LPEC designed to destroy information located on a solid-state digital SSD storage device with surface distributed memory is developed [8].

The device consists of an inductor 1 in the form of two windings 1a and 1b with external electrical terminals 2, between which is located the inductor nonmetallic plate 3 (Fig. 7). The windings of the inductor 1 made in the form of an oval are wound according to the magnetic field from a single ribbon wire and are connected with an inductor plate 3 by means of an epoxy resin.

The device contains an FPA 4 and BPA 5. The inductor 1 is fixed to the object of action – the digital SSD storage device 6 by means of a fixing clip 7 covering their rectilinear sections. The front part of the fixing clip 7a covers the digital storage device 6, and the back part of the clip 7b covers the BPA 5. The parts of the clip are fixed with each other using detachable locks 8.

The impact actuator comprises orderedly arranged sharpened strikers 9 in the form of hardened nails. The hat of each striker is located between the FPA 4 and the impact plate 10, and the striker cores are in the form of a tapered cone and fixed in the holes of the impact plate 10. The FPA 4 and the impact plate 10 are interconnected. FPA 4, BPA 5, inductor plate 3 and shock plate 10 are made in the form of rectangles, which corresponds to the form of a digital SSD storage device 6.

In the angular parts of the inductor plate 3, the guide rails 11 perpendicularly are fixed, which pass through the guide holes of the FPA, the BPA and the impact plate 10.

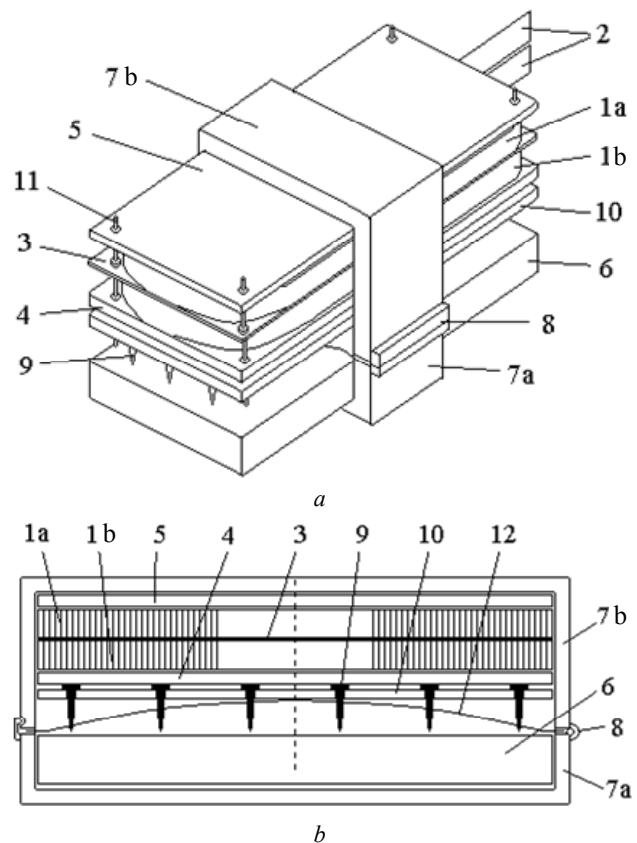


Fig. 7. General view (a) and cross-section (b) of LPEC to destroy information on the SSD storage device

The guide rails are connected to the inductor plate 3. The device comprises a flat spring 12 whose middle part interacts with the shock plate 10 and its ends are fixed relative to the back and front parts of the clip in detachable locks 8. In the initial state of the spring 12, its middle part presses the shock plate 10 together with the FPA 4 to the winding of the inductor 1b, and the winding 1a to the BPA 5.

If it is necessary to destroy information placed on a solid-state digital SSD storage device, for example, when a signal is received about unauthorized access to its information, a capacitive energy storage device is discharged to the inductor. In this case, the shock plate 10 moves with the strikers 9, which penetrate into the digital storage device 6, irrevocably destroying the information on it.

In addition, FPA and BPA screen the magnetic field excited by the inductor, which is favorable for closely located electronic and biological objects [14].

Based on the studies carried out, an experimental LPEC model of an induction type with a double armature was developed.

To conduct experimental studies of the LPEC, a diode-thyristor block, an electronic pulse generating unit with capacitors, a battery and a trigger device were used (Fig. 8,a). In experimental studies, a multilayered structure was used as the object of the impact, made of thin steel sheets backed by sheets of particleboard and fiberglass. Such a design made it possible to visually assess the penetration depth of the strikers into the object of action. As shown by experiments, after the

operation of the LPEC, the striker effectively penetrated almost the entire object of action.

Fig. 9 shows a prototype of LPEC of an induction type with a double armature, designed to destroy information on the SSD storage device and the results of its impact on the multilayer sample.

In the test sample, the inductor was covered with a decorative black film and the fixing clips were improved, which served as the outer casing and fully covered the object of action and the BPA.

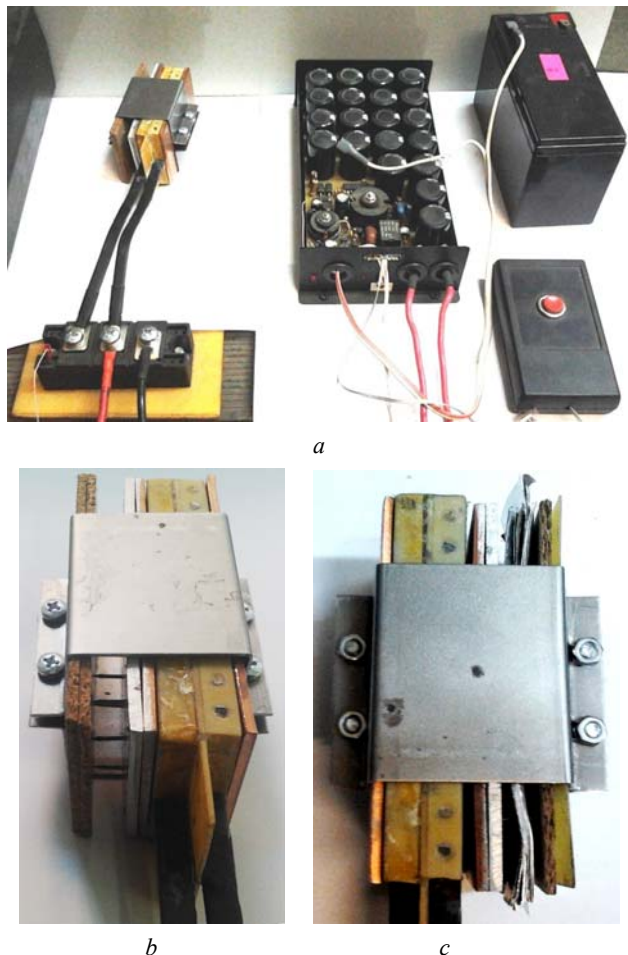


Fig. 8. Equipment for LPEC test (a), experimental LPEC sample in the initial position (b) and after operation (c)

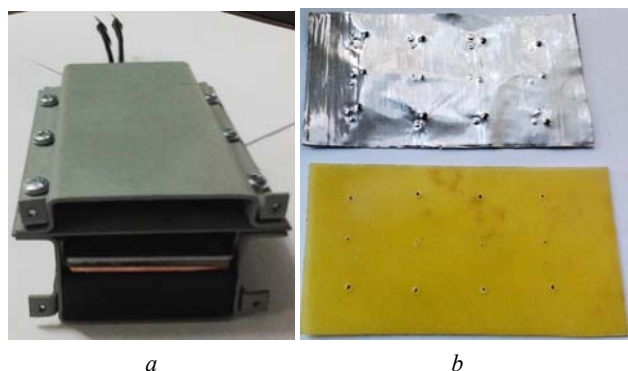


Fig. 9. A LPEC prototype for destroying information on the SSD storage device (a) and the results of its impact on a multilayer sample (b)

Conclusions.

1. Using the mathematical model that takes into account interrelated electrical, magnetic, thermal and mechanical processes, the influence of geometric parameters on the electrodynamic characteristics and indices of the LPEC of the induction type with a double armature covering the inductor from opposite sides was established.

2. The ways of increasing the power indexes of the LPEC are determined – the maximum value and the impulse of the electrodynamic forces between the parts of the double armature. It was established for the first time that the power indexes of the LPEC increase with the maximum approach of both parts of the double armature to the inductor, with an increase in the number of turns and the invariable dimensions of the inductor, with a decrease in the width of the copper bus and the width of the inductor.

3. An induction type LPEC model with a double armature designed to destroy information located on a solid-state digital SSD storage device was developed and experimentally tested.

REFERENCES

1. Tomashevsky D.N., Koshkin A.N. Modeling of linear impulse electric motors. *Russian Electrical Engineering*, 2006, no.1, pp. 24-27. (Rus).
2. Ivashin V.V., Penchev V.P. Features of the dynamics of work and energy diagrams of pulsed electromagnetic drive with parallel and series connection of excitation windings. *Electrical engineering*, 2013, no.6, pp. 42-46. (Rus).
3. Bolyukh V.F., Luchuk V.F., Rassokha M.A., Shchukin I.S. High-efficiency impact electromechanical converter. *Russian electrical engineering*, 2011, vol.82, no.2, pp. 104-110. doi: 10.3103/s1068371211020027.
4. Bolyukh V.F., Shchukin I.S. *Lineinye induktsionno-dinamicheskie preobrazovateli* [Linear induction-dynamic converters]. Saarbrücken, Germany, LAP Lambert Academic Publ., 2014. 496 p. (Rus).
5. Ivanov V.V., Paragin S.N., Nozdrin A.A. Semiautomatic installation of magnetic pulse compaction of powders. *Materialovedenie*, 2011, no.7, pp. 42-45. (Rus).
6. Young-woo Jeong, Seok-won Lee, Young-geun Kim, Hyun-wook Lee. High-speed AC circuit breaker and high-speed OCD. *22nd International Conference and Exhibition on Electricity Distribution (CIRED 2013)*, 2013, 10-13 June, Stockholm, Paper 608. doi: 10.1049/cp.2013.0834.
7. Bolyukh V.F., Shchukin I.S. High-performance electromechanical and electromagnetic pulse devices for destruction of information on digital drives. *Electrical engineering and electromechanics*, 2015, no.5, pp. 36-46. (Rus). doi: 10.20998/2074-272x.2015.5.05.
8. Bolyukh V.F., Luchuk V.F., Shchukin I.S. *Ustroystvo unichtozheniia informatsii, razmeshchennoi na tverdotel'nom tsifrovom SSD nakopitele* [A device for destroying information located on a solid state digital SSD drive]. Patent Russian Federation, no. 2654163, 2018. (Rus).
9. Bissal A., Magnusson J., Engdahl G. Comparison of two ultra-fast actuator concept. *IEEE Transactions on Magnetics*, 2012, vol.48, no.11, pp. 3315-3318. doi: 10.1109/tmag.2012.2198447.
10. Schneider Electric Industries SAS. *Electric switching device with ultra-fast actuating mechanism and hybrid switch comprising one such device*. Patent USA, no.8686814, 2014.
11. Bolyukh V.F., Dan'ko V.G., Oleksenko S.V. The Effect of an External Shield on the Efficiency of an Induction-Type

Linear-Pulse Electromechanical Converter. *Russian Electrical Engineering*, 2018, vol.89, no.4, pp. 275-281. doi: **10.3103/s106837121804003x**.

12. Bolyukh V.F., Kocherga A.I., Schukin I.S. Investigation of a linear pulse-induction electromechanical converter with different inductor power supply circuits. *Electrical engineering & electromechanics*, 2018, no.2, pp. 11-17. (Rus). doi: **10.20998/2074-272X.2018.2.02**.

13. Bolyukh V.F., Kocherga A.I., Schukin I.S. Investigation of a linear pulse-induction electromechanical converter with different inductor power supply circuits. *Electrical engineering & electromechanics*, 2018, no.1, pp. 21-28. (Rus). doi: **10.20998/2074-272X.2018.1.03**.

14. Bolyukh V.F., Kocherga A.A., Shchukin I.S. Comparative analysis of constructive types of combined linear pulse electromechanical converters. *Technical electrodynamics*, 2018, no.4, pp. 84-88. (Ukr). doi: **10.15407/techned2018.04.084**.

V.F. Bolyukh¹, Doctor of Technical Science, Professor,
Yu.A. Kashanskij¹, Master of Science,
A.I. Kocherga¹, Postgraduate Student,
I.S. Schukin², Candidate of Technical Science, Associate Professor,

¹ National Technical University «Kharkiv Polytechnic Institute»,
2, Kyrpychova Str., Kharkiv, 61002, Ukraine,
phone +380 57 7076427,
e-mail: vfbolyukh@gmail.com

² Firm Tetra, LTD,
2, Kyrpychova Str., Kharkiv, 61002, Ukraine,
phone +380 57 7076427,
e-mail: tech@tetra.kharkiv.com.ua

Received 22.06.2018

How to cite this article:

Bolyukh V.F., Kashanskij Yu.A., Kocherga A.I., Schukin I.S. Investigation of linear pulse electromechanical converter of induction type with double armature intended for destroying information on SSD storage device. *Electrical engineering & electromechanics*, 2018, no.5, pp. 17-23. doi: **10.20998/2074-272X.2018.5.03**.

ELECTRIC GENERATOR IN THE RECUPERATION SYSTEM OF THE ENERGY FROM MECHANICAL OSCILLATIONS IN VEHICLES

The paper deals with the system of mechanical energy recuperation of vehicles in the useful electric energy accumulated in the rechargeable battery. This system creates an additional power supply on board of the vehicle and, based on the principle of energy conservation, increases the efficiency of the use of the fuel of the primary engine. One of the main elements of such system is an electric generator, which transforms the mechanical energy of the oscillations of the vehicle's chassis into electric energy. The problem of choosing and optimizing the design and parameters of the generator is considered in the paper. Given the peculiarities of the functioning of the vehicle, the most appropriate type of generator in such system is a synchronous generator with permanent magnet, which has significant structural differences from conventional synchronous machines with permanent magnets. The criterion for optimizing the generator is the largest value of the effective value of the EMF, which is induced in the stator winding. On the basis of simulation results, based on the field mathematical model, a set of values of generalized coefficients that characterize the optimal generator geometry is obtained. References 4, table 1, figures 7.

Key words: electric energy recuperation system, synchronous generator, permanent magnets, mathematical model.

В статье рассматривается система рекуперации энергии механических колебаний транспортных средств в электроэнергию, которая накапливается в аккумуляторной батарее. Одним из основных элементов такой системы является электрогенератор, который преобразует механическую энергию колебаний шасси транспортного средства в электроэнергию. Также рассмотрена проблема выбора и оптимизации конструкции и параметров генератора. Учитывая особенности функционирования транспортного средства наиболее целесообразным типом генератора в такой системе является синхронный генератор с постоянными магнитами, который имеет существенные конструктивные отличия от традиционных синхронных машин с постоянными магнитами. Критерием оптимизации генератора является наибольшая величина действующего значения ЭДС, индуцированной в обмотке статора. По результатам моделирования на основе полевой математической модели получена совокупность значений обобщенных коэффициентов, характеризующих оптимальную геометрию генератора. Библ. 4, табл. 1, рис. 7.

Ключевые слова: система рекуперации электроэнергии, синхронный генератор, постоянные магниты, математическая модель.

Introduction. Requirements for expanding the functionality of modern vehicles of general and special purpose cause the use on board of the vehicles of new devices and systems, operation of which requires additional power supply sources. Since all the energy received by the vehicle for its operation comes from the use of primary energy sources (usually the fuel of an internal combustion engine), additional power sources can only be obtained on the basis of energy saving principles – by detecting unnecessary energy losses in the vehicle and developing systems for the conversion of a part of these losses in useful power storage of battery. One of these is the system of electromechanical conversion of the energy of mechanical oscillations (SCMO) of the vehicle's chassis, which arise during the movement of the vehicle. The development and research of such systems is already being carried out by a number of foreign companies – Bose, Levant Power Corp, Audi [1-3]. For example, the power of the eROT system for an Audi car is up to 613 W in poor coverage, and 100-150 W on conventional roads. In Ukraine, these developments are just beginning, and their use may be the most expedient and effective for heavy duty vehicles.

The goal of the paper is obtaining by the results of mathematical modeling of optimal parameters of the synchronous generator, which is part of the system of electromechanical transformation of the energy of mechanical vibrations of the vehicle chassis.

General analysis. At a uniform motion of the vehicle on an ideally smooth surface (road), there is a balance of the forces of gravity of the subspring mass

(SSM) of the vehicle and the reaction of the elastic element of the suspension. In this case, the SSM does not make vertical vibrations, and the engine power is spent only to overcome the force of friction of the wheels on the surface. In the presence of steps down of the depth h on the road, the wheels of the vehicle are rapidly lowered down and, under the influence of the imbalance of forces, the SSM drops down, reducing its potential energy by the value

$$\Delta W = mgh, \quad (1)$$

where m is the mass of the SSM, g is the acceleration of gravity.

After the occurrence of damped oscillations, as a result of which the indicated energy dissipates in springs of suspension, the mode of uniform movement of the vehicle is restored. In the presence of steps up on the road, the potential energy of the SSM is increased due to the energy of the drive motor. In the process of oscillations, there is a mutual movement of the non-subspring mass (NSSM) and subspring mass of the vehicle in the vertical plane, which allows the creation of systems of electromechanical conversion of the energy of mechanical oscillations into useful electric energy. In the presence of a number of steps (unevenness, pits) on the road, this process is cyclically repeated. In real conditions, the frequency of pits on the road and their depth are random. However, to estimate the additional energy losses caused by vertical fluctuations of the vehicle when driving on a rough road, an equivalent

frequency of the repetition of the oscillation process f can be introduced at the same depth h of pits. Frequency of natural oscillations of the SSM of the vehicle is usually adjusted to a value of 1 ... 2 Hz, and they, due to powerful shock absorbers, damp in a few oscillations.

We consider examples of heavy vehicles: 1) a truck KrAZ-253B, its curb weight (CW) is 11.5 tons; 2) an armored personnel carrier BTR-4 Bucephalus – CW is 21.9 tons. Assuming that the ratio of NSSM and SSM is 1:15, which is typical for any vehicle, the values of SSM are respectively 10.7 and 20.4 tons. At one oscillation of such a mass at a depth $h = 0.05$ m, the change in the potential energy of the SSM will be $\Delta W = 5.24$ and 10 kJ respectively. If, when moving vehicle in rough terrain, such oscillations are constantly repeated, for example, with frequency $f = 0.2$ Hz (period of oscillation is 5 s), then the losses of power in shock absorbers of the vehicle are:

$$\Delta P = \Delta W \cdot f \quad (2)$$

or respectively $\Delta P = 1.05$ and 2 kW. The obtained estimation testifies to considerable losses of power of the engine of the vehicle in shock absorbers, which makes it expedient for its transformation into electric energy, its accumulation in the battery and further use in consumer systems of the vehicle.

For an integral estimation of the power of mechanical oscillations, taking into account the various factors influencing its value, one can introduce the coefficient of power of mechanical oscillations

$$k_e = mhf, \text{ (t}\cdot\text{m/s)}. \quad (3)$$

So, for the examples given, at $\Delta P = 1.05$ kW, we have $k_e = 0.107$, and at $\Delta P = 2$ kW the coefficient is $k_e = 0.204$. It is obvious that the same values of ΔP can be obtained with other values of mass, depth of the step and frequency of repetition of oscillations. For example, $\Delta P = 1.05$ kW can be obtained at $m = 5.36$ t, $h = 0.05$ m and $f = 0.4$ Hz or at $m = 8$ t, $h = 0.06$ m and $f = 0.23$ Hz. Taking into account the expressions (1) and (2) we have a simple universal formula for estimating the power losses during the movement of a vehicle on an uneven road:

$$\Delta P = gk_e. \quad (4)$$

The reciprocal movement of the SSM and NSSM during the drive in difficult road conditions provides a fundamental opportunity for the creation of SCEMO of the vehicle.

Structural flowchart of the SCEMO is presented in Fig. 1.

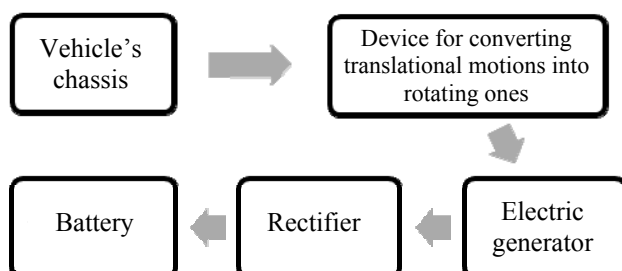


Fig. 1. Structural flowchart of the SCEMO

The operation of SCEMO is as follows. The mutual reciprocating translational displacements of the SSM and

NSSM through a mechanical transforming device are converted into a unidirectional rotational motion of the rotor of the electric generator, in which the conversion of mechanical energy into electrical energy is carried out. The alternating voltage at the output of the generator rectifies in the rectifier and charges the battery. Thus, in SCEMO there is a transformation of energy parameters in the following sequence: «mechanical energy of the reciprocating translational motion – mechanical energy of the rotating motion – electrical energy of alternating current of the electric generator – DC electric power of battery».

The electric generator creates a braking electromagnetic torque that counteracts the forced oscillation of the vehicle chassis. Thus, SCEMO carries out two useful functions: a) converts a part of the energy of mechanical vibrations of the vehicle into the useful electric power of battery; b) promotes dumping of the chassis oscillations, that is, partially serves as a shock absorber. It should be noted that the second function in heavy vehicles is not the main, because SCEMO in heavy vehicles can not replace the traditional shock absorbers, or can only to a small extent supplement them. Thus, the main function of SCEMO is the creation on board of the vehicle of an additional power source.

Modeling and investigations of the electric generator of SCEMO. An important element, which largely determines the efficiency of energy recuperation in SCEMO, is an electric generator. The analysis shows that, taking into account the features of the SCEMO operation, the optimal generator type is a three-phase AC synchronous generator with permanent magnets on the rotor (SGPM).

The use of permanent magnets (PM) as sources of magnetic flux of excitation is the optimal technical solution. In this case, the generator does not have a long stable mode of operation – it always operates in transient modes with variable speed of rotation of the shaft. The mechanical torque leading the generator in rotation has a random impulse character due to the road conditions of the motion of the vehicle. The main issues of the design of an electric generator are: a) optimization of the design of the generator by the chosen criterion, taking into account the probabilistic variables of the characteristics of the traffic of the vehicle; b) estimation of the possible share of the energy of mechanical vibrations of the vehicle, which can be converted into electric energy, taking into account the allowable overall characteristics of SCEMO.

Taking into account the real conditions of the functioning of the SGPM in the SCEMO structure, its design and parameters have a number of significant differences from the SGPM of the traditional execution. Namely:

1. An analysis of the appropriate construction of the SGPM on the vehicle chassis shows that the general configuration of the generator should be «long» – the ratio of the length of the stator core to its outer diameter lies in the range of values $l_s/D_j = 2.5 \dots 3.5$.

2. The average speed of rotation of the rotor, which the generator can receive in the SCEMO, is relatively small:

$n_2 = 200 \dots 400$ rpm. Therefore, in order to obtain an acceptable value of the EMF of the SGPM stator winding, which is proportional to the velocity of the change in the time of magnetic flux linkage (frequency), the generator must have a sufficiently large number of poles – the number of pairs of poles is $p = 4 \dots 5$.

3. Taking into account the possibilities of placing a multipolar three-phase winding of the stator in the core of a small diameter, the number of coils per pole and phase of the stator winding is equal to $q = 1$, and the number of grooves in the stator core is $Z_1 = 24 \dots 30$. Taking into account these data, stator design is performed according to the general methods of designing AC electric machines.

4. In order to ensure a high level of reliability of SGPM it is expedient to use a rotor with PM, which have a radial direction of the magnetization vector and are fixed on the surface of the ferromagnetic yoke of the rotor. Fig. 2, as an example, shows the cross-section of the active zone of the variant of the SGPM.

5. Important is the correct choice of PM parameters. It is necessary to justify the criteria by which this choice should be fulfilled. Unlike the traditional SGPM, for a generator operating in SCEMO there is no requirement for a sinus distribution of magnetic flux density in the air gap along the pole divider. The EMF and the stator currents do not necessarily have to change in time under the sinusoidal law, since the load of the SGPM in the SCEMO is a rectifier and further battery (Fig. 1). The criterion for choosing PM parameters is the *maximum value of the effective value* of the EMF of the stator winding when performing other equal conditions.

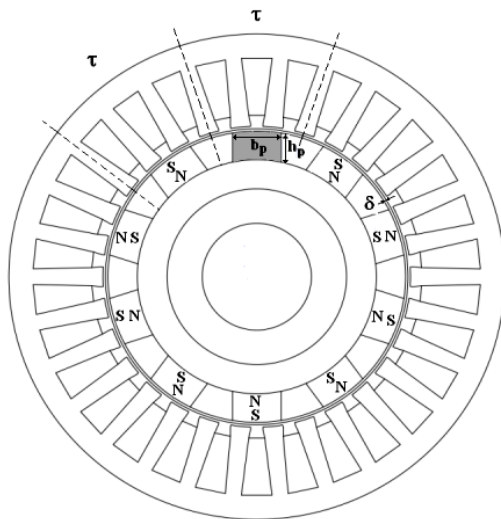


Fig. 2. Cross-section of the active zone of the SGPM

Generalized geometric parameters that characterize PM in the design of SGPM are:

- magnet shape factor – magnet width ratio to its height $k_p = b_p / h_p$. Typically, considering the requirements for the simplicity and performance of the rotor, PM is performed in the as a prism with a rectangular cross-sectional shape;
- coefficient of pole overlap – ratio of the width of the rotor magnet to the pole section of the rotor $\alpha = b_p / \tau$;

- coefficient of height of a magnet that characterizes the ratio of the height of the PM to the radius of the rotor $k_R = h_p / R_2$;

- coefficient of the relative value of air gap – the ratio of the height of the air gap between the stator and the rotor to the pole division of the rotor $k_\delta = \delta / \tau$.

The variation of the indicated coefficients in optimizing the parameters of a magnet should occur under the condition of constant variation in each variant of the cross section (volume) of the PM $S_p = b_p \cdot h_p = \text{const}$, since an increase in the volume of PM, and hence its magnetic flux, in itself increases the EMF of the stator and therefore does not allow to determine the optimal geometry of SGPM.

The indicated coefficients characterize not only the geometry of the PM itself, but also its relation with the geometry of other elements of the active zone of SGPM. Thus, the optimization problem is reduced to finding the extremum of the objective function – *the maximum of the effective value of the EMF of the stator winding* when the specified coefficients are varied, taking into account the constraints on their values, which arise from the possibilities of constructive execution of the generator. This optimization is performed by mathematical modeling.

The mathematical model of SGPM. We consider a field mathematical model of the SGPM with a moving rotor, which allows to analyze in time electromagnetic processes that arise during rotation of a rotor [4]. Equations for temporal functions are written as follows:

$$\nabla \times \left(\frac{1}{\mu} (\nabla \times \mathbf{A} - \mathbf{B}_r) \right) + \gamma \frac{\partial \mathbf{A}}{\partial t} - \gamma \mathbf{v} \times (\nabla \times \mathbf{A}) = \mathbf{J}, \quad (5)$$

$$E_j(t) = \frac{2na\delta}{S_p} \int_{S_i} E_n(t) ds, \quad (6)$$

where: \mathbf{A} is the magnetic vector potential; \mathbf{B}_r is the vector of residual magnetic flux density of the PM; μ , γ are the magnetic permeability and electrical conductivity of the material (given for each sub-region of the calculation area according to their characteristics – PM, air gap, ferromagnetic steel, etc.); \mathbf{v} is the vector of speed of movement of sections of the rotor relative to the system of coordinates of the stator; $\mathbf{J} = I_p n a / S_p$ is the current density in the stator winding, which is determined by the given current values, the number of successively connected conductors in the groove of the stator n and the part of the cross-section of the stator groove S_p , which falls on one parallel branch.

The \mathbf{B}_r vector should reflect the chosen direction of magnetization of the PM. The speed vector is determined by the given angular speed of the rotor ω_R and the radius vector of the current rotor point $\mathbf{v} = \omega_R \mathbf{r}$.

The equation (5) is supplemented by the corresponding boundary conditions. Usually this is the homogeneous boundary conditions of the first kind on the external boundary of the calculated area – the yoke of the stator core.

The instantaneous EMF of the stator phase as a function of time is determined by formula (6), where

integration is performed on the total area of the cross-section of phase conductors. The normal component of the electric field strength vector $E_n(t)$ is integrated – a component of the strength vector, which is directed perpendicular to the cross-section of the conductors of the winding. The electric field strength, provided that the electric scalar potential $\varphi = 0$, is calculated as

$E(t) = -\partial A / \partial t$. The current value of the EMF is calculated on the period T of the change of the function $E_j(t)$

$$E_{rms} = \sqrt{\frac{1}{T} \int_0^T E_j^2(t) dt} . \quad (7)$$

At rotor rotation, the configuration of the calculated area is changed due to changes in the relative position of the stator and elements of the design of the rotor, that is, changes in the coordinates of all points of the rotor. At rotation of a rotor counterclockwise with constant speed, the growth of coordinates of rotor points Δx , Δy in one time step Δt is determined:

$$\begin{cases} \Delta x = \cos[\omega_R \cdot (t + \Delta t) \cdot X - \sin[\omega_R \cdot (t + \Delta t) \cdot Y - X] \\ \Delta y = \sin[\omega_R \cdot (t + \Delta t) \cdot X + \cos[\omega_R \cdot (t + \Delta t) \cdot Y - Y] \end{cases}, \quad (8)$$

where X , Y are the current coordinates of rotor points.

Results of simulation and optimization of SGPM.

SGPM is considered, which has the following data: number of stator phases $m = 3$; number of pairs of poles $p = 5$; active length $l_\delta = 0.26$ m; outer diameter of the yoke of the stator $D = 0.1$ m; inner diameter of the yoke of the rotor, $D_0 = 0.022$ m; nominal power $P_n = 400$ W; rated (active) phase voltage of the stator winding $U_1 = 16$ V; rated rotor rotation speed $n_{nom} = 200$ rpm. The permanent magnet has the following characteristics: $B_r = 1.18$ T, $\mu_r = 1.065$.

Fig. 3 shows the time dependencies of the stator EMF for different values of the pole overlay coefficient: 1 – for $\alpha = 0.69$; 2 – $\alpha = 0.58$; 3 – $\alpha = 0.49$; 4 – $\alpha = 0.36$. From the above dependencies it is seen that the growth of α leads to an increase in the width of the curves, and hence to an increase in the effective value of the EMF at its practically unchanged amplitude. That is, the width of the PM substantially affects the value of E .

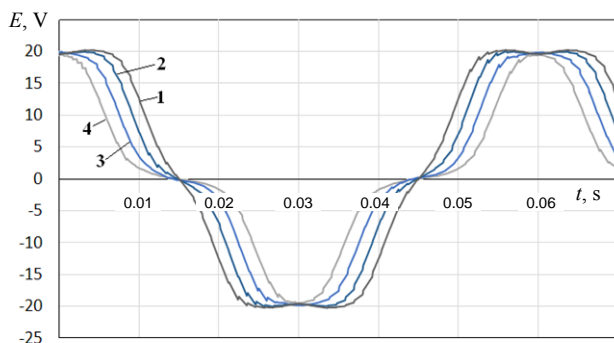


Fig. 3. Temporal dependencies of EMF

Calculations are made in idle mode of the generator. Fig. 4, 5 show the dependencies of the amplitude (dotted line) and the active value (solid line) of the EMF of the stator winding on, respectively, the pole overlay α and the shape coefficient of the magnet k_p on the condition that the volume of the PM is unchanged.

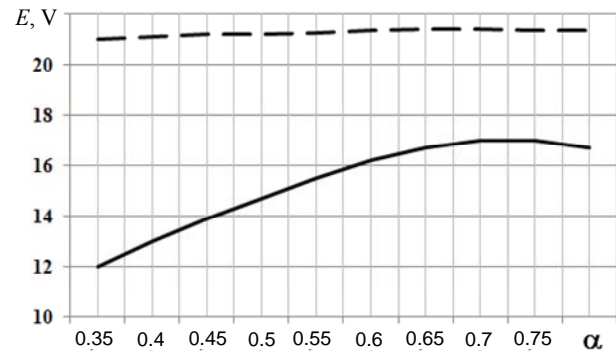


Fig. 4. EMF dependencies on the coefficient α

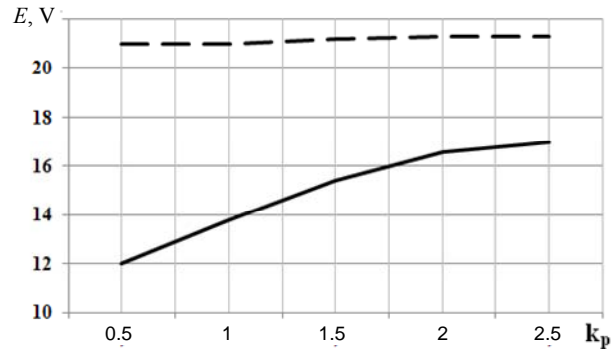


Fig. 5. EMF dependencies on the coefficient k_p

The presented dependencies show that with practically unchanged amplitude of the EMF the use of wider and not high PM leads to an increase in the effective value of EMF.

The excessive increase in the width of the PM is not feasible, since it is limited by an increase in the magnetic scattering fluxes between the PMs that are located near, as well as by constructive factors. The optimal values of the coefficients are: $k_p = 2.5 \dots 3$ and $\alpha = 0.75 \dots 0.8$.

This conclusion is confirmed by the calculated dependences of the EMF on the coefficient of magnet height $k_R = h_p / R_2$, shown in Fig. 6. Calculations are made with constant magnet width $b_p = 6$ mm and variation of the height of the magnet from 3 to 8 mm. With variations, the volume of magnets increases by 2.67 times. The given data testify that at $k_R > 0.2$ the growth of EMF does not occur, that is, the performance of too high magnets is inappropriate.

This is due to the fact that the part of the PM, located near the yoke of the rotor, practically does not «take part» in the creation of the magnetic flux of the mutual induction of the rotor with the winding of the stator, and only creates fluxes of scattering of PM. Therefore, the values of the magnitude of the coefficient of magnet height lie in the range of values $k_R = 0.1 \dots 0.13$.

The size of the air gap between the stator and the rotor affects the EMF of the winding of the stator. Fig. 7 shows the temporal dependencies of the EMF of the winding of the stator for the values: $\delta = 0.5$ mm (indicated by 1); 0.75 mm (2) and 1 mm (3), which correspond to the value of the coefficient of the relative air gap value $k_\delta = \delta / \tau = 0.053$; 0.04 and 0.0265.

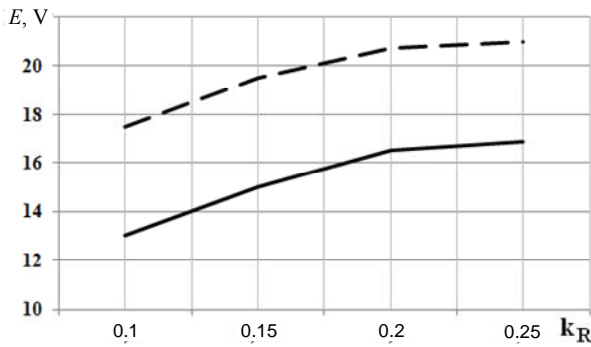


Fig. 6. EMF dependencies on the coefficient k_R

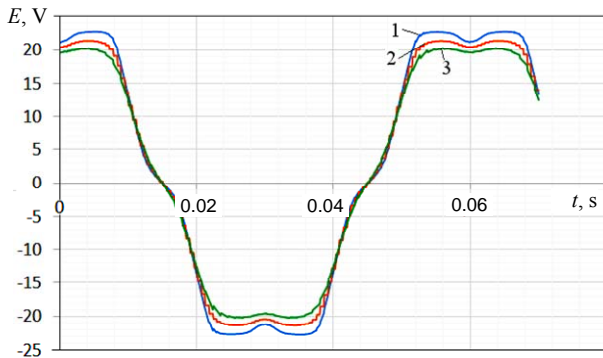


Fig. 7. Temporal EMF dependencies on the coefficient k_δ

Calculations are carried out at a fixed value of the width of the PM. From the data shown, it can be seen that even with a double magnification of δ within the limits which can be due to constructive factors, the amount of EMF decreases by only 13.7 %.

Similar numerical studies were carried out for other standard sizes of SGPM, which resulted in the presented in the Table optimal values of generalized geometric coefficients, which should be used in the design of SGPM, which are intended for operation in SCEMO.

Table

SGPM optimal geometrical coefficients

Coefficient	Numerical value
Ratio of the length of the stator core to its outer diameter l_δ / D_j	2.6...3
Coefficient of pole overlap $\alpha = b_p / \tau$	0.68...0.75
Magnet shape coefficient $k_p = b_p / h_p$	2.1...2.5
Magnet height coefficient $k_R = h_p / R_2$	0.1...0.16
Coefficient of relative air gap value $k_\delta = \delta / \tau$	0.04...0.05

How to cite this article:

Vaskovskyi Yu.M., Poda M.V., Koshikar I.V. Electric generator in the recuperation system of the energy from mechanical oscillations in vehicles. *Electrical engineering & electromechanics*, 2018, no.5, pp. 24-28. doi: 10.20998/2074-272X.2018.5.04.

The value of the EMF of the SGPM, and hence the efficiency of the SCEMO, largely depends on the rotational speed of the generator rotor, which is determined by the traffic conditions of the vehicle. Therefore, the energy intensity and parameters of battery, the time of its charge, etc., require special agreement with the parameters of SGPM taking into account the likely characteristics of the movement of a specific type of vehicle.

Conclusions.

1. An additional power source on board of a vehicle may be a system of electromechanical recuperation of the energy of mechanical oscillations of the vehicle's chassis during its movement into the electric energy of the battery. The analysis confirms the presence of a sufficient amount of energy, which is usually lost in shock absorbers of the vehicle and which can be partially accumulated in battery.

2. The parameters of an important element of the mentioned system – a synchronous generator with permanent magnets, which, due to the peculiarities of its operation, are substantially different from analogous generators of traditional execution, are investigated. The optimal ranges of parameters of SGPM are determined. Their numerical values are presented in the Table and can be used in the development of SGPM in the specified systems.

REFERENCES

1. Drive2 – Automobile Journal. *Electromagnetic suspension Bose*. Available at: <https://www.drive2.ru/b/721443/> (accessed 13 September 2016). (Rus).
2. Drive2 – Automobile Journal. *GenShock – suspension system performing the function of energy regeneration*. Available at: <https://www.drive2.com/b/668040/> (accessed 11 May 2016). (Rus).
3. Audi MediaCenter. *The innovative shock absorber system from Audi*. Available at: <https://www.audi-mediacycenter.com/en/press-releases/the-innovative-shock-absorber-system-from-audi-new-technology-saves-fuel-and-enhances-comfort-6551> (accessed 20 June 2017).
4. Vaskovskyi Yu.M., Haydenko Yu.A. Research of electromagnetic processes in permanent magnet synchronous motors based on a «electric circuit – magnetic field» mathematical model. *Technical Electrodynamics*, 2018, no.2, pp. 47-54. (Ukr). doi: 10.15407/techned2018.02.047.

Received 15.06.2018

Yu.M. Vaskovskyi¹, Doctor of Technical Science, Professor,

M.V. Poda¹, Postgraduate Student,

I.V. Koshikar¹, Master of Science,

¹ National Technical University of Ukraine «Igor Sikorsky Kyiv Polytechnic Institute»,

37, Prospect Peremohy, Kyiv-56, 03056, Ukraine,

e-mail: vun157@gmail.com, poda.mv@gmail.com

V.V. Shevchenko, A.N. Minko, A.V. Strokous

ANALYSIS OF ELECTROMAGNETIC VIBRATION FORCES IN THE ELEMENTS OF THE TURBOGENERATOR STATOR FASTENING TO THE CASE IN NON-NOMINAL OPERATION MODES

Purpose. The purpose of the paper is to determine the value of additional electromagnetic forces (EMF) that are created by the fluxes of scattering of the back of the turbogenerator (TG) stator core in the elements of its fastening to the case when operating in non-nominal modes according to the vibration control data. *Methodology.* The paper used the theory of electromagnetic fields, the method of polynomial approximation, mathematical modeling in the MathCAD-2000 professional package and the provisions of the general theory of electrical machines. *Results.* Analytical and numerical calculations of additional EMF values are performed, which were created by the leakage fluxes of the back of the stator core in the elements of fastening of the TG to the case when operating in non-nominal modes, which is determined by the need for night unloading of the power system. The values of these TG forces are established with a change in the output and consumption of reactive power and with a change in voltage. *Originality.* For the first time for TGs operating in non-nominal modes, the estimation and calculation of additional EMF in the elements of the TG core fastening to the case are carried out, which are created by the leakage fluxes of the back of the stator core and supplement the action of the basic EMF. The definition of these forces is relevant, because turbogenerators of TPPs in Ukraine with a capacity of 200-300 MW are maneuvering capacities and solve the problem of maintaining the power factor of the power system. *Practical value.* It was found that if the TGs often operate in non-nominal modes, the wear of the stator core fastening systems to the case is more significant than in the case of their operation only in nominal modes. The obtained data will allow to more accurately determine the scope of repair work, draw up schedules for their implementation, determine the locations of the sensors for monitoring, and can be used at the design stage of new machines. References 6, tables 2, figures 2.

Key words: turbogenerator, load mode, non-nominal mode, electromagnetic force, reactive power, stator core fastening unit.

Целью статьи является определение величины дополнительных электромагнитных сил (ЭМС), которые создаются потоками рассеяния спинки сердечника статора турбогенератора (ТГ) в элементах его крепления к корпусу при работе в неноминальных режимах по данным вибрационного контроля. Методика. В работе использовали теорию электромагнитных полей, метод аппроксимация полиномами, математическое моделирование в пакете MathCAD-2000 professional, положения общей теории электрических машин. Результаты. Выполнены аналитические и численные расчеты дополнительных величин ЭМС, создаваемых потоками рассеяния спинки сердечника статора в элементах крепления ТГ к корпусу при работе в неноминальных режимах, что определяется необходимостью ночных разгрузок энергосистемы. Установлены значения этих сил ТГ при изменении выдачи и потребления реактивной мощности и при изменении напряжения. Научная новизна. Впервые для ТГ, работающих в неноминальных режимах, выполнены оценка и расчет дополнительных ЭМС в элементах крепления сердечника ТГ к корпусу, которые создаются потоками рассеяния спинки сердечника статора и дополняют действие основных ЭМС. Определение этих усилий актуально, т.к. турбогенераторы ТЭС Украины мощностью 200-300 МВт являются маневренными мощностями и решают задачу поддержания коэффициента мощности энергосистемы. Практическое значение. Было установлено, что если ТГ часто работают в неноминальных режимах, износ систем крепления сердечников статора к корпусам более значителен, чем в случае их работы только в номинальных режимах. Полученные данные позволяют более точно определять объемы проведения ремонтных работ, составлять графики их проведения, определять места установки датчиков контроля, могут быть использованы на этапе проектирования новых машин. Библ. 6, табл. 2, рис. 2.

Ключевые слова: турбогенератор, режим нагрузки, неноминальный режим, электромагнитная сила, реактивная мощность, узел крепления сердечника статора.

Introduction. Currently, there is a high degree of aging of the park equipment of thermal power plants (TPPs). Therefore, taking into account the national economic situation, the strategic task for Ukraine is to extend the life and increase the reliability of long-term operating turbogenerators (TGs), improve their maintenance and optimize the costs of upgrading and technical re-equipment of TPPs and nuclear power plants (NPPs).

One of the most effective solutions to these challenges is to improve the quality, implementation and development of new ones, as well as to improve existing methods for diagnosing TG, which ensure timely and complete detection of defects (including at an early stage of their development), as well as the completeness and quality of their elimination. The reliability of the TG and its physical life is largely determined by the technical state of the stator core, including the system of its

fastening to the case. Reliable execution of the fastening unit provides the necessary level of core rigidity, vibration isolation of the stator case and the foundation from vibrations caused by electromagnetic forces (EMFs) of the active zone. In turn, a reliable fastening system protects the stator core from external vibrations transmitted from the foundation through the supports and sliding bearings to the case of the TG, which is especially important in maneuvering operation modes [1, 2].

The goal of the paper is determination of the value of additional EMFs that are created by the leakage fluxes of the back of the stator core of the turbogenerator in the elements of its fastening to the case when operating in non-nominal modes according to the vibration control data.

The main material of the study. According to the statistics collected by the operating personnel of power

© V.V. Shevchenko, A.N. Minko, A.V. Strokous

plants, the state of the cases and cores of TG stators, which for a long time operated in non-nominal modes (at a load of 70, 50, 30 % of the nominal) on TPP units, it was found that compared to the TGs that operated only in nominal modes, the value of vibration is higher. Vibration of the stator case is monitored periodically, and vibration measurement of the fastening elements of the active steel of the stator core to the frame of the case is carried out very rare, only in cases of obvious symptoms of deterioration of their vibration state or in the unsatisfactory state of the stator steel structures (contact corrosion, damage to attachment points, etc.), i.e. already in the presence of a defect. At the same time, it is known from the operating experience that the volume and efficiency of repair work depends on the stage of defect development.

Conducting a vibration examination of the core fastening system is associated with certain difficulties, which is determined by the need to take into account the design of the hydrogen or air exhaust assemblies, the terminals of the measuring systems from the case through gas tight fingers and other elements, the presence of sensors inside the generator. But, if you install the

vibration monitoring system of the case in advance, it is possible to detect defects in time, which can lead to serious damages and require expensive repairs, and in some cases a complete replacement of the generator.

Usually the vibration spectrum obtained from vibration signals taken from the case of the operating generator includes a fundamental harmonic with frequency of 100 Hz and a number of harmonic components that are multiples of the fundamental harmonic. Thus, when servicing the turbogenerators of the unit No. 4 of the Gusinozerskaya TPP (2014), unit No. 1 of the Gomel TPP-2 (2011, 2012), unit No. 15 of the Luganskaya TPP (2014) and unit No. 3 of the Zuevskaya TPP (2013), measurements of the vibrations of the stator cases were performed. It was found that in modes other than nominal, the vibration was maximum, especially in the middle sections of the cases. Table 1 shows the data of tests of the stator case of the turbogenerator TTB-300-2Y3 of the block № 3 of the Zuevskaya TPP. Fig. 1 shows the layout of the control sensors on the left side «L».

The sensors 1R – 9R on the right are arranged symmetrically.

Table 1

Stator case vibration of the TG TTB-300-2Y3 of the unit No. 3 of the Zuevskaya TPP

Power of the TG	Vibration value, 2A, μm																	
	Point No.																	
	1L	2L	3L	4L	5L	6L	7L	8L	9L	1R	2R	3R	4R	5R	6R	7R	8R	9R
$P = 288 \text{ MW}$, $Q = 60 \text{ MVar}$	10	13	11	23	33	26	25	40	26	19	28	17	41	48	40	39	47	38
$P = 220 \text{ MW}$, $Q = 52 \text{ MVar}$	11	15	11	26	34	27	29	42	29	23	29	16	43	51	43	41	53	46
$P = 154 \text{ MW}$, $Q = 52 \text{ MVar}$	15	15	9	28	37	31	31	45	33	28	34	14	49	59	47	47	57	50

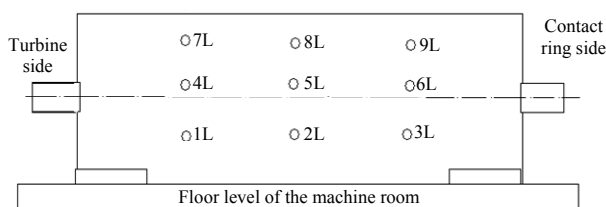


Fig. 1. The location of the vibration measurement points on the left side of the TG case (if viewed from the side of the contact rings)

During investigations it was also noted the weakening of pressing of the laminated packages and the more frequent destruction of the stator winding insulation of the slotted and frontal parts, the destruction of the stator core fastening system to the case [3].

To determine the reasons for the increase in vibration in non-nominal modes, we consider changes in the action of eddy currents, which are induced in the stator core and in the elements of its fastening to the case of the TG. These currents, which are induced by scattering fluxes in the elements of the system of fastening the laminated stator core to the case, and, consequently, the value of the electromagnetic forces acting on the clamp prisms of the TG, depend on the

degree of saturation of the core back. The value of the flux of scattering per unit surface (the flux that is displaced from the core into the fastening zone to the case) can be represented [1, 2], Wb/m:

$$\Phi_{dis} = \frac{\mu_0 \cdot H_S \cdot \tau}{\pi} \cdot \left[1 + \left(\frac{R_S}{R_k} \right)^{2p} \right] \cdot \left[1 - \left(\frac{R_S}{R_k} \right)^{2p} \right]^{-1}, \quad (1)$$

where $\mu_0 = 4\pi \cdot 10^{-7} \text{ H/m}$ is the magnetic constant; H_S is the amplitude of the tangential component of the magnetic field strength on the surface of the stator back, A/m; R_S is the outer radius of the stator core back, m; τ is the pole division, m; R_k is the inner radius of the stator case, m; $2p$ is the number of poles.

Thus, the flow displaced from the core is directly proportional to the magnetic field strength in the back of the core, which in turn depends on magnetic flux density, i.e. from the operating mode of the generator [3].

When the operating mode changes, the temperature of the active and structural parts of the stator changes, which affects their linear dimensions. The coefficient of linear expansion of steel is 0.12 - 0.15 mm per 1 °C [4]. If the temperature of the stator core is increased by 30 °C, its linear dimensions will increase only by 0.04 % of the initial value. Therefore, the thermal

expansion of the linear dimensions of the prisms, core packages, and the fastening system can be neglected. Also in calculations it is possible to neglect the influence of heating on the resistance of the circuits of the closure of eddy currents [5].

The permissible non-nominal modes of operation of the TG are regulated by the instruction manual and are determined from the diagram of permissible loads [5]. Therefore, we select the active power (P), reactive power (Q) and the line voltage of the stator winding (U_s) to characterize the operating modes. Let us determine the analytical relationship of the indicated parameters with the value of the EMF acting on the fastening elements. The sequence of the analytical calculation of electromagnetic forces is described in detail in [2].

The amplitude of magnetic flux density on the outer line of the back of the stator core can be determined:

$$B_s = \frac{E_r}{2 \cdot \sqrt{2} \cdot \pi \cdot f \cdot \omega_s \cdot k_0 \cdot S_s} \cdot k_c, \quad (2)$$

$$E_r = \sqrt{\left(\frac{U_s}{\sqrt{3}} + x_\sigma \cdot I_s \cdot \cos\left(\frac{\pi}{2} - \varphi\right) \right)^2 + \left(x_\sigma \cdot I_s \sin\left(\frac{\pi}{2} - \varphi\right) \right)^2}$$

When calculating the values of the magnetic field strength in the back of the core and the clamp prisms, magnetic flux density in the surface layer of the active steel, the magnetization characteristics of the relevant materials are used, which are selected from the tables [5], but to solve the problem it is advisable to present them in the form of functional dependencies.

The amplitude of the magnetic field strength on the surface of the back of the stator core is related to the magnetic flux density value by a nonlinear dependence and in the range of inductions 0.6 to 1.7 T is approximated with sufficient accuracy by a polynomial of the 6th degree:

$$H_s = f(B_s) = \sum_{n=0}^6 h_n \cdot B_s^n. \quad (4)$$

We determine the amplitude of the magnetic field strength on the upper line of the back of the stator core, then we find the values of the magnetic flux linked to the contour of the fastening elements and the back surface, and determine the electromotive forces induced by it on the prisms. When calculating the resistance of the contour of the formation of the eddy current Z_k , it must be taken into account that the resistance of the prism Z_p and the end package depends on the degree of saturation of the material.

However, taking into account that the resistance of the eddy current shortage contour is approximately 80 % determined by the resistance value of the fastening elements, in the further calculations the resistance of the end core packets is assumed to be constant, the effect of saturation of the active steel on the resistance value of the contour Z_k is neglected.

The relative magnetic permeability of the prism material μ_p also depends nonlinearly on the magnetic field strength and can be represented as:

where f is the network current frequency; k_0 is the winding factor; ω_s is the number of turns of stator winding; S_s is the stator back section; k_c is the coefficient that characterizes the uneven distribution of magnetic flux density in the stator back; E_r is the electromotive force, which is induced by the magnetic fluxes of the scattering of the back of the stator core in the clamp prisms in the non-nominal operating modes:

$$E_r = \sqrt{\left(\frac{U_s}{\sqrt{3}} + x_\sigma \cdot I_s \cdot \cos\left(\frac{\pi}{2} - \varphi\right) \right)^2 + \left(x_\sigma \cdot I_s \sin\left(\frac{\pi}{2} - \varphi\right) \right)^2}.$$

The angle between the stator voltage and current vectors, as well as the stator current, A:

$$\varphi = \arccos\left(\frac{P}{\sqrt{P^2 + Q^2}}\right); \quad I_s = \frac{1}{U_s} \cdot \sqrt{\frac{P^2 + Q^2}{3}}. \quad (3)$$

Taking into account (3), the value of the resulting electromotive force in the stator back and in the elements of its fastening to the case:

$$\mu_p = \sum_{n=0}^6 m_n \cdot H_s^n. \quad (5)$$

The change in the magnetic permeability μ_p on the magnetic field strength for the steel St 3, of which the prisms of the fastening are made, is considered in the interval 100-1250 A/m.

The magnetic flux density amplitude, which corresponds to the value of the magnetic field strength H_s on the surface of the back of the core, can be represented as:

$$B_{s, \max} = \sum_{n=0}^3 b_n \cdot H_{s, \max}^n. \quad (6)$$

When examining the dependence of the EMF value in different modes, we change the value of one of the parameters (P , Q , U_s) within the limits determined by the power diagram and a typical operating instruction, while the other two parameters do not change.

To carry out the calculations, we introduce the dimensionless quantity ε_N , which is the ratio of the EMF changes to the change in physical quantities (P , Q , U_s) in one of the non-nominal modes N : 70, 50 and 30 % of the generator load from the nominal (100 %):

$$\varepsilon_N = \frac{(F_B - F_N) / F_b}{(N_B - N_N) / N_b}, \quad (7)$$

where N_B , N_N , N_b are the upper boundary, lower boundary and base values of the selected parameter N (P , Q or U_s), depending on the mode of operation of the TG; F_B , F_N , F_b are the upper boundary, lower boundary and base values of the EMF.

We accept changes in the values of the parameters that characterize the changes in the modes (P , Q , U_s):

- 1) $P_N = 0$ MW, $P_B = P_b = 300$ MW;
- 2) $Q_N = -80$ MVar, $Q_B = Q_b = 186$ MVar;
- 3) $U_N = 0.95$ kV, $U_B = U_b = U_{sN} = 20$ kV.

To verify analytically obtained results, we solve the problem also by numerical methods on the developed mathematical model using the MathCAD-2000 Professional package. We study the fastening element (prism), which has been in operation for a long time, in connection with which the metal was worked out: the dimensions of the side gaps of the prism fastening are taken to be 0.435 mm (data obtained on turbogenerator that operates on the block No. 2 of the Zmievska TPP, [6]).

We perform the expansion of the distribution of EMF, its radial and tangential components in Fourier series:

$$F(\theta) = F_{\cos\theta} + \sum_{v=1}^N F_{v,m} \cdot \sin(v\theta) + \sum_{v=1}^N F_{v,m} \cdot \cos(v\theta),$$

where θ is the load angle of the TG, electrical degrees; v is the harmonic number; $F_{v,m}$ is the amplitude of the v -th harmonic of the EMF:

$$F_{v,m} = \sqrt{(F_{v,m}^s)^2 + (F_{v,m}^c)^2}, \text{ N}$$

φ_v is the phase of the v -th harmonic of the EMF

$$\varphi_v = \arctg\left(\frac{F_{v,m}^c}{F_{v,m}^s}\right),$$

where $F_{v,m}^s, F_{v,m}^c$ are the coefficients of the Fourier series for odd and even harmonic components of the v -th order, varying from 1 to v .

The results of calculating the EMF induced by eddy currents in the stator core fastening elements to the case, obtained analytically and numerically for various operating modes of the TG, are given in Table 2 and in Fig. 2.

Comparison of the results of analytical calculations and the results obtained by numerical methods (Table 2, Fig. 2) allows us to conclude that the results obtained are fairly close. This confirms the reliability of the calculations performed.

Table 2

The results of calculating the EMF, acting on the elements of fastening the stator core to the case, obtained analytically and numerically for various modes of operation of the TG

Active power influence			Reactive power influence			Voltage influence		
P , MW	Value of the EMF first harmonic amplitude, N		Q , MVar	Value of the EMF first harmonic amplitude, N		U_s , kV	Value of the EMF first harmonic amplitude, N	
	Analytical calculation	Numerical calculation		Analytical calculation	Numerical calculation		Analytical calculation	Numerical calculation
0	104.8	179	-80	107.3	163.6	19	132.4	173.7
150	141.5	179	0	115.7	174.2	19.5	135	185
100	145.2	189	186	145.2	189	20	145.2	189
ε_N	0.03	0.053	ε_Q	0.183	0.094	ε_P	1.763	1.619

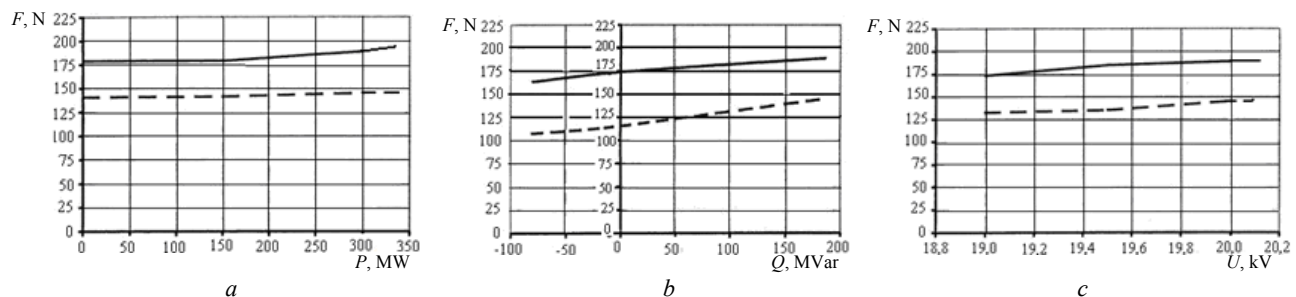


Fig. 2. Dependence of the electromagnetic forces acting on the stator core fastening system to the case on the active power (a), reactive power (b) and stator voltage (c) for various operating modes of the turbogenerator by analytical and numerical methods (--- data of analytical calculation; — data obtained by numerical methods)

Conclusions.

1. The results of analytical and numerical calculations showed that in nominal operating modes of the TG (within the load diagram), the value of the EMF acting on the stator core fastening elements varies little. However, when calculating EMF in non-nominal modes, its change is significant. Thus, for a TG with a power of 300 MW, the maximum change in EMF was observed when the reactive power was changed from the largest value (+186 MVar) to the limiting value of the reactive power consumed (-80 MVar), which is 13 % (based on the results of numerical calculations).

2. Quantitative characteristics of the change in EMF are obtained depending on the value of active P , reactive power Q and on the voltage of the stator U_s . It is established that under non-nominal operating modes of the TG, the change in the value of these forces is

practically independent on the active and reactive power: when P and Q change by 1 %, the change in EMF is only hundredths and tenths of a percent, respectively. The dependence of EMF on voltage is more significant, it is quadratic (with a change of U_s by 2 %, EMF increases by approximately 4 %).

3. When operating the TG in non-nominal modes, the wear of the TG stator core fastening system to the case is more significant than when operating in nominal modes. This should be taken into account when installing sensors for monitoring the status of the TG in on-line mode, when drawing up schedules for carrying out repairs and determining their volumes.

REFERENCES

1. Vaskovskyi Yu.M., Melnyk A.M. The electromagnetic vibration disturbing forces of turbogenerator in maneuverable

- operating conditions. *Technical Electrodynamics*, 2016, no.2, pp. 35-41. (Ukr). doi: **10.15407/techned2016.02.035**.
2. Kuznetsov D.V. Investigation of electromagnetic forces acting on the coupling prisms of the stator core of the turbogenerator. *Electricity*, 2006, no.10, pp. 42-48. (Rus).
 3. Stepanov A., Sikora R. *Modelirovanie elektromagnitnyh polej v elektricheskikh ustroystvah* [Modeling of electromagnetic fields in electrical devices]. Kiev, Tehnika Publ., 1990. 188 p. (Rus).
 4. Griscenko M., Vitols R. Stator core vibration and temperature analysis of hydropower generation unit at 100 Hz frequency. *Proceedings of 14th International Scientific Conference Engineering for Rural Development*. 20-22 May, 2015. Jelgava, Latvia, pp. 383-388.
 5. Shevchenko V.V., Strokous A.V. Forecasting the operating resource of turbogenerators on vibration control data. *Norwegian Journal of development of the International Science*, 2017, vol.1, no.10, pp. 78-83. (Rus).
 6. Minko A.N., Gordienko V.Yu. Turbogenerators with the optimal mass-size parameters in place of the exhausted

resources without destroying the original foundation. *Energetic and electrification*, 2011, no.6, pp. 37-42. (Rus).

Received 10.05.2018

V.V. Shevchenko¹, Candidate of Technical Science, Associate Professor,

A.N. Minko², Candidate of Technical Science,

A.V. Strokous¹,

¹ National Technical University «Kharkiv Polytechnic Institute»,

2, Kyrpychova Str., Kharkiv, 61002, Ukraine,

phone +380 50 4078454,

e-mail: zurbagan8454@gmail.com, anton220579@gmail.com

² Private Scientific and Production Company «Ankor-Teploenergo»,

19, Kirgizska Str., build 1, Kharkiv, 61105, Ukraine,

phone +380 97 7924889, e-mail: alexandr.minko@i.ua

How to cite this article:

Shevchenko V.V., Minko A.N., Strokous A.V. Analysis of electromagnetic vibration forces in the elements of the turbogenerator stator fastening to the case in non-nominal operation modes. *Electrical engineering & electromechanics*, 2018, no.5, pp. 29-33. doi: **10.20998/2074-272X.2018.5.05**.

B.I. Kuznetsov, T.B. Nikitina, V.V. Kolomiets, I.V. Bovdai, A.V. Voloshko, E.V. Vinichenko

SYNTHESIS OF ROBUST ACTIVE SHIELDING SYSTEMS OF MAGNETIC FIELD GENERATED BY GROUP OF HIGH-VOLTAGE POWER LINES

Aim. The synthesis of robust active shielding system of magnetic field, generated by group of high voltage power lines for reducing the induction of the initial magnetic field to the sanitary standards level and reducing the sensitivity of the system to variations in the plant parameters is given. **Methodology.** The synthesis is based on the solution of a multi-criteria stochastic game, in which the gain vector is calculated on the basis of the Maxwell equations solutions in the quasi-stationary approximation. The equilibrium state of the game is based on the stochastic multiagent optimization algorithms of the multiswarm particles. The initial parameters for the synthesis of active shielding system are the location of the high voltage power lines with respect to the protected from transmission line space, geometry and number of cables, operating currents, as well as the size of the protected space and normative value magnetic field induction, which should be achieved as a result of screening. The objective of the synthesis of the active shielding system is to determine their number, configuration, spatial arrangement, wiring diagrams and compensation cables currents, setting algorithm of the control systems as well as the resulting value of the induction magnetic field at the points of the protected space. **Results.** Robust active shielding system synthesis results for reduction of a magnetic field generated by group of high voltage power lines is given. The possibility of a significant reduction in the level of induction of the magnetic field source within and reducing the sensitivity of the system to variations in the plant parameters is given. **Originality.** For the first time carried out the synthesis of the robust active shielding systems of magnetic field generated by group of high voltage power lines within a given region of space. **Practical value.** Practical recommendations on reasonable choice of the number and spatial arrangement of compensating cables of robust active shielding systems of the magnetic field generated by the group of high voltage power lines is given. References 18, figures 5.

Key words: high voltage power lines, power frequency magnetic field, robust active screening system, a multi-criteria stochastic game.

Цель. Проведен синтез робастной системы активного экранирования магнитного поля, создаваемого группой высоковольтных линий электропередачи для снижения индукции исходного магнитного поля до уровня санитарных норм и уменьшения чувствительности системы к изменениям параметров системы. **Методология.** Синтез основан на решении многокритериальной стохастической игры, в которой векторный выигрыш вычисляется на основании решений уравнений Максвелла в квазистационарном приближении. Равновесное состояние игры находится на основе алгоритмов стохастической мультиагентной оптимизации мультироем частиц. Исходными параметрами для синтеза системы активного экранирования являются расположение высоковольтных линий электропередачи по отношению к защищаемому пространству, геометрические размеры, количество проводов и рабочие токи линии электропередачи, а также размеры защищаемого пространства и нормативное значение индукции магнитного поля, которое должно быть достигнуто в результате экранирования. **Целью** синтеза системы активного экранирования является определение количества, конфигурации, пространственного расположения, схем электропитания и токов компенсационных кабелей, алгоритма работы системы управления, а также результирующего значения индукционного магнитного поля в точках защищаемого пространства. **Результаты.** Приводятся результаты синтеза робастной системы активного экранирования для уменьшения магнитного поля, создаваемого группой высоковольтных линий электропередачи. Показана возможность существенного снижения уровня индукции исходного магнитного поля внутри заданного пространства и снижения чувствительности системы к изменениям параметров системы. **Оригинальность.** Впервые проведен синтез робастной системы активного экранирования магнитного поля, создаваемого группой высоковольтных линий электропередач в данной области пространства. **Практическая ценность.** Приводятся практические рекомендации по обоснованному выбору количества и пространственного расположения компенсирующих обмоток робастных систем активного экранирования магнитного поля, создаваемого группой высоковольтных линий электропередач. Библ. 18, рис. 5.

Ключевые слова: высоковольтные линии электропередачи, магнитное поле промышленной частоты, робастная система активного экранирования, многокритериальная стохастическая игра.

Introduction. Methods of active contour shielding of power frequency magnetic field (MF) created by high voltage power lines (HVPL) [1-6] are the most acceptable and economically feasible for ensuring the sanitary norms of Ukraine in the magnetic field of the industrial frequency [7-8]. The method of synthesis of active shielding systems (ASS) for MF, created by air power lines, was developed in [9]. The initial data for the synthesis of the system is the parameters of the transmission lines (working currents, geometry and number of wires, location of the transmission lines relative to the protected space) and the dimensions of the protected space and the standard value of the induction of the MF, which should be achieved as a result of

screening. In the process of synthesis, it is necessary to determine the parameters of the compensation coil (their number, configuration, spatial arrangement, connection diagram), compensating coil currents and the resulting induction values of the MF at the points of the protected space, as well as the algorithm of the ASS. However, this method [9] does not take into account the uncertainty of the system parameters due to the inaccurately known model of the control object, as well as changes in the parameters of the system during its operation [10].

Ukraine's electricity networks are characterized by high density, and especially near high-voltage power substations. There is usually a group of overhead HVPL, in the immediate vicinity of which can be located

residential buildings. In this case, the main uncertainty in the synthesis of this system is the variation of the currents of different power lines, which leads not only to a change in the level of magnetic field induction, but also to a change in the position of the space-time characteristics (STC) of the MF in the shielding zone.

The goal of this work is the synthesis of robust active shielding systems of power frequency magnetic field created by group of high voltage power lines, which allows to reduce the magnetic field level to sanitary norms and to reduce the sensitivity of the system to variations of plant parameters.

Problem statement considers the formulation of the problem of synthesis of the robust ASS. In the synthesis of the ASS, the mathematical model of the original MF is known inaccurately [10]. In particular, currents in current conductors that have daily, weekly, seasonal variations are approximately known. The geometric dimensions of the compensating coil, the parameters of the regulators, etc. are not accurately realized. Therefore, we introduce a vector of deviations of the system parameters from their nominal values δ used in the synthesis of the system. The problem of synthesizing a robust ASS is reduced to the determination of such a vector of spatial arrangement and geometric sizes of compensated windings, as well as parameters of the regulator X and the vector of variable parameters δ , at which the maximum value of the magnetic field induction at selected points P_j of the considered space P assumes a minimum value for the regulator parameter vector X , but the maximum value for the vector of variable parameters δ so that

$$X^* = \arg \min_{X \in X} \max_{\delta \in \Delta} \max_{P_j \in P} B(X, \delta, P_j). \quad (1)$$

This technique corresponds to the standard approach to the synthesis of robust systems for the worst-case [10], when the variations of the parameters δ lead to the greatest deterioration in the compensation of the initial MF created by HVPL. The problem (1) can be formulated in the form of the following multi-criteria game [11] with vector gain

$$B(X, \delta) = [B(X, \delta, P_1), B(X, \delta, P_2), \dots, B(X, \delta, P_m)]^T, \quad (2)$$

the components of which $B(X, \delta, P_i)$ are the MF induction vector module in the m points P_i of the space under consideration. In this case, of course, it is necessary to take into account the constraints on the control vector and the state variables of the system, the vector of the unknown and variable parameters in the form of a vector inequality

$$G(X, \delta) \leq G_{\max}. \quad (3)$$

In the multi-criteria game (2), the first player is the parameter vector of the regulator X and its strategy is the minimization of the vector gain (2), and the second player is a vector δ of variable parameters characterizing the uncertainty of the plant parameters and the strategy of this player is maximization of the same vector gain [11].

Note that the components of the vector gain (2) are nonlinear functions of the required parameters vectors X and δ are calculated on the basis of the solutions of the Maxwell equations in the quasi-stationary approximation [12-16].

Method of synthesis. Consider the algorithm for finding the equilibrium of the game problem. To find the equilibrium state of the multi-criterion game (2) from Pareto-optimal solutions taking into account the preference relations [11], we construct an algorithm for stochastic multi-agent optimization based on the set of particle swarms [17], the number of which m is equal to the number of components of the vector gain (2). The motion of i particle of j swarm is described by the following expressions

$$v_{ij}(t+1) = w_j v_{ij}(t) + c_{1j} r_{1j}(t) H(p_{1j} - \varepsilon_{1j}(t)) [y_{ij}(t) - \dots] \quad (4)$$

$$u_{ij}(t+1) = w_j u_{ij}(t) + c_{2j} r_{2j}(t) H(p_{2j} - \varepsilon_{2j}(t)) [z_j^*(t) - x_{ij}(t)] \quad (5)$$

$$\begin{aligned} x_{ij}(t+1) &= x_{ij}(t) + v_{ij}(t+1) \\ \delta_{ij}(t+1) &= \delta_{ij}(t) + u_{ij}(t+1), \end{aligned} \quad (6)$$

where $x_{ij}(t)$, $\delta_{ij}(t)$ and $v_{ij}(t)$, $u_{ij}(t)$ is the position and velocity of i particle of j swarm; $y_{ij}(t)$, $z_j^*(t)$ and y_j^* , z_j^* – the best local – lbest and global – gbest positions of the i -th particle, found respectively by only one i -th particle and all the particles of j swarm.

Moreover, the «best» position of the j particle of j swarm on a vector $x_{ij}(t)$ is understood in the sense of a minimum of the scalar gain $B(X, \delta, P_j)$, and by the vector $\delta_{ij}(t)$ is understood in the sense of the maximum of the same scalar gain. Positive constants c_1 , c_2 , random numbers $r_{1j}(t)$, $r_{2j}(t)$, inertia coefficients w_j and switching functions H are tuning parameters of the algorithm.

Note that in connection with the fact that the vector of the solutions of the game (2) is represented in the form of strategies of two players X – the vector of the parameters of the regulators and the δ – the vector of the variable parameters of the plant, where it is necessary to minimize the vector gain (2) along the regulators parameter vector X and maximize the same vector gain (2) with respect to the of plant parameters variable vector δ . Therefore, each i particles of j swarm has two components of position $x_{ij}(t)$, $\delta_{ij}(t)$ and two components of velocity $v_{ij}(t)$, $u_{ij}(t)$ to find the two desired components of the regulators parameters vector X and the variable parameters vector δ .

In conclusion, we note that the original multi-criteria game (2), (3), taking into account the algorithm for its solution (4) – (7), is a multi-criteria stochastic dynamic game, since it clearly has time and random search [6, 7].

Computer simulation results. Consider the result of synthesis of robust ASS of MF created by group of HVPL. This situation is typical for the outskirts of cities, where several power lines are suitable, as well as near power line substations. The layout of group of HVPL, compensating coil and screening zone of the system under consideration is shown in Fig. 1. In the immediate vicinity of the shielding zone there are two double-circuit 110 kV HVPL-1 and HVPL-2, a double-circuit 330 kV HVPL-3 and a single-circuit 330 kV HVPL-4.

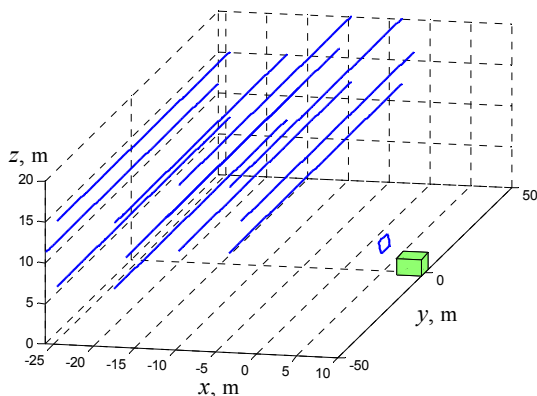


Fig. 1. Layout of group of high voltage power lines, compensating coil and screening zone

For the synthesis of ASS, in addition to the geometric dimensions of the transmission lines and the shielding zone, the values of the currents in the current conductors of the all HVPL are necessary. To this, first, experimental studies of the level of the magnetic field both in the shielding zone and near the transmission lines were carried out. Based on the obtained experimental data, the problem of current identification in current conductors of the power line is solved, under which the sum of the squares of the errors of the measured and model-them magnetic field induction values at given points is minimized.

In Fig. 2 shows the equal level lines of the initial magnetic field induction vector module.

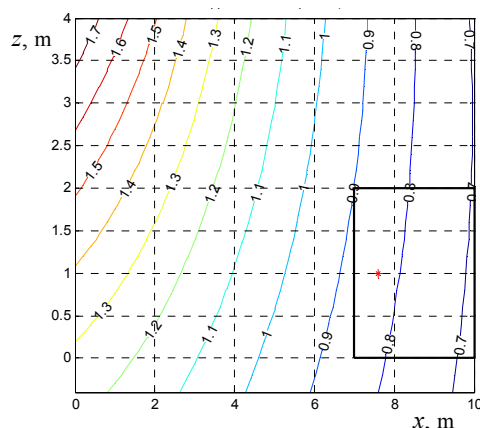


Fig. 2. Equal level lines of the initial magnetic field induction vector module

The MF initial induction generate by HVPL in the space under consideration is $0.9 \mu\text{T}$, which is 1.8 times higher than the MF sanitary standards of Ukraine.

Based on the model of MF created by group of HVPL, the problem of synthesis of a robust ASS was solved. The ASS contains one compensation coil.

On the basis of experimental research, it was found that in the shielding zone, the MF generated by group of HVPL has the space-time characteristics (STC) of such MF is a strongly elongated ellipse [9] and, consequently, the initial MF has a negligible polarization. Active screening of such MF is possible with the use of single compensation coil. It should be noted that such systems have become most widespread in the world practice [2].

In Fig. 3 shows the equal level lines of the compensation coil magnetic field induction vector: module (a), component along Z axes (b) and component along X axes (c) with the robust active screening system is on.

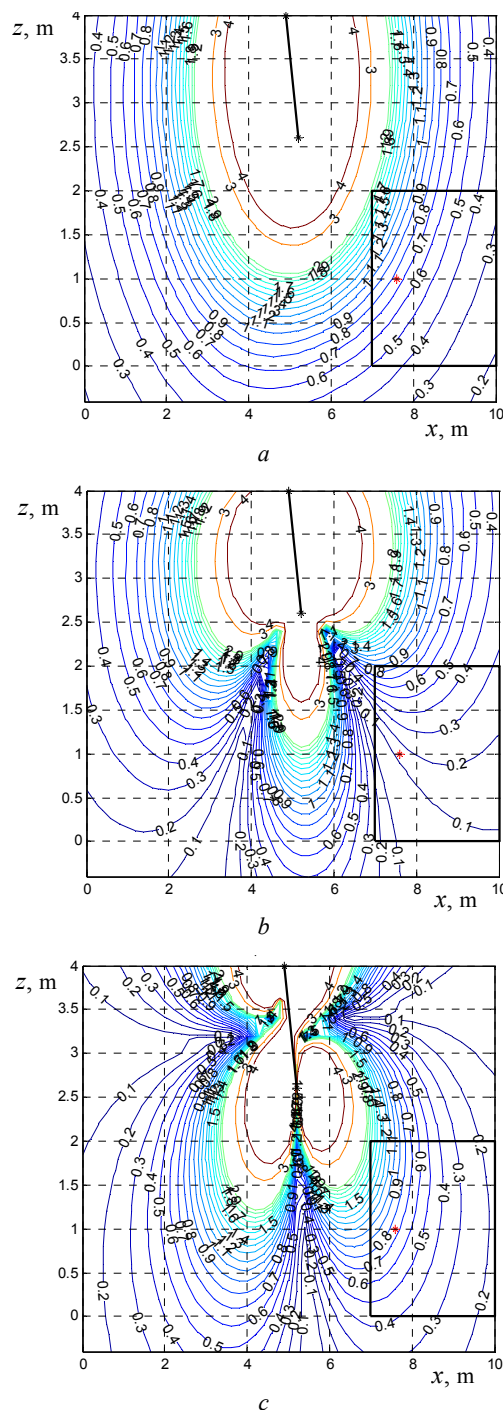


Fig. 3. Equal level lines of the compensation coil magnetic field induction vector: module (a), component along Z axes (b) and component along X axes (c) with the robust active screening system is on

In Fig. 4 shows the equal level lines of the magnetic field induction vector: module (a), component along Z axes (b) and component along X axes (c) with the robust active screening system is on. When the active shielding system is on, as can be seen from Fig. 3, the MF induction level in the residential space under consideration does not exceed $0.5 \mu\text{T}$.

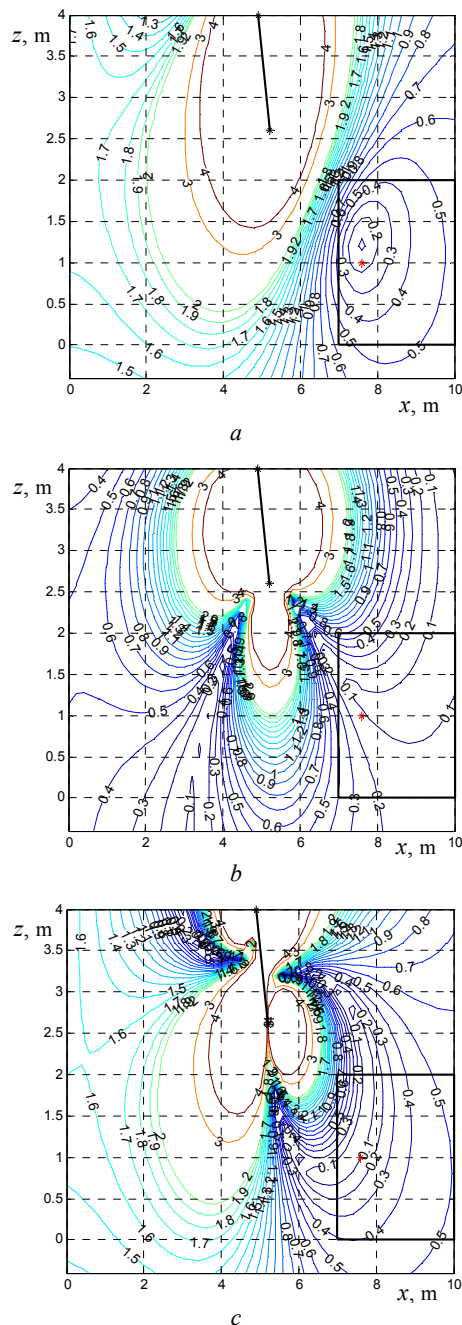


Fig. 4. Equal level lines of the magnetic field induction vector: module (a), component along Z axes (b) and component along X axes (c) with the robust active screening system is on

In Fig. 5 shows the STC of MF, created by group of HVPL (1); compensating coil (2) and total MF with the ASS is on (3). Naturally, such a MF can be effectively compensated for using a single-loop ASS. With single coil, the big axis of the STS ellipse of the initial MF is compensated, so that the STS of the total MF with the ASS is on is an ellipse with an ellipse coefficient 0.8.

In the robust system, the maximum value of the magnetic induction in the protected zone does not exceed $0.5 \mu\text{T}$, which corresponds to the sanitary norms of Ukraine [7]. For the worst-case scenario, when vector parameters variations lead to the greatest deterioration in the compensation of the initial magnetic field by a robust system, the maximum value of the level of magnetic induction in the protected zone increases by 10 %

compared to the robust system at nominal values of the parameters when the vector $\delta = 0$. In spite of the fact that in the initial optimal system with nominal values of the parameters, the maximum value of the level of magnetic induction in the protected zone is approximately 10 % less than in robust systems and is $0.4 \mu\text{T}$. However, when the vector of variable parameters is changed for the worst-case case, the maximum value of the level of magnetic induction in the initial optimal system increases to $0.6 \mu\text{T}$.

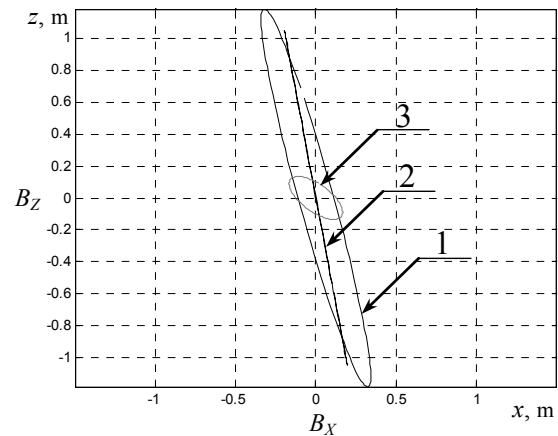


Fig. 5. Space-time characteristics of magnetic field: initial (1), compensation coil (2) and resultant magnetic field with the robust active screening system is on (3)

Note that the position of the compensating coil of the robust system, shown in Fig. 3, slightly differs from the position of the compensating coil of the optimal system [9]. Also, the parameters of the controllers of the robust and original optimal system are not significantly different, as a result of which the robustness of the synthesized system with respect to the optimal system is ensured.

Thus, the synthesized robust ASS makes it possible to reduce the sensitivity of the system to changes in the parameters of the control object in comparison with the initial ASS.

Experimental research results. Consider the field experimental research of the full scale ASS layout [18]. Compensation coil of the full scale ASS layout is a square shape, the upper branch of which is located at a height of 4 m from the ground, and the lower branch is located at a height of 2.6 m from the ground. The compensation coil contains 20 winds and is powered by amplifier type TDA7294.

The ASS contains an external MP induction controller and an internal current controller. An inductive sensor is used as an MF induction sensor, and the MP measurement is performed by EMF-828 type magnetometer of the Lutron Firm. The ASS is powered by an autonomous source. Field experimental research of a single-loop MF ASS with open and closed-loop control algorithms were carried out. The results of comparison of experimental and calculated of MP induction values in a residential zone are given. It is shown that the experimental and calculated MF induction values differ by not more than 10 %.

Conclusions.

1. For the first time the synthesis of robust active screening system of magnetic field, generated by group of

high voltage power lines for reducing the induction of the initial magnetic field to the sanitary standards level and reducing the sensitivity of the system to variations in the plant parameters is given.

2. The synthesis of a robust active screening system is based on multi-criteria stochastic game decision, the equilibrium state of which is based on multiswarm stochastic multi-agent optimization from Pareto-optimal solutions.

3. As a result of active screening system synthesis the spatial position of one compensation coil and the parameters of the regulator are determined. System reduce the level of the initial magnetic field induction throughout the considered residential area up to the Ukraine sanitary norms level and has less sensitivity to plant parameters variations in comparison with the known systems.

REFERENCES

1. Rozov V.Yu., Reutskyi S.Yu., Pelevin D.Ye., Pyliugina O.Yu. The magnetic field of power transmission lines and the methods of its mitigation to a safe level. *Technical Electrodynamics*, 2013, no.2, pp. 3-9. (Rus).
2. Active Magnetic Shielding (Field Cancellation). Available at: <http://www.emf-services.com/afcs.html> (accessed 10 September 2012).
3. Ter Brake H.J.M., Huonker R., Rogalla H. New results in active noise compensation for magnetically shielded rooms. *Measurement Science and Technology*, 1993, Vol. 4, Issue 12, pp. 1370-1375. doi: 10.1088/0957-0233/4/12/010.
4. Celozzi S., Garzia F. Active shielding for power-frequency magnetic field reduction using genetic algorithms optimization. *IEE Proceedings – Science, Measurement and Technology*, 2004, Vol.151, no.1, pp. 2-7. doi: 10.1049/ip-smt:20040002.
5. Shenkman A., Sonkin N., Kamensky V. Active protection from electromagnetic field hazards of a high voltage power line. *HAIT Journal of Science and Engineering. Series B: Applied Sciences and Engineering*, Vol. 2, Issues 1-2, pp. 254-265.
6. Beltran H., Fuster V., García M. Magnetic field reduction screening system for a magnetic field source used in industrial applications. *9 Congreso Hispano Luso de Ingeniería Eléctrica (9 CHLIE)*, Marbella (Málaga, Spain), 2005, pp. 84-99.
7. *Electrical installation regulations. 5th ed.* The Ministry of Energy and Coal Mining of Ukraine, 2014. 277 p. (Ukr).
8. Rozov V.Yu., Grinchenko V.S., Pelevin D.Ye., Chumikhin K.V. Simulation of electromagnetic field in residential buildings located near overhead lines. *Technical electrodynamics*, 2016, no.3, pp. 6-8. (Rus).
9. Kuznetsov B.I., Nikitina T.B., Voloshko A.V., Bovdyj I.V., Vinichenko E.V., Kobilyanskiy B.B. Synthesis of an active shielding system of the magnetic field of power lines based on multiobjective optimization. *Electrical engineering & electromechanics*, 2016, no.6, pp. 26-30. (Rus). doi: 10.20998/2074-272X.2016.6.05.
10. Ren Z., Pham M.-T., Koh C.S. Robust Global Optimization of Electromagnetic Devices With Uncertain Design Parameters: Comparison of the Worst Case Optimization Methods and Multiobjective Optimization Approach Using Gradient Index. *IEEE Transactions on Magnetics*, 2013, vol.49, no.2, pp. 851-859. doi: 10.1109/tmag.2012.2212713.
11. Ummels M. *Stochastic Multiplayer Games: Theory and Algorithms*. Amsterdam University Press, Amsterdam, 2010. 174 p. doi: 10.5117/9789085550402.
12. Rozov V.Yu., Reutskyi S.Yu., Pyliugina O.Yu. The method of calculation of the magnetic field of three-phase power lines. *Technical electrodynamics*, 2014, no.5, pp. 11-13. (Rus).
13. Panchenko V.V., Maslii A.S., Pomazan D.P., Buriakovskiy S.G. Determination of pulsation factors of the system of suppression of interfering harmonics of a semiconductor converter. *Electrical engineering & electromechanics*, 2018, no.4, pp. 24-28. (Rus). doi: 10.20998/2074-272X.2018.4.04.
14. Buriakovskiy S., Maslii A., Maslii A. Determining parameters of electric drive of a sleeper-type turnout based on electromagnet and linear inductor electric motor. *Eastern-European Journal of Enterprise Technologies*, 2016, vol.4, no.1(82), pp. 32-41. (Rus). doi: 10.15587/1729-4061.2016.75860.
15. Zagirnyak M., Chornyi O., Nykyforov V., Sakun O., Panchenko K. Experimental research of electromechanical and biological systems compatibility. *Przegląd Elektrotechniczny*, 2016, no.1, pp. 128-131. doi: 10.15199/48.2016.01.31.
16. Buriakovskiy S.G., Maslii A.S., Panchenko V.V., Pomazan D.P., Denis I.V. The research of the operation modes of the diesel locomotive CHME3 on the imitation model. *Electrical engineering & electromechanics*, 2018, no.2, pp. 59-62. (Ukr). doi: 10.20998/2074-272X.2018.2.10.
17. Shoham Y., Leyton-Brown K. *Multiagent Systems: Algorithmic, Game-Theoretic, and Logical Foundations*. Cambridge University Press, 2009. 504 p.
18. Kuznetsov B.I., Nikitina T.B., Voloshko A.V., Bovdyj I.V., Vinichenko E.V., Kobilyanskiy B.B. Experimental research of magnetic field sensors spatial arrangement influence on efficiency of closed loop of active screening system of magnetic field of power line. *Electrical engineering & electromechanics*, 2017, no.1, pp. 16-20. (Rus). doi: 10.20998/2074-272X.2017.1.03.

Received 10.05.2018

B.I. Kuznetsov¹, Doctor of Technical Science, Professor,
T.B. Nikitina², Doctor of Technical Science, Professor,
V.V. Kolomiets², Candidate of Technical Science,
I.V. Bovdui¹, Candidate of Technical Science,
A.V. Voloshko¹, Candidate of Technical Science,
E.V. Vinichenko¹, Candidate of Technical Science,
¹ State Institution «Institute of Technical Problems
of Magnetism of the NAS of Ukraine»,
19, Industrialna Str., Kharkiv, 61106, Ukraine,
phone +380 50 5766900,
e-mail: kuznetsov.boris.i@gmail.com
² Kharkov National Automobile and Highway University,
25, Yaroslava Mudroho Str., Kharkov, 61002, Ukraine,
e-mail: tatjana55555@gmail.com

How to cite this article:

Kuznetsov B.I., Nikitina T.B., Kolomiets V.V., Bovdui I.V., Voloshko A.V., Vinichenko E.V. Synthesis of robust active shielding systems of magnetic field generated by group of high-voltage power lines. *Electrical engineering & electromechanics*, 2018, no.5, pp. 34-38. doi: 10.20998/2074-272X.2018.5.06.

N.I. Suprunovska, M.A. Shcherba

METHOD FOR VOLTAGE CONTROL IN CHARGE CIRCUIT OF ELECTRIC DISCHARGE INSTALLATIONS WITH TWO CAPACITORS UNDER NONZERO INITIAL CONDITIONS

Purpose. To analyze the transient processes in the charge circuit of electric discharge installations with two capacitors, taking into account the change in the initial conditions of such processes (initial voltage on the capacitors and the initial current in the charge circuit) as well as to develop the method for charge voltage control of such installations using purposeful change of these initial conditions. **Methodology.** We have applied the concepts of theoretical electrical engineering, the principles of theory of electrical circuits, and mathematical simulation in the software package MathCAD 12. **Results.** We have obtained analytical expressions and graphical dependencies establishing a quantitative relationship between the value of the maximum charge voltage of an electric discharge installation and the values of the initial voltage on its capacitors and the initial current in the circuit. This allows us to propose the method for the charge voltage control of electric discharge installations with two reservoir capacitors, using a purposeful change in their initial voltages and initial current in the charge circuit. **Originality.** For the first time, we have found that the charge voltage of the installation can be controlled using two influence mechanisms – either changing the initial current in the charge circuit (by interrupting the transient process of the first capacitor charge at a certain time) or using a nonzero initial voltage on the charged second capacitor. In this case the charge voltage can be varied by 2 times. **Practical value.** The use of this method makes it possible to obtain discharge pulses of complex shape in the technological load, since the maximum charge voltages of the first capacitor and second one can differ by a factor of 1.5. References 10, figures 4.

Keywords: electric discharge installation, capacitor charge, charge voltage, transients, nonzero initial conditions.

Цель. Целью статьи является анализ переходных процессов в зарядной цепи электроразрядных установок с двумя конденсаторами с учетом изменения начальных условий протекания таких процессов (начального напряжения на конденсаторах и начального тока в зарядной цепи), а также разработка метода регулирования зарядного напряжения таких установок, используя целенаправленное изменение указанных начальных условий. **Методика.** Для проведения исследований использовались положения теоретической электротехники, теория электрических цепей, математическое моделирование в программном пакете MathCAD 12. **Результаты.** Получены аналитические выражения и графические зависимости, устанавливающие количественную связь между значением максимального зарядного напряжения установок и величинами начального напряжения на ее конденсаторах и начального тока в цепи. Предложен метод регулирования напряжения заряда электроразрядных установок с двумя накопительными конденсаторами, использующий целенаправленное изменение их начальных напряжений и начального тока в зарядной цепи. **Научная новизна.** Установлено, что напряжение заряда установки можно регулировать, используя два механизма влияния – как изменяя начальный ток в зарядной цепи (прерыванием переходного процесса заряда первого конденсатора в определенный момент времени), так и используя ненулевое начальное напряжение на заряжаемом втором конденсаторе. При этом напряжение заряда можно изменять в 2 раза. **Практическое значение.** Использование данного метода позволяет получить разрядные импульсы сложной формы в технологической нагрузке, поскольку максимальные напряжения заряда первого и второго конденсаторов могут отличаться в 1,5 раза. Библи. 10, рис. 4.

Ключевые слова: электроразрядная установка, заряд конденсатора, зарядное напряжение, переходные процессы, ненулевые начальные условия.

Introduction. Electric discharge installations (EDIs) with capacitive energy storage devices (reservoir capacitors) have found wide application in the development of new technologies for electric pulse treatment of materials and media (in particular, electro-erosion, electro-hydraulic, magneto-pulse treatments, etc.) [1-8].

The use of parallel connection of capacitors with different capacities is one of the most common methods for control of the EDIs dynamic parameters.

So, for example, several capacitors with different capacities, which are discharged through a load with a time delay, are used in many schemes of electric discharge installations in order to control the shape of the pulse currents in the load [1, 2, 9]. In the installations containing semiconductor DC voltage shapers with filtering capacitors of high-capacity, additional dosing capacitors are used to more accurately control the energy in the load [1, 7, 8, 10]. Additional low-capacity dosing capacitors are also used in the input circuits of semiconductor converters to stabilize

the power consumed by them from the electrical network [2, 3, 5, 10].

It should be noted that in most of considered electric discharge installations, the initial charge voltages and the final discharge voltages of their capacitors were equal to zero [1, 3-6].

At the same time, the reservoir capacitor is not completely discharged in the EDIs for volumetric electro-spark dispersion (VESD) of metal granules in a dielectric liquid. The residual voltage of the capacitor is used as information for changing the voltage of the subsequent charge of the capacitor [7]. In these installations, the dependence of the resistance of the electric spark load on the magnitude and duration of the discharge current is used for parametric stabilization of the dispersion modes [7, 8].

If an oscillatory discharge of the capacitor through the load occurs and the capacitor is partially recharged to a reverse polarity voltage, then the negative feedback

of the subsequent charge voltage of the capacitor with its previous discharge voltage is realized in the installation. If an aperiodic discharge occurs, then a positive feedback between these voltages is realized. In fact, high-speed control and parametric stabilization of electrical technological modes is implemented in such installations [7, 8].

Thus, the change in the magnitude and sign of the initial voltage of the capacitor can be used to develop methods for high-speed control of energy in the capacitor, discharge pulse parameters, EDIs efficiency, as well as for parametric stabilization of discharge processes in a circuit with a nonlinear load [7, 8].

The solution of the problems of improving the energy characteristics of such EDIs is much more complicated when you change the initial and final conditions of the transients in circuits of reservoir capacitors that are part of such installations.

In addition, the analysis of transient processes with a nonzero initial current in the charging circuit of the EDIs with several reservoir capacitors has not been carried out previously.

Therefore, **the purpose** of this paper is to analyze the transient processes in the charge circuit of electric discharge installations for the VESD with two reservoir capacitors, taking into account the change in the initial conditions of such processes (initial capacitors voltage and the initial current in the charge circuit), as well as to develop the method for control of the charge voltage of such installations using purposeful change of these initial conditions.

As a typical example of such EDIs, we have considered the installation for electro-spark dispersion of conductive granules in a dielectric liquid, the charge circuit of which includes two reservoir capacitors.

Features of the capacitor charge when the initial current changes. The electric schematic diagram of the charge circuit of the EDI, where the transient processes are analyzed, is shown in Fig. 1.

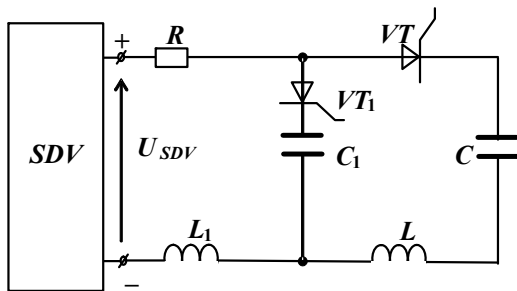


Fig.1. Electric schematic diagram of the charge circuit of EDI with two reservoir capacitors

The capacitor C (Fig. 1) is charged from a shaper of direct voltage (SDV) with an output voltage U_{SDV} through a resistor R , thyristor commutator VT , and inductance coils L and L_1 . The thyristor VT_1 was locked up to a certain time $t = t_1$. There is an oscillatory charge of capacitor C in the charge circuit, since the parameters of the circuit elements (R, C, L, L_1) were chosen in such a way as to realize high Q -factor of the circuit ($Q \geq 10$).

At time $t = t_1$, when the charge voltage of the capacitor C becomes higher than the SDV voltage $U_C > U_{SDV}$, the thyristor commutator VT_1 is unlocked.

The capacitor C_1 begins to charge from the SDV . We assume that in the general case there is some voltage on the capacitor C_1 ($U_{0C_1} \neq 0$) before starting its charge.

Since $U_C > U_{SDV}$, then the capacitor C tries to discharge to the capacitor C_1 , however, the occurrence of reverse current in the circuit leads to the locking of the thyristor VT . Inductance L is needed to limit the reverse current in the circuit when the thyristor VT is locked.

Thus, there are two transient processes in the charge circuit of an EDI with two capacitors: the first process is the charge of the capacitor C from the SDV in the time interval $0 \leq t \leq t_1$ and the second process is the charge of the capacitor C_1 from the SDV at $t > t_1$.

In the analysis of transient processes we have assumed that the thyristors VT and VT_1 are ideal switches (without energy losses and with instantaneous commutation), and the inductance value L is less by two orders of the inductance L_1 , therefore, value L can be ignored in the analysis of the first transient process.

Since the first transient is the ordinary oscillating charge of the capacitor C from the SDV under zero initial conditions, then we have analyzed in detail only the second transient process – the charge of the capacitor C_1 from the SDV , which occurs under a nonzero initial conditions in voltage U_{0C_1} and in current I_1 (due to the first transient process and the presence of inductance in the circuit) after switching thyristor VT_1 .

The initial current I_1 is determined by the known formulas for the oscillatory charge of the capacitor from a direct voltage source. The parameters of the charge circuit of the capacitor C_1 (R, C_1, L_1) are also chosen so there was an oscillatory transient process.

Transient analysis of the capacitor charge under nonzero initial voltage and current conditions. The initial time of the second transient process is $t = t_1$ and we denote it as t_0^* . The current time of this transient process, denoted by t^* , is defined as $t^* = t - t_1 = t - t_0^*$.

According to the second Kirchhoff's law the current in the SDV - R - VT_1 - C_1 - L_1 - SDV circuit (Fig. 1) is given by formula

$$i(t^*) = (U_{SDV} - u_{C_1}(t^*) - u_{L_1}(t^*)) / R, \quad (1)$$

here $u_{C_1}(t^*)$ and $u_{L_1}(t^*)$ are the voltage drop across the capacitor C_1 and the inductance L_1 , respectively.

Since $i(t^*) = C_1 du_{C_1}(t^*) / dt^*$, and $u_{L_1}(t^*) = L_1 di(t^*) / dt^* = L_1 C_1 d^2 u_{C_1}(t^*) / dt^{*2}$, then equation (1) can be reduced to the form:

$$\frac{d^2 u_{C_1}(t^*)}{dt^{*2}} + \frac{R}{L_1} \frac{du_{C_1}(t^*)}{dt^*} + \frac{du_{C_1}(t^*)}{L_1 C_1} = \frac{U_{SDV}}{L_1 C_1}. \quad (2)$$

Taking into account that in the general case there are the certain voltage $U_{0C_1} \neq 0$ on the capacitor C_1 before start of its charge and nonzero current of value I_1 in the circuit (determined in the first transient process of charging the capacitor C), then we can write the solution of such a non-uniform equation in the form:

$$u_{C_1}(t^*) = U_{SDV} + \left[\left\{ p_2 (U_{0C_1} - U_{SDV}) / (p_2 - p_1) - I_1 / C_1 \right\} e^{p_1 t^*} + \left\{ I_1 / C_1 - p_2 (U_{0C_1} - U_{SDV}) \right\} e^{p_2 t^*} \right] \quad (3)$$

Since $i(t^*) = C_1 du_{C_1}(t^*)/dt^*$, the expression for the current in the charge circuit can be written as:

$$i(t^*) = (U_{0C_1} - U_{SDV}) \left(e^{p_1 t^*} - e^{p_2 t^*} \right) / L_1 (p_2 - p_1) + I_1 \left(p_2 e^{p_2 t^*} - p_1 e^{p_1 t^*} \right) / (p_2 - p_1). \quad (4)$$

Since charge circuit parameters are selected so that the circuit has a high Q -factor, then there is an oscillatory transient process, and consequently the roots of the characteristic equation are conjugate complexes:

$$p_1 = -R/2L_1 + j\sqrt{1/L_1 C_1 - R^2/4L_1^2} = -b + j\omega,$$

$$p_2 = -R/2L_1 - j\sqrt{1/L_1 C_1 - R^2/4L_1^2} = -b - j\omega,$$

here $\omega = \sqrt{1/L_1 C_1 - R^2/4L_1^2}$, $b = R/2L_1$.

After substituting the values of p_1 and p_2 in (3) and (4) and performing the transformations, we obtain expressions for $u_{C_1}(t^*)$ and $i(t^*)$:

$$u_{C_1}(t^*) = U_{SDV} - \chi e^{-bt^*} \left((b/\omega - I_1/\omega \cdot \chi \cdot C_1) \sin \omega t^* + \cos \omega t^* \right), \quad (5)$$

$$i(t^*) = e^{-bt^*} \left[(\chi/L_1 \omega - I_1 b/\omega) \sin \omega t^* + I_1 \cos \omega t^* \right], \quad (6)$$

here $\chi = U_{SDV} - U_{0C_1}$.

The value of the current I_1 , which is the initial current for second transient (charge transient of the capacitor C_1), we determine by the formula for the oscillatory charge of the capacitor C (in general having some initial voltage U_{0C}) from the SDV :

$$I_1 = i(t = t_1) = (U_{SDV} - U_{0C}) e^{-bt_1} \cdot \sin \omega t_1 / L_1 \omega, \quad (7)$$

here $\omega_1 = \sqrt{1/L_1 C - R^2/4L_1^2}$.

Calculations and data processing for the charge circuit (Fig. 1) with parameters $U_{SDV} = 500$ V, $L = 2 \cdot 10^{-6}$ H, $L_1 = 2 \cdot 10^{-4}$ H, $C = 10^{-4}$ F, $C_1 = 4 \cdot 10^{-5}$ F, $R = 0.1$ Ohm we have performed using the software package MathCAD 12. As mentioned above, the inductance L is two orders of magnitude smaller than L_1 , so we did not take it into account when performing calculations.

Table 1 shows the results of the calculation of the first transient process (the currents in the charge circuit and the charge voltage of capacitor C in the time interval from $t \approx \tau_{charge}/2$ (when the current is $I_1 = I_{1max}$) to $t = \tau_{charge}$ (when current $I_1 = 0$). Here τ_{charge} is the charge duration of capacitor C . These results are required for further analysis.

Analysis of the results of Table 1 shows that interrupting the charging process of capacitor C , when the charge circuit current reaches values in the range $I_{1max} \div 0$, we can change the control conditions of the charge voltage of the capacitor C , i.e. we can adjust the charge voltage (to perform so-called a tune-up) in the range of $7 \div 50$ %.

Fig. 2 represents the time dependence of the current in the charge circuit of the EDI $i(t^*)$ for various values

of the initial current I_1 : $(0, I_{1max}/2, 2I_{1max}/3, I_{1max})$ and the initial voltage $U_{0C_1} = 0$.

Table 1

The results of calculation of currents and charge voltages of capacitor C in the time interval from $t \approx \tau_{charge}/2$ to $t = \tau_{charge}$

$t_1 \cdot 10^{-6}$, s	$i(t_1)$, A	$u(t_1) = U_{Cmax}$, V
217.9	$I_1 = I_{1max} = 335$	469
337.9	$I_1 = 2I_{1max}/3 = 223$	824
366.9	$I_1 = I_{1max}/2 = 168$	881
444.4	$I_1 = 0$	947

$i(t^*)$, A for $U_{0C_1} = 0$

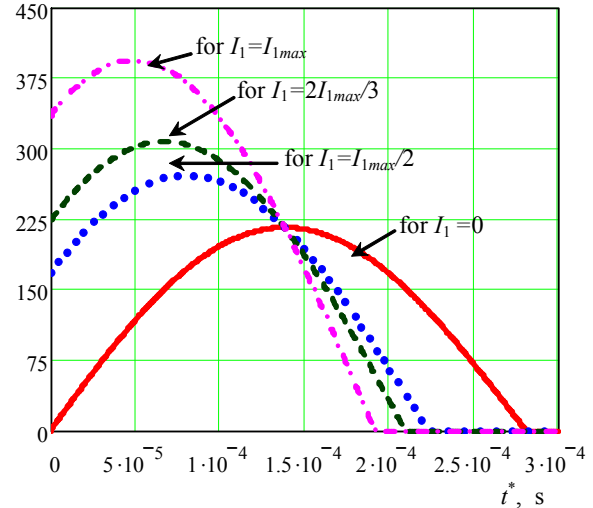


Fig. 2. The time variation in the charging current of capacitor C_1 with initial voltage $U_{0C_1} = 0$ at different initial circuit current values

As can be seen from Fig. 2, with a decrease in the value of the initial current I_1 the amplitude value of the current in the charge transient process of the capacitor C_1 decreases, and the duration of current flow increases. In other words, the earlier the first transient is interrupted, the faster and with the higher currents the second one proceeds.

Fig. 3, a-c shows the time dependence of the voltage $u_{C_1}(t^*)$, and Table 2 represents the values of the maximum charge voltage of the capacitor C_1 for different initial current I_1 $(0, I_{1max}/2, 2I_{1max}/3, I_{1max})$ and initial voltage U_{0C_1} $(0, U_{SDV}/2, 2U_{SDV}/3)$.

Analyzing dependences shown in Fig. 3 and the data in Table 2, we can conclude that with a decrease in the initial current I_1 , the maximum charging voltage of the capacitor C_1 in the second transient process also decreases.

So if the initial current decreases from I_{1max} to zero, the voltage value U_{C_1max} decreases by 30 % at $U_{0C_1} = 0$ and by 47 % at $U_{0C_1} = 2U_{SDV}/3$. Thus, the magnitude of the initial voltage U_{0C_1} also affects the value of U_{C_1max} , and with increasing U_{0C_1} the voltage U_{C_1max} also decreases.

For example, if the initial voltage U_{0C_1} of the capacitor C_1 increases from zero to $2U_{SDV}/3$ when the value of the current in the $SDV-R-VT-C-L-L_1-SDV$ circuit $I_1 = I_{1max}$, the value of the maximum charge voltage U_{C_1max} of the capacitor C_1 decreases by 9 %, and at current value $I_1 = 0$ this voltage decreases by 32 %. In other words, the later the first charge transient of capacitor C is interrupted, and the higher initial voltage on capacitor C_1 , the lower its maximum charge voltage after second transient.

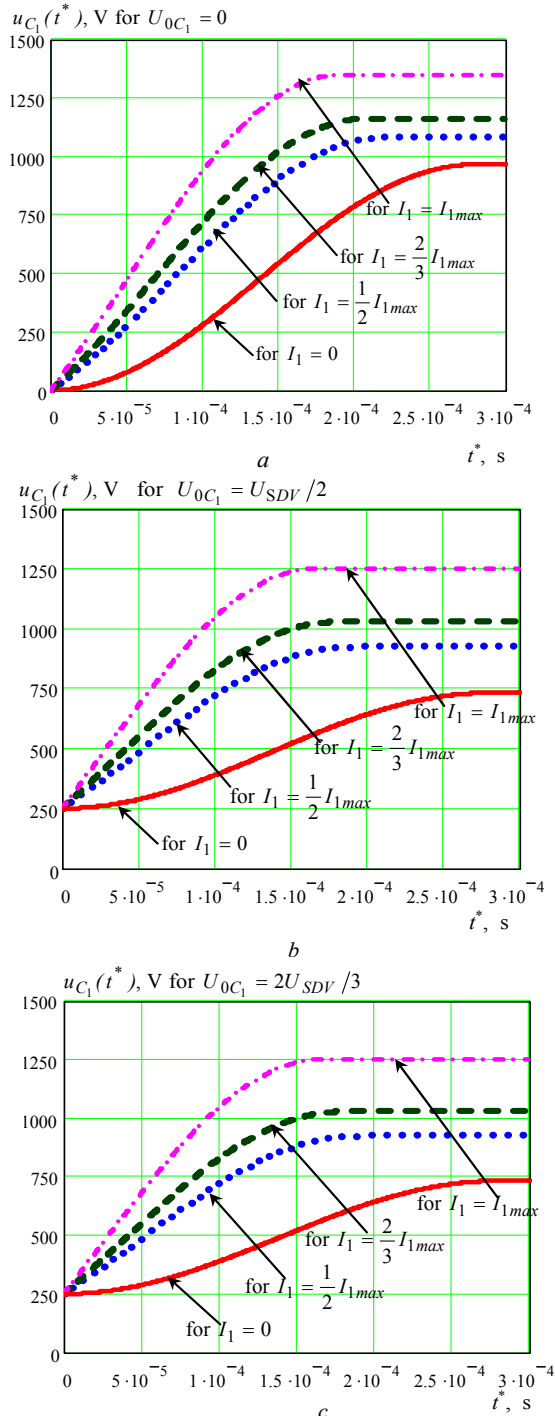


Fig. 3. The change with time of the charge voltage $u_{C_1}(t^*)$ of the capacitor C_1 at its various initial voltages and different initial values of the current in the circuit ($0, I_{1max}/2, 2I_{1max}/3, I_{1max}$): a – for $U_{0C_1} = 0$; b – for $U_{0C_1} = U_{SDV}/2$; c – $U_{0C_1} = 2U_{SDV}/3$

Fig. 4 represents the dependence of maximum voltage U_{C_1max} on the initial current I_1 for different initial voltages U_{0C_1} on the capacitor C_1 .

Table 2
Maximum charge voltage U_{C_1max} for different values I_1 and U_{0C_1}

U_{0C_1}, V	0	$U_{SDV}/2$	$2U_{SDV}/3$
$I_1 = I_{1max}$	1349	1252	1234
$I_1 = 2I_{1max}/3$	1163	1029	1001
$I_1 = I_{1max}/2$	1084	925	889
$I_1 = 0$	966	733	655

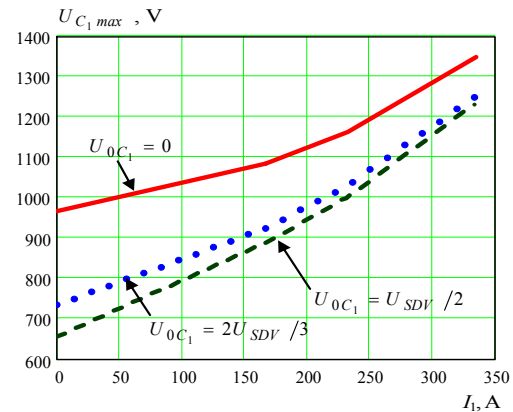


Fig. 4. The change in the maximum charge voltage U_{C_1max} of the capacitor C_1 as a function of the magnitude of the initial current I_1 , at which the transient of charge C_1 begins

As can be seen in Fig. 4, the charge voltage of the capacitor C_1 can be controlled by changing the initial current in its charge circuit by means of varying the duration of the charge process of the capacitor C .

The charge voltage of the capacitor C_1 can also be adjusted by changing its initial voltage before the start of the charge process. Of course, we can simultaneously use both methods for control of voltage U_{C_1max} . In this case, the control range can be $655 \div 1349$ V, that is, the charge voltage can be changed by 2 times.

The charge voltage of the capacitor C_1 can be almost 1.5 times higher than the charge voltage of the capacitor C (see Tables 1 and 2). This fact can be used to produce discharge pulses of complex shapes in spark load.

Conclusions.

1. We have carried out the transient analysis in the charge circuit of the capacitors of electric discharge installation, taking into account the change in the initial conditions of such transients (initial voltage on the capacitors and the initial current in the charging circuit). As the results we have defined the analytical expressions for determining the current in the circuit and the capacitor voltage during its charge under nonzero initial current and voltage conditions.

2. From the formula for the capacitor charge voltage under nonzero initial conditions in such installations follows that it depends on two factors: the initial voltage of this capacitor and the value of the initial current in this transient process. The numerical experiment of capacitor charge under nonzero initial conditions has shown that the

maximum capacitor voltage decreases both with increasing its initial voltage and with decreasing initial circuit current.

3. Based on the revealed dependencies, we proposed a method for charge voltage control of such installations by changing the initial current in the charge circuit (by interrupting the first transient at a certain time), and by using a nonzero initial voltage on the second charged capacitor. The difference in capacitors voltage of the installation can be used to produce discharge pulses of complex shape in the technological load.

REFERENCES

1. Vovchenko A.I., Tertilov R.V. Synthesis of capacitive nonlinear- parametrical energy sources for discharge and pulse technologies. *Proceedings of the National University of Shipbuilding*, 2010, no.4, pp. 118-124. (Rus).
2. Onishchenko L., Gunko V., Grebennikov I., Bandura A. Capacitors for various electrophysical and technological pulsed power applications. *Proceedings of the 1st Intl Congress on Radiation Physics, High Current Electronics, and Modification of Materials*. Tomsk, HCEI, 2000, vol.2, pp. 366-367.
3. Casanueva R., Azcondo F.J., Branas C., Bracho S. Analysis, Design and Experimental Results of a High-Frequency Power Supply for Spark Erosion. *IEEE Transactions on Power Electronics*, 2005, vol.20, no.2, pp. 361-369. doi: **10.1109/tpe.2004.842992**.
4. Ivanov A.V., Sinchuk A.V., Ruban A.S. Effect of the technological parameters of the melt treatment by a electric pulse current on the mixing process. *Surface Engineering and Applied Electrochemistry*, 2012, vol.48, no.2, pp. 180-186. doi: **10.3103/s106837551202007x**.
5. Sen B., Kiyawat N., Singh P.K., Mitra S., Ye J.H., Purkait P. Developments in electric power supply configurations for electrical-discharge-machining (EDM). *The Fifth International Conference on Power Electronics and Drive Systems PEDS 2003*. Singapore, 17-20 November 2003, vol.1, pp. 659-664. doi: **10.1109/PEDS.2003.1282955**.
6. Sunka P., Fuciman M., Babicky V., Clupek M., Benes J., Pouckova P., Soucek J. Generation of focused shock waves by multi-channel electrical discharges in water. *Conference Record of the Twenty-Fifth IEEE International Power Modulator Symposium*, Hollywood, California, USA, 2002, pp. 174-177. doi: **10.1109/MODSYM.2002.1189444**.
7. Suprunovska N.I. Analysis of interdependent charge-discharge processes of capacitor in circuits with positive voltage feedback. *Technical electrodynamics*, 2017, no.4, pp. 14-21. (Rus). doi: **10.15407/techned2017.04.014**.
8. Shcherba A.A., Suprunovska N.I. Cyclic transients in the circuits of electric discharge installations taking into account the influence of magnitude and rate of discharge currents rise on resistance of electric spark load. *Technical electrodynamics*, 2018, no.2, pp. 3-10. (Rus). doi: **10.15407/techned2018.02.003**.
9. Kim J.-S., Rim G.-H., Jin Y.-S., Lee H.-S., Suk H.-Y., Kim K.-S., Jung J.-W., Sung G.-Y. A flexible control scheme for current wave forming using multiple capacitor bank units. *PPPS-2001 Pulsed Power Plasma Science 2001. 28th IEEE International Conference on Plasma Science and 13th IEEE International Pulsed Power Conference*. Digest of Papers (Cat. No.01CH37251). doi: **10.1109/ppps.2001.1001846**.
10. Suprunovska, N.I.; Shcherba, A.A. Features of the energy interchange between capacitors in the circuit using unidirectional commutator or bidirectional one. *Proceedings IEEE International Conference on Intelligent Energy and Power Systems (IEPS-2016)*, June 7-11, 2016, Kyiv, Ukraine, pp. 6-10. doi: **10.1109/IEPS.2016.7521843**.

Received 22.05.2018

N.I. Suprunovska¹, Doctor of Technical Science,
M.A. Shcherba¹, Candidate of Technical Science,
¹ The Institute of Electrodynamics of the NAS of Ukraine,
56, prospekt Peremogy, Kiev, 03057, Ukraine,
phone +380 44 3662493,
e-mail: iednat1@gmail.com, m.shcherba@gmail.com

How to cite this article:

Suprunovska N.I., Shcherba M.A. Method for voltage control in charge circuit of electric discharge installations with two capacitors under nonzero initial conditions. *Electrical engineering & electromechanics*, 2018, no.5, pp. 39-43. doi: **10.20998/2074-272X.2018.5.07**.

M.I. Baranov, S.G. Buriakovskiy, S.V. Rudakov

THE METROLOGY SUPPORT IN UKRAINE OF TESTS OF OBJECTS OF ENERGY, AVIATION AND SPACE-ROCKET ENGINEERING ON RESISTIBILITY TO ACTION OF PULSES OF CURRENT (VOLTAGE) OF ARTIFICIAL LIGHTNING AND COMMUTATION PULSES OF VOLTAGE

Purpose. Presentation and analysis of the modern state of the metrology support in Ukraine of model tests of equipment of objects of energy on resistibility to the action of pulsed current (voltage) of artificial lightning and commutation pulses of voltage, and also objects of aviation and space-rocket engineering on resistibility to lightning. Methodology. Electrophysics bases of engineering of high-voltage and large pulsed currents, theoretical bases of the electrical engineering, technique of the strong electric and magnetic fields, and also measuring technique. Scientific methods of analysis of scientific and technical information. Results. Information is resulted, touching the modern consisting of Ukraine of providing high-voltage measuring facilities conducted on requirements of the normative documents of the USA of SAE ARP 5412:2013, SAE ARP 5416:2013, International Standard of IEC 62305-1:2010 and Standard GOST 1516.2-97 model tests of equipment of objects of energy on resistibility to lightning and commutation resistibility, and also objects of aviation and space-rocket engineering on resistibility to lightning. It is marked that similar measuring facilities are not made by domestic industry. It is indicated that R&DPCI «Molniya» of the NTU «KhPI» disposes the proper measuring facilities of the own making, passing a state metrology check (calibration). Basic technical descriptions are described developed and created at this Institute: high-voltage high-current shunts of type of SC-300M1 and SC-300M2, intended for measuring of micro- and millisecond pulses of current amplitude to ± 220 kA with the integral of their action to $15 \cdot 10^6$ J/Ohm; capacitive (type of CDV-100 and CDV-1,2) and ohmic (type of ODV-1,2 and ODV-2,5) dividers of pulsed voltage of micro- and millisecond duration, capable not only to measure but also form on the tested electric loading standard (non-standard) storm and commutation pulses of voltage amplitude to ± 2 MV. Originality. First in the generalized kind possibilities are developed and created by the domestic scientific and technical workers of high-voltage high-current measuring facilities, intended for the aims of the metrology providing of model tests in obedience to the requirements of domestic and foreign normative documents of equipment of objects of energy on resistibility to lightning and commutation resistibility, and also objects of aviation and space-rocket engineering on resistibility to lightning. Practical value. Application in practice of model tests on powerful high-voltage pulsed current (voltage) of artificial lightning and commutation pulses of voltage of electrical equipment and component elements of objects of energy, aviation and space-rocket engineering on resistibility to lightning and commutation resistibility of the described special high-voltage measuring facilities will be instrumental in the decision of global in the world problem of protection from lightning of ground and air-based technical objects and to the increase of their strength security. References 23, tables 4, figures 16.

Key words: high-voltage generators of pulses of current (voltage) of artificial lightning and commutation pulses of voltage, objects of energy, aviation and space-rocket engineering, measuring facilities for the model tests of technical objects on resistibility to the action of pulses of current (voltage) of artificial lightning and commutation pulses of voltage.

Изложено современное состояние метрологического обеспечения в Украине натурных испытаний объектов промышленной энергетики, авиационной и ракетно-космической техники на стойкость к прямому воздействию на них мощных импульсов тока (напряжения) искусственной молнии и аperiodических коммутационных импульсов напряжения. Показано, что подобные испытания технических объектов на молниестойкость и коммутационную стойкость могут проводиться в соответствии с требованиями нормативных документов США SAE ARP 5412: 2013, SAE ARP 5416: 2013, международного стандарта IEC 62305-1: 2010 и стандарта ГОСТ 1516.2-97 в полевых условиях на уникальных отечественных высоковольтных силовых электроустановках, оснащенных современными измерительными средствами. Описаны основные технические характеристики разработанных и созданных в НИПКИ «Молния» НТУ «ХПИ» для метрологического обеспечения натурных испытаний указанных технических объектов на молниестойкость и коммутационную стойкость: измерительных коаксиальных силовых шунтов типа ШК-300М1 и ШК-300М2, емкостных и омических высоковольтных и сверхвысоковольтных делителей напряжения типа ЕДН-100, ЕДН-1,2, ОДН-1,2 и ОДН-2,5. Приведены примеры практического использования при натурных испытаниях на молниестойкость и коммутационную стойкость отмеченных технических объектов указанных нестандартизованных измерительных средств собственного изготовления. Библ. 23, табл. 4, рис. 16.

Ключевые слова: высоковольтные генераторы импульсов тока (напряжения) искусственной молнии и коммутационных импульсов напряжения, объекты энергетики, авиационной и ракетно-космической техники, измерительные средства для натурных испытаний технических объектов на стойкость к действию импульсов тока (напряжения) искусственной молнии и коммутационных импульсов напряжения.

Introduction. In accordance with the requirements of the current US regulatory documents SAE ARP 5412:2013 [1], SAE ARP 5416:2013 [2] and International Standard IEC 62305-1:2010 [3] for field testing of aviation, rocket and space equipment and power objects to lightning resistibility to the latter pulses of artificial lightning current with different amplitude-time parameters (ATPs) from powerful high-voltage lightning

current generators (LCG) are applied. In this case, the amplitudes I_{mL} of lightning current pulses flowing through the test objects can vary from tens of Amperes to hundreds of thousands of Amperes, and their duration τ_p is from hundreds of microseconds to one thousand milliseconds [1-3]. In the documents [1-3], the numerical values of the normalized ATPs used in the tests for the

© M.I. Baranov, S.G. Buriakovskiy, S.V. Rudakov

lightning resistibility of the considered technical objects of the current pulses of artificial lightning are described in more detail. In [4], the authors described the technical characteristics of unique domestic powerful high-voltage LCG, which realizes the requirements of documents [1-3]. The current Standard GOST 1516.2-97 [5] defines normalized ATPs of voltage pulses of lightning nature and commutation aperiodic voltage pulses used in testing the electrical strength of external (internal) insulation of industrial power engineering objects with capacitive characteristics (for example, switches, disconnectors, bushings, insulators, current transformers, capacitors, etc.). In this case, the thunderstorm aperiodic voltage pulse generated on the tested load by the pulsed voltage generator (PVG), constructed according to the classical Arkadiev-Marx scheme, is characterized by the time shape $\tau_f/\tau_p=1.2 \mu\text{s}/50 \mu\text{s}$ (with tolerances on: front $\tau_f \pm 30\%$, voltage amplitude $U_{mL} \pm 3\%$, pulse duration τ_p at the level $0.5 U_{mL} \pm 20\%$), the normalized maximum value of which U_{mL} usually does not exceed 1 MV [5]. We point out that the amplitude U_{mk} of commutation aperiodic voltage pulses, reproduced on electric load by the commutation voltage pulse generator (CVPG), reaches a level of several Megavolts. The time of rise T_{rise} of such voltage pulses to the level U_{mk} is several hundred microseconds, and their duration T_p at the level of $0.5 U_{mk}$ is up to several thousand microseconds [5]. For the prompt registration of the ATP of the specified current and voltage pulses, appropriate measuring means are required. It should be noted that the domestic industry does not produce such measuring aids. In this regard, the developers and creators of LCG, PVG and CVPG, as well as the operating engineering and technical personnel serving them, are required to independently solve the problems of metrology support of contractual works and applied scientific research carried out with the help of these high-voltage current and voltage generators in the considered relevant worldwide scientific and technical field of engineering and electrophysics of high currents and high (superhigh) voltages.

The goal of the paper is the presentation and analysis of the current state of metrology support in Ukraine of testing equipment of industrial power facilities for lightning resistibility and commutation stability, as well as for aviation and rocket and space equipment for lightning resistibility.

1. Metrology support of testing of technical objects for lightning resistibility. First, let us dwell on the issues of metrology support for the testing of aviation and rocket and space equipment and energy facilities for resistibility to the impact of artificial lightning current pulses on them. For aircraft and rocket and space equipment, such tests are regulated by the requirements of US regulations SAE ARP 5412:2013 [1] and SAE ARP 5416:2013 [2]. According to [1, 2], the following components of the artificial lightning current generated in high-voltage high-current LCG circuits can flow through the tested objects of the indicated technique: pulsed *A*- (or repetitive pulsed *D*-), intermediate *B*- and prolonged *C*- (or shortened long *C** -) components of artificial lightning current. The main ATPs of the component of the pulsed current of artificial lightning are given in Table 1. The

following combinations of these lightning current components are most often used [1, 2, 6]: *A*-, *B*- and *C*-components; *A*-, *B*- and *C**- components; *D*-, *B*- and *C**-components.

Table 1

Normalized ATPs of the main components pulsed current of artificial lightning [1, 2, 4]

Artificial lightning component	I_{mL} , kA	I_c , kA	q_L , C	J_L , 10^6 J/ Ω	τ_f , μs	τ_p , ms
<i>A</i>	200±20	—	—	2±0.4	≤50	≤0.5
<i>B</i>	—	2±0.4	10±1	—	—	5±0.5
<i>C</i>	0.2-0.8	—	200±40	—	—	(0.25÷1)·10 ³
<i>C*</i>	—	0.4	6-18	—	—	15-45
<i>D</i>	100±10	—	—	0.25±0.05	≤25	≤0.5

Note. I_{mL} is the amplitude of the current pulse; I_c is the average value of the current; q_L is the amount of electric charge leaking through the object under test; J_L is the integral of the action of the current pulse; τ_f , τ_p are, respectively, the pulse front duration between the levels (0.1-0.9) I_{mL} and the current pulse at the level $\leq 0.1 I_{mL}$.

For industrial power facilities, the high-voltage high-current tests for lightning resistibility under consideration are governed by the requirements of the International Standard IEC 62305-1:2010 [3] and the national Standard GOST R IEC 62305-1:2010 [7] developed in Russia on this basis. An aperiodic pulsed current of artificial lightning of the time shape $\tau_f/\tau_p=10 \mu\text{s}/350 \mu\text{s}$ of both polarities, characteristic of a direct short thunderstorm attack to terrestrial objects protected by a number of engineering services of power supply companies, is fed from the powerful LCG to the test object. Table 2 shows the main ATPs of this powerful test current pulse of artificial lightning.

Table 2

Normalized ATPs of the aperiodic current pulse of lightning of temporary shape $10 \mu\text{s}/350 \mu\text{s}$ [3, 4]

Name of the lightning current pulse parameter	Lightning protection level of the facility according to the Standard IEC 62305-1: 2010		
	I	II	III-IV
Front duration τ_f , μs	10±2	10±2	10±2
Pulse duration at half-descend τ_p (at the level $0.5 I_{mL}$), μs	350±35	350±35	350±35
Current amplitude I_{mL} , kA	200±20	150±15	100±10
Integral of action J_L , 10^6 J/ Ω	10±3.5	5.6±1.96	2.5±0.875
Charge q_L , C	100±20	75±15	50±10

With regard to testing the electrical strength of external and internal insulation of power facilities to the effects of lightning discharges, according to [5], they are carried out using the above-mentioned thunderstorm voltage pulse of the time shape $1.2 \mu\text{s}/50 \mu\text{s}$. In this case, for its measurement we can use measuring standard balls with a diameter from 125 mm to 1.5 m [8], as well as high-voltage capacitive (CDV) and ohmic (ODV) dividers of voltage for pulsed voltages of $\pm(0.1-2.5)$ MV, having in the composition of high-voltage and low-voltage arms [5, 9].

1.1. Measuring coaxial disk shunts type SC-300M1 and SC-300M2. To record the current pulses of

artificial lightning with the ATPs according to the data of Table 1, 2, generated at the objects under test with powerful LCG [4], satisfying the requirements [1-3], special measuring high-voltage high-current disk shunts of SC-300M1 (Fig. 1) and SC-300M2 (Fig. 2) type of the coaxial design were developed and created at the R&DPCI «Molniya» of the NTU «KhPI». Similar shunt designs are characterized by their small inductance values (not more than 10 nH) and active resistance (no more than 0.2 mΩ), which provides insignificant influence of the own electrical parameters of the measuring shunt on the electromagnetic processes occurring in the load. A significant difference between the designs of these high-current shunts from known (for example, described in [6]) is the use in them instead of a thin-walled (with a thickness of not more than 0.3 mm) high-resistance manganin disk from which the drop in the pulsed voltage from the passage of a measured current pulse is taken, a disk of thickness of 1 to 2 mm from stainless steel 12X18H10T [10, 11].



Fig. 1. External view of the improved coaxial disk shunt type SC-300M1, intended for measurement in the micro- and millisecond ranges of damped sinusoidal and aperiodic current pulses of artificial lightning with amplitude up to ± 220 kA in the high-current discharge circuit of a powerful high-voltage LCG with their integral of action up to $3 \cdot 10^6$ J/Ω [10]



Fig. 2. External view of the improved coaxial shunt type SC-300M2 designed to measure in the coordinated mode of operation of its cable signal transmission line in the micro- and millisecond ranges of current pulses of artificial lightning with amplitude up to ± 220 kA in the high-current discharge circuit of high-voltage LCG with their integral of action up to $15 \cdot 10^6$ J/Ω [11]

Such a technical improvement of the design of the high-resistance measuring disk in the high-voltage high-current shunt (see Fig. 1, 2) has made it possible to significantly increase its electrothermal resistivity to high impulse currents (HICs) flowing along it and to avoid the development of the phenomenon of electric explosion (EE) of its metal dangerous for the mechanical stability of the shunt.

As is known [12, 13], the EE of the metal measuring disk of the shunt at registration of the HIC is accompanied by a sharp increase in the gas-dynamic pressure inside the shunt (up to hundreds of atmospheres [14]), usually leading to its destruction and failure. Fig. 3 is a schematic view of a shunt of the SC-300M2 type in the longitudinal section.

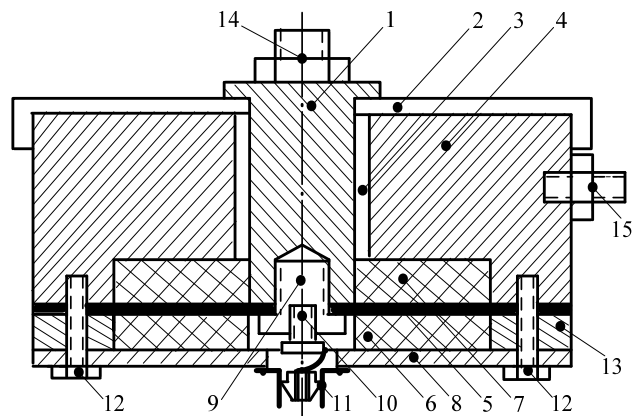


Fig. 3. Schematic view of the design of a coaxial disk shunt of the SC-300M2 type in its longitudinal axial section (1 – a massive inner cylindrical brass electrode, 2, 3 – an insulating sleeves made of fluoroplastic, 4 – a massive outer cylindrical brass electrode, 5 – a measuring high-resistance steel disk, 6, 7 – massive clamping insulating disks, 8 – banded brass disk, 9, 10, 12 – steel fastening screws, 11 – CP-75 output coaxial connector, 13 – massive clamping brass ring, 14, 15 – respectively input (potential) and output (grounded) elements of the brass bolt connection of the shunt to the high-voltage high-current discharge circuit of the LCG) [11]

For the simultaneous measurement of several components of the total current of artificial lightning generated in a high-voltage high-current discharge circuit of the LCG, it was required to develop and create a special measuring matching voltage divider (MVD), which is connected to the output of an additional shielded coaxial communication line (Fig. 4). In the shown in Fig. 4 divider of the type SDN-300 there are two coaxial connectors 1:1 and 1:2, intended for the coordinated connection of their outputs to the inputs of the measuring channels of digital storage oscilloscopes (DSO) [6, 10].

Fig. 5 is a general view of the placement of three DSO type Tektronix TDS 1012 in a buried screened measuring hopper for field testing of aircraft equipment for direct impact in them according to [1, 2] of lightning current.



Fig. 4. External view of the SC-300M1 measuring shunt connected to the input of an additionally shielded coaxial RF cable of the RK 75-7-11 type with a length of 70 m, the output of which is connected to a shielded matching voltage divider of the type SDN-300 with two output coaxial connectors 1:1 and 1:2 for the coordinated connection of the measuring channels of the three DSO (for example, Tektronix TDS 1012 series) to them, while simultaneously registering of three components of the total current pulse of the artificial lightning in the high-current discharge circuit of the LCG with different ATPs [6, 10]



Fig. 5. External view of the placement of three Tektronix TDS 1012 digital storage oscilloscopes that register in parallel useful electrical signals from one SC-300M1 measuring shunt in a buried screened measuring hopper designed for metrology support of field testing of various technical objects for lightning resistibility [9]

It should be noted that the DSO used by us in testing technical facilities for lightning resistibility have the corresponding certificates of metrological verification and calibration of the State Enterprise «Kharkivstandartmetrologiya» (for example, No. 08/2128K dated May 16, 2017).

Table 3 shows the main technical characteristics of the described shunts of the type SC-300M1 and SC-300M2 that passed the state metrological certification at the State Enterprise «Kharkivstandartmetrologiya» (inspection certificate No. 06/184 of June 27, 2017 and certificate of conformity No. 06/0206 of July 19, 2017) [11].

Using the data of Table 3 and the readings (in fractions or units of volts) recorded on the screen of the DSO from the measuring shunt of the drop of the U_S pulsed voltage, the required value of the measured lightning current pulse I_{mL} is determined as: $I_{mL} = K_S U_S$.

Table 3
The main technical characteristics of high-voltage high-current shunts SC-300M1 and SC-300M2

Shunt name	Characteristic value		
	R_S , m Ω	K_S , A/V	Mass, kg
SC-300M1	$0.158 \pm 1\%$	$K_{SA} = 12625$	3.1
		$K_{SC} = 6312$	
SC-300M2	$0.080 \pm 1\%$	$K_{SA} = 25000$	3.2
		$K_{SC} = 12500$	

Note. R_S is the active resistance of the shunt disk, m Ω ; $K_S = 2/R_S$ is the shunt transform coefficient, A/V; K_{SA} is the shunt conversion factor for measuring in the discharge circuit of the LCG of the ATPs of A - and D - components of the lightning current and lightning pulse of the shape $10 \mu s / 350 \mu s$, A/V (from the 1:1 coaxial connector of the SDN-300 divider); K_{SC} is the shunt conversion factor when measuring in the discharge circuit of the GTM of the ATPs of B -, C - and C^* - artificial lightning current component, A/V (from the coaxial connector 1:2 of the SDN-300 divider).

1.2. Capacitive and ohmic voltage dividers type CDV-100, CDV-1,2, ODV-1,2 and ODV-2,5. In 2011, when studying the behavior of high-voltage insulation samples (in particular, wood) of test electrical installations of Department No. 4 of the Institute under the influence of large pulsed currents and high voltages on them, we found it necessary to have a small mobile capacitive voltage divider of amplitude up to ± 100 kV (CDV-100) operating in the microsecond time range. Fig. 6 shows the connection diagram of the CDV-100 to the measuring circuit of the installation.

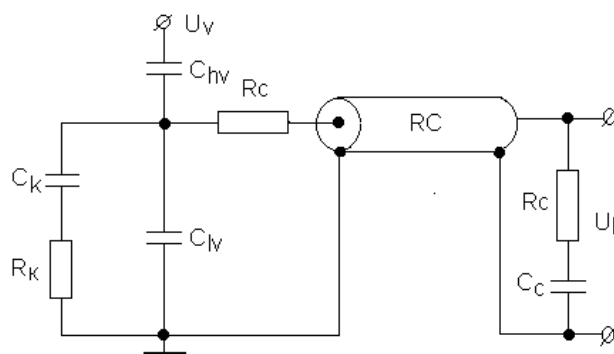


Fig. 6. Connection diagram of CDV-100 to the input of the DSO [15]

The measurement circuit in Fig. 6 of the high voltage U_V applied to the high-voltage divider arm with capacitance C_{hv} , connected in series with the low-voltage divider arm of with capacitance $C_{lv} \gg C_{hv}$, is based on the agreed operating mode of the CDV-100 measuring circuit. To implement this mode, the coaxial RF cable (PC) with the impedance Z_B of the transmission line of the useful electrical signal from the low-voltage arm of the $R_C = Z_B$ matching impedance divider and the connection on the low-voltage side of the circuit with the voltage U_L of the matching $R_C C_C$ chain are used in the circuit of the wire (see Fig. 6). We indicate that the connection of the resistance R_C in accordance with the circuit in Fig. 6 reduces twice the useful signal with the level of voltage U_L applied to the measuring channel of the DSO. To improve the transmission characteristics of the divider under consideration, its low-voltage arm contains a

corrective $R_k C_k$ chain. In accordance with the circuit of Fig. 6 the following numerical values of the main electrical parameters of the CDV-100 divider were used (Fig. 7): $C_{hv}=0.47$ nF; $C_h=C_c=0.54$ μ F; $R_c=Z_B=75$ Ω ; $R_k=27$ Ω ; $C_k=2.8$ nF.

We point out that high-voltage ceramic capacitors of the K-15-10 type (with a capacitance of 4700 pF for a rated voltage of ± 50 kV) were used to create a high-voltage arm of the CDV-100 pulsed voltage divider. In this connection, the capacitance C_{hv} consisted of 10 series-connected capacitors of the indicated type, placed in air in an insulating pipe made of glass textolite of STEF brand (length of 915 mm and inner diameter of 151 mm with wall thickness 12 mm). The low-voltage arm of the divider under consideration with capacitance of $C_h=0.54$ μ F was realized on the basis of two parallel capacitors of the K-73-11 type with capacitance of 0.27 μ F at a voltage of 250 V [15]. The matching active resistance R_c was assembled from two parallel-connected resistors of the MLT-2 type with a rating resistance of 150 Ω . The electrical part of the low-voltage arm of the described divider was placed in a rectangular aluminum casing with a CR-75 coaxial connector rigidly fixed to the isolator base of the divider and connected to the grounding bus of the test setup. The calculated value of the division factor for CDV-100 in the circuit according to Fig. 6 was numerically $K_{D1}=2C_h/C_{hv}=2298$. The performed high-voltage experiments showed that the experimental value of the CDV-100 division factor is $K_{D2}\approx 2515$ [15].

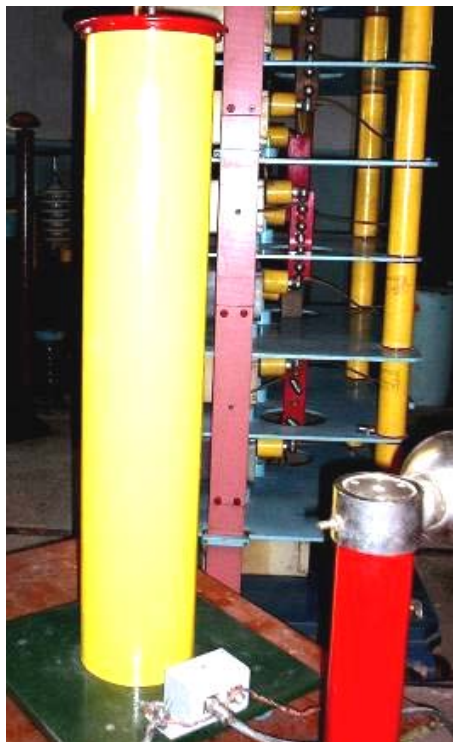


Fig. 7. General view of the mobile high-voltage pulsed voltage divider CDV-100 for a rated voltage of ± 100 kV, placed on the test field of a superhigh voltage pulsed voltage generator of the GIN-1,2 type of our own flooring design (the GIN-1,2 generator is located behind the CDV-100 divider; to the right of the CDV-100 divider there are movable standard measuring balls with a diameter of 125 mm) [15]

In Fig. 8 shows the electrical circuit with the use of a high-voltage capacitive voltage divider of the type CDV-1,2, designed to form a non-standard commutation aperiodic pulse of a time shape of 250 μ s/5000 μ s of amplitude up to ± 1 MV in the long air gap between the electrodes E_1 (disk) and E_2 (rod) [16]. In this circuit, the CDV-1,2 divider at a nominal voltage of ± 1.2 MV performs not only the role of the measuring mean, but also the role of the superhigh voltage forming capacitance.

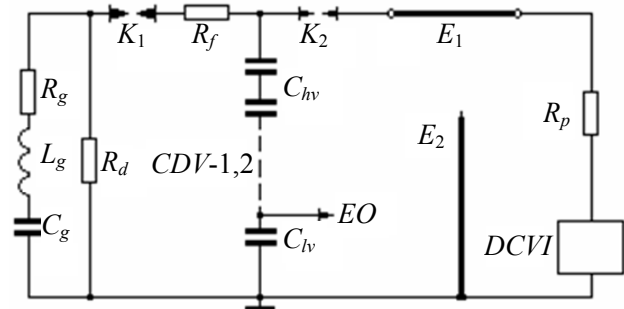


Fig. 8. A schematic electrical circuit for the forming in the GIN-1,2 type generator discharge circuit in a long air gap of a commutation aperiodic voltage pulse of a time shape of 250 μ s/5000 μ s with an amplitude up to ± 1 MV based on the use of a capacitive voltage divider of the CDV-1,2 type [16]

In the circuit according to Fig. 8 to the potential electrode E_1 of the air gap from the DC voltage installation (DCVI) through a protective resistance R_p of 1.4 G Ω (14 resistors of the KEV-5-100 M Ω type with a total length of 2.05 m), a DC voltage of up to ± 50 kV can be applied. The generator of pulsed voltages of type GIN-1,2 had following own electric parameters [16]: $R_g=48$ Ω ; $L_g=6$ μ H; $C_g=20.8$ nF; discharge resistance $R_d=340$ k Ω . The front active resistance R_f , connected to the circuit in Fig. 8 between the cut-off K_1 and the isolating K_2 switches was 360 k Ω . The capacitance C_{hv} of the high-voltage arm of the divider CDV-1,2 was chosen equal to 130 pF, and the capacitance C_h of its low-voltage arm, connected to the oscilloscope or DSO, was 2.6 μ F. At the same time, the calculated division factor for CDV-1,2 had a numerical value equal to $K_{DC} = C_h C_{hv} = 20 \cdot 10^3$ [16].

Fig. 9 shows a general view of a high-voltage test stand, which uses as a base of its design the electrical circuit in accordance with Fig. 8 with a capacitive voltage divider of the type CDV-1,2.

Fig. 10 shows a general view of the ultrahigh-voltage ohmic voltage divider ODV-1,2 developed and created at the Department No. 4 of the Institute.

The insulating supporting structure (ISS) of the divider ODV-1,2 is assembled from five rigid hollow fiberglass sections fixed in a single rack, inside which high-voltage ceramic resistors of the type TVO-5-250 Ω were placed on the getinax plates [17]. Each divider section contains 40 consistently and zigzag connected on both sides of the getinax plate of the indicated resistors with a total active resistance of 10 k Ω . In the case of using the four specified sections in the divider, the design of an ohmic divider of the ODV-1 type for a nominal voltage of ± 1 MV (Fig. 11) can be realized [17].



Fig. 9. General view of the high-voltage test stand of the R&DPCI «Molniya» of the NTU «KhPI», intended for testing lightning protection equipment of technical objects with commutation aperiodic voltage pulse with amplitude up to ± 1 MV of time shape $250 \mu\text{s}/5000 \mu\text{s}$ and containing in the scheme a mobile superhigh voltage capacitor voltage divider of the type CDV-1, 2 [16]



Fig. 10. General view of a mobile superhigh-voltage ohmic voltage divider of the type ODV-1,2 at a rated voltage ± 1.2 MV, located at the factory test field of a high-voltage test stand SVI-1,2, designed to determine in the laboratory conditions the pulsed electrical strength of polymer insulation of its own production (enterprise ES «Polymer», Bakhmut city, Ukraine, 2006) [9, 17]



Fig. 11. General view of the high-voltage test stand of the R&DPCI «Molniya» of the NTU «KhPI», on the test field of which mobile generator of pulsed voltages of the type GIN-1,2, the divider of the type ODV-1 and standard measuring balls with a diameter of 250 mm are placed [17]

For the divider of the type ODV-1,2, the high-voltage arm is characterized by an active resistance $R_{hv}=50 \text{ k}\Omega$. Its low-voltage arm is made of two parallel-connected resistors of the MLT-2 type with a total active resistance $R_n=2.5 \Omega$. In this connection, the calculated division factor for the divider ODV-1,2 is $K_{DR}=R_{hv}/R_n=20 \cdot 10^3$. In practical use in the measuring path, connected to the low-voltage arm of a divider of the type ODV-1,2, the matching circuit, which is similar to that shown in Fig. 6, the coefficient of its division K_{DR} is doubled and numerically is about $40 \cdot 10^3$. Experimental verification of the K_{DR} value using standard balls of diameter of 250 mm (see Fig. 11) according to the requirements of [8] showed that it takes a numerical value of about $39.8 \cdot 10^3$. From Fig. 10, 11 it can be seen that above the ISS of dividers of the type ODV-1,2 and ODV-1, anti-crown metal shields are installed, which simultaneously improve the distribution of a strong electric field along their upper sections [17].

The use in the discharge circuit of shown in Fig. 8, 11 the generator of pulsed voltages of the type GIN-1,2 at a rated voltage of ± 1.2 MV with an own discharge resistance $R_d=240 \text{ k}\Omega$ and an additional shaping resistance $R_{f1}=1.98 \text{ k}\Omega$ (Fig. 12) of the ohmic voltage divider of the type ODV-1,2 (or ODV-1) makes it possible to form following requirements [5] a standard lightning aperiodic wave of a voltage of $1.2 \mu\text{s}/50 \mu\text{s}$ with the above tolerances and the required values of its amplitude $U_{mL} \leq \pm 1 \text{ MV}$ [16, 18]. Here, the capacitive nature of the load ($C_L \approx 10 \text{ pF}$) and the parasitic capacitance of the ODV-1,2 divider, approximately 50 pF , should be taken into account in the calculation circuit for the formation of a standard lightning pulse of the shape $1.2 \mu\text{s}/50 \mu\text{s}$.

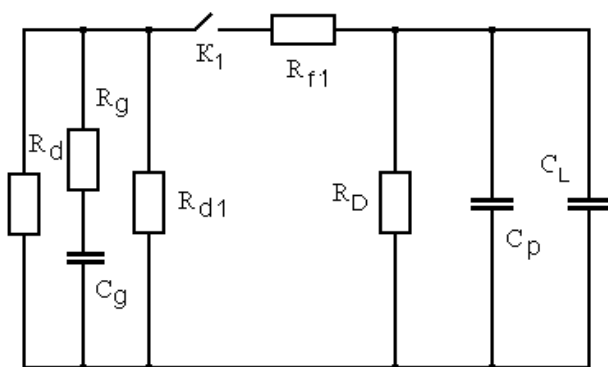


Fig. 12. Electric circuit for obtaining in the discharge circuit of the generator GIN-1,2 on the tested load with the capacitive characteristic of a standard lightning voltage pulse of the time shape of 1.2 μ s/50 μ s with the use of the ohmic voltage divider of the type ODV-1,2 with an active resistance $R_D=50$ k Ω ($R_d=240$ k Ω is the own discharge resistance of GIN-1,2, $R_{d1}=3.91$ k Ω is the additional discharge resistance of GIN-1,2; $R_g=48$ Ω ; $C_g=20.8$ nF; $R_{f1}=1.98$ k Ω ; $C_L\approx 10$ pF; $C_p\approx 50$ pF) [9, 18]

The utilization in the discharge circuit of the pulsed voltage generator of the GIN-1,2 type to a rated voltage of ± 1.2 MV of a capacitive voltage divider of the CDV-1,2 type (Fig. 13) allows on the electrical load under test with the indicated capacitive characteristic ($C_L\approx 10$ pF) to form a standard commutation pulse of voltage of a time shape of 250 μ s/2500 μ s with an amplitude $U_{mk}\leq \pm 700$ kV with normalized tolerances (for a rise time $\pm 20\%$, for a half-decay time $\pm 30\%$, for the amplitude $U_{mk} \pm 3\%$) [5, 18]. It should be noted that the mobile capacitive voltage divider CDV-1,2 contains three C- sections connected in series, each of which is placed in a 900 mm diameter glass-fiber plastic pipe of TSEF brand with an outer diameter of 300 mm with a wall thickness of 35 mm. Each of its C- sections consists of 12 series-connected high-voltage ceramic capacitors of type K 15-10-4700 pF at ± 50 kV. Each of these sections of the divider is filled with transformer oil of T-1500 grade, and its upper and lower terminals are connected to round metal flanges with a diameter of 350 mm [16, 18].

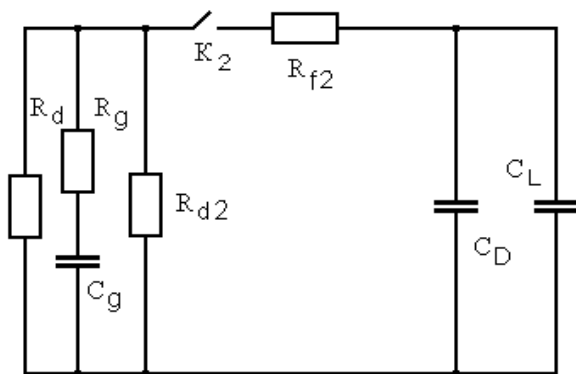


Fig. 13. Electric circuit for obtaining in the discharge circuit of the generator GIN-1,2 on the tested load with the capacitive characteristic of a standard commutation pulse of a time shape of 250 μ s/2500 μ s with the use of a capacitive voltage divider of the type CDV-1,2 with a total capacitance $C_D=130$ pF ($R_d=240$ k Ω is the own discharge resistance of the GIN-1,2; $R_{d2}=840$ k Ω is the additional discharge resistance of the GIN-1,2; $R_g=48$ Ω ; $C_g=20.8$ nF; $R_{f2}=395$ k Ω ; $C_L\approx 10$ pF; K_2 is the cut-off high-voltage switch of the generator GIN-1,2) [9, 18]

To measure with an error of no more than 5 % at industrial power facilities of aperiodic lightning and commutation voltage pulses up to ± 2.5 MV, an ultrahigh-voltage ohmic voltage divider of the ODV-2,5 type was created in the Department No. 4 of the Institute [19, 20]. The main technical characteristics of this pulsed voltage divider are given in Table 4 [20].

Table 4
The main technical characteristics of a superhigh-voltage ohmic voltage divider ODV-2,5

No.	Characteristic name	Value
1	The maximum level of the measured voltage U_m , kV	± 2500
2	The active resistance of the high-voltage divider's arm R_{hv} , k Ω	107.3
3	The active resistance of the low-voltage divider's arm R_n , Ω	4
4	Division coefficient, K_{DR}	$26.82 \cdot 10^3$
5	Height (length), m	12.6
6	Mass, kg	350

General view of a superhigh-voltage ohmic voltage divider of the type ODV-2,5, functioning as a part of a unique CVPG at ± 2.5 MV, is shown in Fig. 14. The high-voltage arm of the ODV-2,5 divider is made up of nine R- sections connected in series and placed outside and inside the glass-fiber pipe of the TSEF brand with an outer diameter of 120 mm and a wall thickness of 10 mm. Each R- section contains 20 series-parallel-connected high-voltage ceramic resistors of the TVO-10-2,4 k Ω type, assembled on two glass-fiber plates with a length of 1400 mm and a thickness of 5 mm. As a result, the resistance of each section of the high-voltage divider arm is about 12 k Ω , and its total resistance is $R_{hv}\approx 107.3$ k Ω [20].



Fig. 14. General view of a superhigh-voltage ohmic voltage divider of the ODV-2,5 type for a rated voltage of ± 2.5 MV, connected in the CVPG discharge circuit to a two-electrode «needle-plane» system with an air gap length of 3 m (the upper steel rod-electrode of this electric discharge system is located at the center of its lower flat electrode made of thin galvanized steel with a plan size of 5 m \times 5 m) [23]

The low-voltage arm of the ODV-2.5 divider is made of small-sized ceramic resistors of the TBO-2-2 Ω

type with a total active resistance $R_h=4\ \Omega$. In this connection, the calculated division coefficient K_{DR} for the considered voltage divider of the type ODV-2,5 is approximately equal to $K_{DR}=R_{hv}/R_h=26,82\cdot 10^3$. With the agreed mode of measuring the pulsed voltage on the load, the division coefficient for the divider of the type ODV-2,5 will be doubled and take a numerical value of about $53,65\cdot 10^3$. An experimental estimate of the reaction time T_R of the ohmic divider of the type ODV-2,5 on the action of a rectangular voltage pulse [21] showed that for this type of divider $T_R\approx 170\text{ ns}$ [19]. In this regard, the voltage divider of the type ODV-2,5 can be used to measure voltage pulses with an amplitude of $U_m\leq\pm 2,5\text{ MV}$, varying in micro- and millisecond time bands. A comparison of the metrological characteristics of a superhigh-voltage ohmic divider of the ODV-2,5 type with the characteristics of the known high and ultra high voltage meters [22] indicates that the domestic voltage divider of the ODV-2,5 type meets modern requirements and developments in the field of high-voltage measuring equipment.

Fig. 15 shows the oscillogram of a superhigh-voltage pulse of microsecond duration, obtained with the help of the ohmic voltage divider of the ODV-2,5 type on a long air gap of 3 m at its electrical breakdown in the «rod-rod» system [20]. From the oscillogram of Fig. 15 it can be seen that the cut-off voltage U_C in our case is approximately $U_C\approx 25\text{ V}\times 53,65\cdot 10^3\approx 1341,3\text{ kV}$. Here, the pre-discharge time T_C for this insulating air gap is about $T_C\approx 5\times 2,5\cdot 10^{-6}\approx 12,5\ \mu\text{s}$, and the cut-off time T_{DC} of the microsecond voltage wave does not exceed the value $5,47\ \mu\text{s}$.

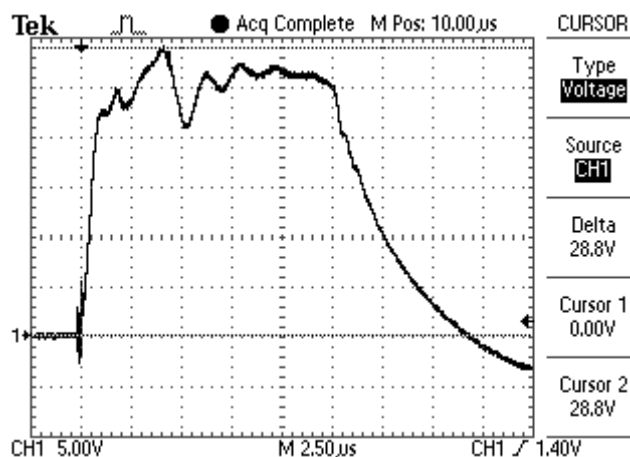


Fig. 15. Oscillogram of a superhigh voltage pulse of positive polarity on the air gap of 3 m long in a «rod-rod» system cut at its rising part and registered with the ohmic voltage divider ODV-2,5 (cut-off voltage $U_C\approx 1341,3\text{ kV}$, pre-discharge time $T_C\approx 12,5\ \mu\text{s}$, the cut-off time $T_{DC}\approx 5,47\ \mu\text{s}$, the vertical scale is 268 kV/cell ; the horizontal scale is $2,5\ \mu\text{s/cell}$) [20]

2. Metrological support of testing of technical objects for commutation stability. In order to conduct full-scale testing of power engineering facilities for commutation stability, a unique CVPG was created at the R&DPCI «Molniya» of the NTU «KhPI» at the experimental range of the Institute (Andreevka, Kharkiv

region) in 2012. The CVPG is rated for a voltage of $\pm 2\text{ MV}$ [23]. This outdoor CVPG allows, in the field conditions, to reliably form, in accordance with the requirements of [5], a standard aperiodic commutation pulse of the time shape of $205\ \mu\text{s}/1900\ \mu\text{s}$ of both polarities in the field conditions on a large-sized electrical load under test.

To measure the ATPs of voltage pulses formed in the CVPG generator circuit, a superhigh-voltage ohmic voltage divider of the ODV-2,5 type described above can be used [20]. The data in Fig. 14 clearly illustrate the practical use of a superhigh-voltage ohmic voltage divider of the ODV-2,5 type at metrology support for testing the electrical strength of long air gaps in electric power devices for commutation stability. Fig. 16 shows the oscillogram of a full standard commutation pulse of time shape of $205\ \mu\text{s}/1900\ \mu\text{s}$ of positive polarity obtained in the discharge circuit of the CVPG generator in field conditions in the open air using an ohmic voltage divider of the ODV-2,5 type [23]. From the oscillogram of Fig. 16 it follows that the amplitude U_{mk} of the commutation voltage wave in this case is approximately $U_{mk}\approx 9\text{ V}\times 53,65\cdot 10^3\approx 483\text{ kV}$. For the voltage commutation pulse formed on a long air gap, the rise duration T_{rise} reaches a numerical value of about $T_{rise}\approx 205\ \mu\text{s}$. In this case, the duration of the commutation voltage pulse T_p at the level of $0,5U_{mk}$ equals approximately $1900\ \mu\text{s}$.

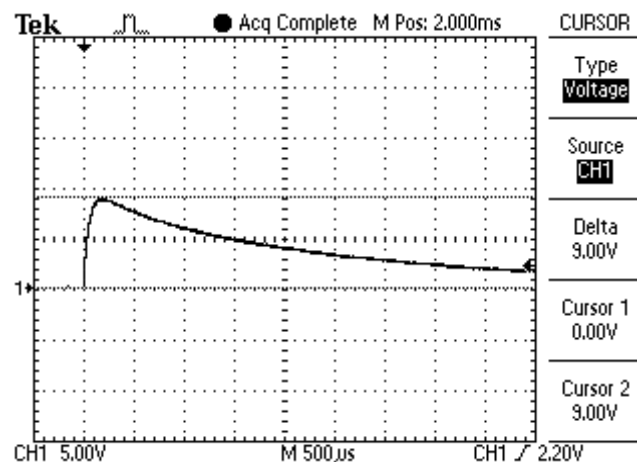


Fig. 16. Oscillogram of the full standard aperiodic commutation voltage pulse of positive polarity generated in the discharge circuit of the superhigh voltage generator of the CVPG on a two-electrode «needle-plane» system with an air gap length of 3 m and recorded with an ohmic voltage divider ODV-2,5 ($U_{mk}\approx 483\text{ kV}$; rise duration of the voltage pulse is $T_{rise}\approx 205\ \mu\text{s}$, duration of the voltage pulse is $T_p\approx 1900\ \mu\text{s}$, the vertical scale is 268 kV/cell , the horizontal scale is $500\ \mu\text{s/cell}$) [23]

Conclusions.

1. Analysis of the current state of metrology support of full-scale testing of industrial power engineering objects, aircraft and rocket and space equipment on lightning resistibility and commutation stability in Ukraine shows that the R&DPCI «Molniya» of the NTU «KhPI» currently has not only high-voltage pulsed technology reproducing in this area required by the

requirements of domestic and foreign regulatory documents test pulses of current and voltage by powerful high-voltage electrical installations, placed outdoor and in heated special laboratory premises, but also the corresponding measurement means, passed state metrological calibration.

2. The composition of these high-voltage measuring instruments used in the practice of full-scale tests at testing the durability of energy facilities, aircraft and rocket and space equipment to affect their electrical equipment, components and components of lightning current (voltage) pulses and commutation voltage pulses include the following non-standardized devices of own manufacture: high-voltage high-current shunts of type SC-300M1 and SC-300M2, intended for measurement of micro- and millisecond pulses of a current of amplitudes up to ± 220 kA with an integral of their action up to $15 \cdot 10^6$ J/ Ω ; capacitive (CDV-100 and CDV-1,2 type) and ohmic (ODV-1,2 and ODV-2,5 type) dividers of pulsed voltage of micro- and millisecond duration, capable both of measuring with the help of metrologically attested DSO, and forming the standard (non-standard) lightning and commutation voltage pulses with amplitude up to ± 2 MV on a tested certain electrical load with a capacitive characteristic.

REFERENCES

1. SAE ARP 5412: 2013. Aircraft Lightning Environment and Related Test Waveforms. SAE Aerospace. USA, 2013. – pp. 1-56.
2. SAE ARP 5416: 2013. Aircraft Lightning Test Methods. SAE Aerospace. USA, 2013. – pp. 1-145.
3. IEC 62305-1: 2010 «Protection against lightning. Part 1: General principles». Geneva, IEC Publ., 2010.
4. Baranov M.I., Buriakovskiy S.G., Rudakov S.V. The tooling in Ukraine of model tests of objects of energy, aviation and space-rocket engineering on resistibility to action of pulsed current of artificial lightning. *Electrical engineering & electromechanics*, 2018, no.4, pp. 45-53. doi: **10.20998/2074-272X.2018.4.08**.
5. GOST 1516.2-97. *Elektrooborudovanie i elektroustanovki peremennogo toka na napryazhenie 3 kV i vyshe. Obshchie metody ispytaniy elektricheskoi prochnosti izolatsii* [GOST 1516.2-97. Electrical equipment and electrical options of alternating current voltage 3 kV and above. Common test methods for dielectric strength]. Minsk, Publishing house of standards, 1998. 31 p. (Rus).
6. Baranov M.I., Koliushko G.M., Kravchenko V.I., Nedzel'skii O.S., Dnyshchenko V.N. A Current Generator of the Artificial Lightning for Full-Scale Tests of Engineering Objects. *Instruments and Experimental Technique*, 2008, no.3, pp. 401-405. doi: **10.1134/S0020441208030123**.
7. GOST R MEK 62305-1-2010. *Menedzhment riska. Zashhita ot molnii. Chast' 1: Obshhie principy* [GOST R IEC 62305-1-2010. Risk management. Protection from lightning. Part 1: General principles]. Moscow, Standartinform Publ., 2011, 46 p. (Rus).
8. GOST 17512-82. *Elektrooborudovanie i elektroustanovki na napryazhenie 3 kV i vyshe. Metody izmereniya pri ispytaniyah vysokim napryazheniem* [GOST 17512-82. Electrical equipment and electric options on voltage 3 kV and higher. Measuring methods at tests by high voltage]. Moscow, State standard of the USSR Publ., 1982. 32 p. (Rus).
9. Baranov M.I. *Izbrannye voprosy elektrofiziki: Monografiya v 3-h tomah. Tom 3: Teoriya i praktika electrofizicheskikh zadach* [Selected topics of Electrophysics: Monograph in 3-th vols. Vol.3: Theory and practice of electrophysics tasks]. Kharkiv, Tochka Publ., 2014. 400 p. (Rus).
10. Baranov M.I., Kniaziev V.V., Rudakov S.V. The coaxial shunt for measurement of current pulses of artificial lightning with the amplitude up to ± 220 kA. *Instruments and Experimental Technique*, 2018, vol.61, no.4, pp. 501-505. doi: **10.1134/S0020441218030156**.
11. Baranov M.I., Kniaziev V.V., Rudakov S.V. A coaxial disk shunt for measurement in the high-current circuit of high-voltage generator of storm discharges of pulses of current of artificial lightning with the integral of action up to $15 \cdot 10^6$ J/ Ω m. *Electrical engineering & electromechanics*, 2017, no.5, pp. 45-50. doi: **10.20998/2074-272X.2017.5.07**.
12. Knopfel' G. *Sverkhshil'nye impul'snye magnitnye polia* [Ultra strong pulsed magnetic fields]. Moscow, Mir Publ., 1972. 391 p. (Rus).
13. Baranov M.I., Kniaziev V.V., Rudakov S.V. Calculation and experimental estimation of results of electro-thermal action of rationed by the international standard IEC 62305-1-2010 impulse current of short blow of artificial lightning on the thin-walled coverage from stainless steel. *Electrical engineering & electromechanics*, 2017, no.1, pp. 31-38. doi: **10.20998/2074-272X.2017.1.06**.
14. Baranov M.I., Rudakov S.V. Approximate calculation of basic characteristics of plasma at the air electric explosion of metal conductor. *Electrical engineering & electromechanics*, 2017, no.6, pp. 60-64. doi: **10.20998/2074-272X.2017.6.09**.
15. Baranov M.I., Zin'kovskiy V.M., Ziyabko Yu.P., Ignatenko N.N., Lysenko V.O. Development and creation of movable capacity divider of impulsive voltage amplitude to ± 100 kV. *Bulletin of NTU «KhPI». Series: Technique and electrophysics of high voltage*, 2011, no.49, pp. 3-10. (Rus).
16. Baranov M.I., Bocharov V.A., Ziyabko Yu.P. Complex high-voltage electrophysical equipment for testing lightning protection of technical objects via storm and switching micro and millisecond voltage impulses with up to 1 MV amplitude. *Electrical engineering & electromechanics*, 2006, no.4, pp. 60-65. (Rus).
17. Baranov M.I., Bocharov V.A., Zin'kovskiy V.M., Ziyabko Yu.P., Ignatenko N.N. Ohmic divider of voltage for measuring of proof-of-concept storm and interconnect impulses of voltage amplitude to ± 1 MV. *Bulletin of NTU «KhPI». Series: Technique and electrophysics of high voltage*, 2007, no.20, pp. 20-30. (Rus).
18. Baranov M.I., Bocharov V.A., Ziyabko Yu.P., Mel'nikov P.N. Complex of electrophysics equipment for generating of micro- and millisecond impulses of voltage to 1,2 MV and current to 200 kA. *Technical electrodynamics*, 2003, no.5, pp. 55-59. (Rus).
19. Baranov M.I., Bocharov V.A., Ignatenko N.N., Kolobovskiy A.K. Powerful generators of impulsive voltages and currents of maximum parameters for testing of power electroenergy equipment. *Electrical Engineering & Electromechanics*, 2003, no.2, pp. 75-80. (Rus).
20. Baranov M.I., Koliushko G.M. Experimental estimation of electric durability of long air intervals in the electrode system «bar-bar» for the microsecond impulses of voltage. *Bulletin of NTU «KhPI». Series: Technique and electrophysics of high voltage*, 2011, no.49, pp.11-20. (Rus).

21. Shvab A. *Izmereniya na vysokom napryazhenii* [Measuring on high voltage. Trans. with German]. Moscow, Energy Publ., 1973. 233 p. (Rus).
22. Gurov S.A., Vladimirov G.A. Universal measuring complexes on voltages to 4 MV. *Electrical Engineering*, 1978, no.11, pp. 51-53. (Rus).
23. Baranov M.I., Koliushko G.M., Kravchenko V.I. A switching aperiodic superhigh-voltage pulse generator for testing the electric strength of insulation of technical objects. *Instruments and Experimental Technique*, 2013, vol.56, no.6, pp. 653-658. doi: 10.1134/s0020441213050126.

Received 19.07.2018

M.I. Baranov¹, Doctor of Technical Science, Chief Researcher,
S.G. Buriakovskiy¹, Doctor of Technical Science,
S.V. Rudakov², Candidate of Technical Science, Associate
Professor,

¹ Scientific-&-Research Planning-&-Design Institute «Molniya»,
National Technical University «Kharkiv Polytechnic Institute»,
47, Shevchenko Str., Kharkiv, 61013, Ukraine,
phone +380 57 7076841,

e-mail: baranovmi@kpi.kharkov.ua, sergbyr@i.ua

² National University of Civil Protection of Ukraine,
94, Chernyshevska Str., Kharkiv, 61023, Ukraine,
phone +380 57 7073438,

e-mail: serg_73@i.ua

How to cite this article:

Baranov M.I., Buriakovskiy S.G., Rudakov S.V. The metrology support in Ukraine of tests of objects of energy, aviation and space-rocket engineering on resistibility to action of pulses of current (voltage) of artificial lightning and commutation pulses of voltage. *Electrical engineering & electromechanics*, 2018, no.5, pp. 44-53. doi: 10.20998/2074-272X.2018.5.08.

V.O. Brzhezytskyi, R.V. Vendychanskyi, Ye.O. Trotsenko, Ya.O. Haran, O.M. Desyatov, V.I. Khominich

CHARACTERISTICS OF SPECIALIZED SINGLE-PHASE HIGH VOLTAGE DOUBLER RECTIFIER

Introduction. To obtain a high voltage direct current, voltage multipliers with a number of cascades of three or more are widely used. At the same time, for voltage levels of 100...200 kV there are several advantages of using a specialized single-phase high voltage doubler rectifier. **Problem.** The main difficulty is that at the moment mathematical modeling has not been worked out for describing modes that use the built-in R , C -filter, as well as a nonlinear load in the form of Zener diodes. **Goal.** Generalization of the results of the authors' previous publications on the development of an analytical method for calculating the modes of a typical high-voltage direct current installation based on a specialized single-phase voltage doubler rectifier. **Methodology.** Compilation of a system of algebraic linear and nonlinear equations that describe the current and voltage modes in the elements of a typical high-voltage direct current installation with a nonlinear load. **Results.** It is shown that with the use of linearization of the current-voltage characteristics of Zener diodes used in the load circuits of a typical high-voltage direct current installation, an analytical solution for the voltages and currents in its elements can be obtained. **Originality.** The theoretical basis of the complex solution of the system of equations for the currents, voltages and power of the elements of a typical high-voltage direct current installation with the account of nonlinear pulsations is formulated for the first time. **Practical value.** The obtained theoretical results can be used for calculations, design, optimization of the modes for a wide range of high-voltage direct current installations of technical, technological, and measuring purposes in the range up to 100...200 kV. References 16, tables 2, figures 3.

Key words: voltage doubler rectifier, high-voltage Zener diode, current-voltage characteristic.

Цель. Обобщение результатов предыдущих публикаций авторского коллектива по разработке аналитического метода расчёта режимов типовой установки высокого напряжения постоянного тока на основе специализированного однофазного выпрямителя с удвоением напряжения. **Методика.** Составление системы алгебраических линейных и нелинейных уравнений, описывающих режимы тока и напряжения в элементах типовой схемы установки высокого напряжения постоянного тока с нелинейной нагрузкой. **Результаты.** Показано, что с применением линейзации вольт-амперных характеристик стабилитронов, используемых в цепях нагрузки типовой установки высокого напряжения постоянного тока, может быть получено аналитическое решение для напряжений и токов в её элементах. **Научная новизна.** Впервые сформулирован теоретический базис комплексного решения системы уравнений для токов, напряжений и мощности элементов типовой установки высокого напряжения постоянного тока с учётом нелинейных пульсаций. **Практическая значимость.** Полученные теоретические результаты могут быть использованы для расчётов, проектирования, оптимизации режимов широкого спектра установок высокого напряжения постоянного тока технического, технологического, а также измерительного назначения в диапазоне до 100...200 кВ. Библ. 16, табл. 2, рис. 3.

Ключевые слова: выпрямитель с удвоением напряжения, высоковольтный стабилитрон, вольт-амперная характеристика.

Introduction. The variety of high voltage applications for steady-state modes of technological equipment (electrostatic precipitators of coal-fired power plants, electro-coloring and coating sputtering devices, electric separators) necessitates the improvement of their power supplies to a level of 100...200 kV. In connection with this, recently interest in various variants of the improvement of the classical Cockcroft-Walton direct current voltage generator [3] with a number of stages of three or more [1, 2] has appeared. At the same time, since high-voltage diodes [4] are of high quality, in order to obtain the above voltage level, it is more efficient to use the Cockcroft-Walton generator with only doubling the rectified voltage, and to reduce output voltage ripple – to supplement it with the «built-in» R , C – filter [5].

It should be noted that to date no rigorous mathematical model of the Cockcroft-Walton generator has been created. The available publications on this topic give different results on the magnitude of voltage ripples, and there are also no analytical expressions for the shape of pulsing voltage, etc.

In this connection, a new development of the authors' team [6-8] on the creation of elements of the theory of voltages and currents of the Cockcroft-Walton generator with voltage doubling, together with the integrated R , C – filter,

and, in addition, the possibility of attaching to its load nonlinear elements such as Zener diodes.

The goal of the paper is to generalize the results of previous publications of the authors' group, to formulate and analyze the final analytical expressions for both voltages and currents in the rectifier circuit with voltage doubling in Fig. 1, and for the powers of the elements of the Cockcroft-Walton generator with voltage doubling and its integrated R , C – filter, taking into account the nonlinear pulsation modes. To reduce the terminology, we will call such a generator a specialized single-phase high voltage doubler rectifier.

The subject of the research is a specialized high-voltage single-phase rectifier with voltage doubling, its generalized circuit is shown in Fig. 1.

In Fig. 1: VT – high-voltage step-up transformer; VD_1 , VD_2 – high-voltage diodes; C_1 , C_2 , C_3 – capacitors; R_f , R_{LV} , r – resistors. The branch of n Zener diodes ZD_1, \dots, ZD_n , resistor r and voltmeter V forms the «built-in» high-precision measuring group of the load voltage U_{LV} . In this case, the voltage source in the circuit diagram in Fig. 1 is of interest for both technological applications and measuring equipment [9, 10]. The peculiarity of this voltage source is that by changing the parameters of the elements it is possible to adjust the amplitude and shape

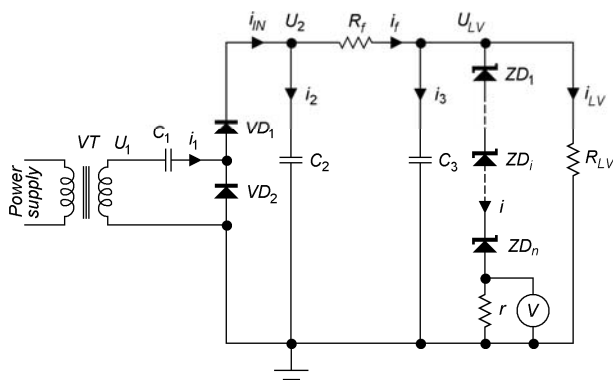


Fig. 1. Functional diagram of rectifier with voltage doubling [5]

of the output voltage ripple U_{LV} in a wide range. The problems of the synthesis of circuits with capacitive energy storage devices, including those using nonlinear electrical loads, are considered in modern publications [11-13]. However, the features of the high-voltage source in Fig. 1 in the well-known publications of other authors have not been studied. The calculated relationships for the voltages and currents of the circuit in Fig. 1 were first obtained in [6-8].

The initial prerequisites for the research are based on a number of conditions:

- a typical current-voltage characteristic of a Zener diode has the form shown in Fig. 2, where u_0 , I_0 denote the selected point of its operating mode;
- a differential resistance of a Zener diode $r_d = du_{ZD}/di_{ZD}$ in its operating domain is far less than the impedance u_0/I_0 (number 1 denotes the linearized current-voltage characteristic of a Zener diode);
- a capacitance current $C_{ZD} \frac{du_{ZD}}{dt}$ of a Zener diode is far less than its through-current I_0 (here C_{ZD} is the inter-electrode capacitance of a Zener diode);
- placement of a Zener diode in a metal casing (Fig. 3) completely shields its internal active element from the influence of external electric fields [5].

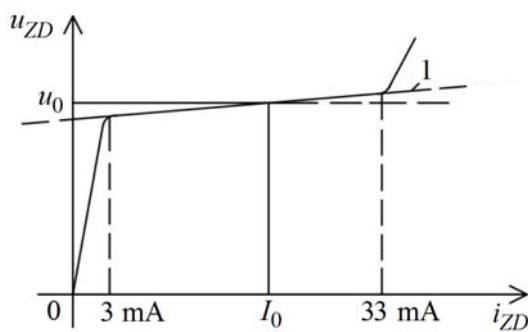


Fig. 2. Current-voltage characteristic of the Zener diode D818D

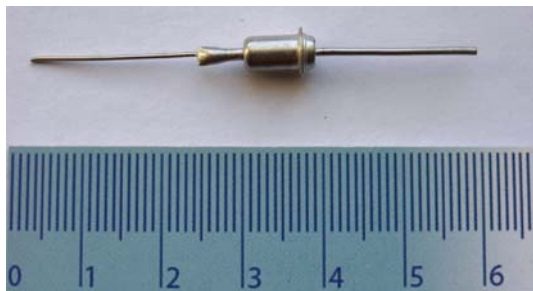


Fig. 3. Photograph of the Zener diode D818D

When these conditions are fulfilled, a series connection of the same type of Zener diodes in the steady state is characterized by the flow of the same current I_0 through their circuit with the voltage operating point

$$U_0 = u_{01} + u_{02} + \dots + u_{0i} + \dots + u_{0n},$$

as well as the total differential resistance

$$R_d = r_{d1} + r_{d2} + \dots + r_{di} + \dots + r_{dn},$$

that corresponds to the conclusion of [4] on the admissibility of a serial connection of any number of Zener diodes. The typical «high-voltage» design of insulation of a series of similar Zener diodes eliminates the need to take into account the corona and other phenomena of distributed currents [9].

Derivation of the initial expressions. Then for the instantaneous load voltage $u_{LV}(t)$, one can write:

$$u_{LV}(t) = U_0 + I_0 r + (i(t) - I_0)(R_d + r), \quad (1)$$

where: $i(t)$ – instantaneous current through a Zener diode and resistor r branch. From here one can get:

$$i(t) = \frac{u_{LV}(t) - U_0 - I_0 r}{R_d + r} + I_0. \quad (2)$$

The expressions (1) and (2) are valid within the stabilized domain of the current-voltage characteristic of Zener diodes (Fig. 2) and, therefore, are applicable up to a current ripple level of ~50 % (when I_0 is selected in the middle part of this domain). The peculiarity of the expressions (1) and (2) is also that they can provide (with an appropriate selection of the parameters U_0 , R_d) any variants of a series connection of Zener diodes and a resistor r , up to the limit: «only the Zener diode» load or «only resistive» load.

Let us write

$$u_{LV}(t) = U_0 + I_0 r + \Delta u(t),$$

where $\Delta u(t)$ – load voltage ripple as a function of time.

Wherein

$$\int_0^T \Delta u(t) dt = 0,$$

where $T = 1/f$ – voltage period of sinusoidal voltage $u_1(t) = U_m \cdot \sin(\omega t)$, $\omega = 2\pi f$ – angular frequency, f – voltage frequency.

Let us write $i_3 = C_3 \cdot du_{LV}(t)/dt$ (taking into account the losses in the capacitors of the circuit in Fig. 1 slightly refines the results obtained [6]) and $i_{LV} = u_{LV}(t)/R_{LV}$.

Then the current flowing through the resistor R_f is:

$$i_f = I_0 + \frac{\Delta u(t)}{R_d + r} + \frac{U_0 + I_0 r + \Delta u(t)}{R_{LV}} + C_3 \frac{du_{LV}(t)}{dt},$$

and voltage is:

$$u_{C2}(t) = u_{LV}(t) + i_f R_f.$$

In its turn, $i_2 = C_2 \cdot du_{C2}(t)/dt$ and the total current at the input of the right-hand side of the circuit is

$$\begin{aligned} i_{IN} &= i_f + i_2 = \\ &= I_0 + \frac{u_0 + I_0 r}{R_{LV}} + \Delta u(t) \left(\frac{1}{R_{LV}} + \frac{1}{R_d + r} \right) + \\ &+ \frac{d\Delta u(t)}{dt} \left(C_3 + C_2 \left(1 + \frac{R_f}{R_{LV}} + \frac{R_f}{R_d + r} \right) \right) + \\ &+ C_2 C_3 R_f \frac{d^2 \Delta u(t)}{dt^2}. \end{aligned} \quad (3)$$

Since the process occurs cyclically, let us assume that at time instant t_1 , the diode VD_1 «opens», and the current $i_1=i_{IN}$ flows (the resistance of the diode VD_1 in the open state is neglected). At time instant $t_2>t_1$, the diode VD_1 «closes» (the resistance of the diode in the closed state is assumed to be infinitely large). In the time interval $t_2 \leq t \leq T+t_1$, the current $i_{IN} = 0$. Proceeding from this for a given period of time, from (3) one can obtain an equation for a function of $\Delta u_1(t)$ in the form:

$$\frac{d^2 \Delta u_1(t)}{dt^2} + a_1 \frac{d\Delta u_1(t)}{dt} + a_2 \Delta u_1(t) = I_0 + \frac{1}{R_{LV}}(U_0 + I_0 r) = -\frac{C_2 C_3 R_f}{C_2 C_3 R_f}, \quad (4)$$

where

$$a_1 = \frac{C_3 + C_2 \left(1 + \frac{R_f}{R_{LV}} + \frac{R_f}{R_d + r}\right)}{C_2 C_3 R_f},$$

$$a_2 = \frac{\frac{1}{R_{LV}} + \frac{1}{R_d + r}}{C_2 C_3 R_f}.$$

A study of the roots p_1, p_2 of the characteristic equation $p^2 + a_1 p + a_2 = 0$ shows that its discriminant $D > 0$. Thus, one can find the solution for $\Delta u_1(t)$ in the form:

$$\Delta u_1(t) = A_1 e^{p_1 t} + A_2 e^{p_2 t} + \Delta u_{1s}, \quad (5)$$

where Δu_{1s} – steady-state voltage.

For the industrial power supply frequencies of the circuit in Fig. 1, one can ignore the inductance of its elements. Therefore, in the open state of VD_1 (during the time interval $t_1 \leq t \leq t_2$) one can obtain [6]:

$$i_{IN}(t) = i_1(t),$$

$$u_{C2} = U_m \sin(\omega t) + U_m - \frac{1}{C_1} \int_{t_1}^t i_1(t) dt.$$

After differentiating this expression, one can get:

$$\frac{du_{C2}(t)}{dt} = \omega U_m \cos(\omega t) - \frac{1}{C_1} i_1(t)$$

and, consequently:

$$i_1(t) = C_1 \omega U_m \cos(\omega t) - C_1 \frac{du_{C2}(t)}{dt}. \quad (6)$$

Using the expression $u_{C2}(t) = u_{LV}(t) + i_f(t) \cdot R_f$ and performing its differentiation, and also substituting (6) in (3), one obtain the equation for the function $\Delta u_2(t)$ during the time period $t_1 \leq t \leq t_2$:

$$\frac{d^2 \Delta u_2(t)}{dt^2} + b_1 \frac{d\Delta u_2(t)}{dt} + b_2 \Delta u_2(t) = \frac{C_1 \omega U_m \cos(\omega t)}{R_f C_3 (C_1 + C_2)} - \frac{I_0 + \frac{1}{R_{LV}}(U_0 + I_0 r)}{R_f C_3 (C_1 + C_2)}, \quad (7)$$

where

$$b_1 = \frac{C_3 + (C_1 + C_2) \left(1 + \frac{R_f}{R_{LV}} + \frac{R_f}{R_d + r}\right)}{R_f C_3 (C_1 + C_2)},$$

$$b_2 = \frac{\frac{1}{R_{LV}} + \frac{1}{R_d + r}}{R_f C_3 (C_1 + C_2)}.$$

The discriminant of the characteristic equation in this case is also greater than zero, and the solution for $\Delta u_2(t)$ is found in the form:

$$\Delta u_2(t) = A_3 \sin(\omega t + \psi) + A_4 e^{p_3 t} + A_5 e^{p_4 t} + \Delta u_{2s}, \quad (8)$$

where Δu_{2s} – steady-state voltage, p_3, p_4 – roots of the characteristic equation $p^2 + b_1 p + b_2 = 0$. Values of A_3 and ψ are given by following expressions:

$$A_3 = \frac{C_1 \omega U_m}{R_f C_3 (C_1 + C_2) \sqrt{b_1^2 \omega^2 + (b_2 - \omega^2)^2}},$$

$$\psi = \arctan \left(\frac{b_2 - \omega^2}{b_1 \omega} \right).$$

Comparing (5) and (8), one can find:

$$\Delta u_{1s} = \Delta u_{2s} = \Delta u_s = -\frac{I_0 + \frac{1}{R_{LV}}(U_0 + I_0 r)}{\frac{1}{R_{LV}} + \frac{1}{R_d + r}},$$

where Δu_s – continuous component of the ripple voltage.

Using the invariance of u_{C2} and u_{C3} at the time instants t_1, t_2 , as well as the determination of t_1 from the condition $U_m(1 + \sin(\omega t_1)) = u_{C2}(t_1)$, and the time instant t_2 from the condition $i_1(t_2) = 0$, and also the expression

$$\int_{t_2}^{T+t_1} \Delta u_1(t) dt + \int_{t_1}^{t_2} \Delta u_2(t) dt = 0, \quad \text{one can get a system of}$$

seven algebraic equations (9) – (15) with seven unknowns: $A_1, A_2, A_3, A_4, A_5, t_1, t_2$

$$\omega A_3 \cos(\omega \Delta t + \psi) + p_3 A_4 e^{p_3 \Delta t} + p_4 A_5 e^{p_4 \Delta t} = p_1 A_1 + p_2 A_2; \quad (9)$$

$$\omega A_3 \cos(\psi) + p_3 A_4 + p_4 A_5 = p_1 A_1 e^{p_1(T-\Delta t)} + p_2 A_2 e^{p_2(T-\Delta t)}; \quad (10)$$

$$A_3 \sin(\psi) + A_4 + A_5 = A_1 e^{p_1(T-\Delta t)} + A_2 e^{p_2(T-\Delta t)}; \quad (11)$$

$$A_3 \sin(\omega \Delta t + \psi) + A_4 e^{p_3 \Delta t} + A_5 e^{p_4 \Delta t} = A_1 + A_2; \quad (12)$$

$$\frac{A_3}{\omega} (\cos(\psi) - \cos(\omega \Delta t + \psi)) = -\Delta u_s T - \frac{A_1}{p_1} (e^{p_1(T-\Delta t)} - 1) - \frac{A_2}{p_2} (e^{p_2(T-\Delta t)} - 1) - \frac{A_4}{p_3} (e^{p_3 \Delta t} - 1) - \frac{A_5}{p_4} (e^{p_4 \Delta t} - 1); \quad (13)$$

$$t_1 = \frac{1}{\omega} \arcsin \left(\frac{F_1}{U_m} - 1 \right); \quad (14)$$

$$t_2 = \frac{1}{\omega} \arccos\left(\frac{F_2}{\omega U_m}\right). \quad (15)$$

In (14) F_1 is given by the expression:

$$F_1 = I_0 R_f + (U_0 + I_0 r) \left(1 + \frac{R_f}{R_{LV}}\right) + (\Delta u_s + A_3 \sin(\psi) + A_4 + A_5) \left(1 + \frac{R_f}{R_{LV}} + \frac{R_f}{R_d + r}\right) + C_3 R_f (\omega A_3 \cos(\psi) + p_3 A_4 + p_4 A_5).$$

In its turn, in (15) F_2 is given by the expression:

$$F_2 = C_3 R_f \left(-\omega^2 A_3 \sin(\omega \Delta t + \psi) + p_3^2 A_4 e^{p_3 \Delta t} + p_4^2 A_5 e^{p_4 \Delta t}\right) + \left(1 + \frac{R_f}{R_{LV}} + \frac{R_f}{R_d + r}\right) (\omega A_3 \cos(\omega \Delta t + \psi) + p_3 A_4 e^{p_3 \Delta t} + p_4 A_5 e^{p_4 \Delta t}).$$

It should be noted that $\Delta t = t_2 - t_1$, while the relation between A_3 and U_m is defined above.

Equations (9) – (13) are linear with respect to A_1, \dots, A_5 , and therefore the system of equations (9) – (15) can be reduced to three equations with three unknowns t_1, t_2, A_j . Our experience in calculating (9) – (15) confirms the possibility of obtaining in each particular case a unique solution of the system in a set of real numbers.

Development of theory. The initial expressions (1) – (15) obtained above are derived from the publications of the authors [6-8] and are necessary for the further presentation of the materials in this article.

The advantage of the obtained analytical solution of this problem implies its logical conclusion in the derivation of expressions for the power of the elements of the circuit in Fig. 1 taking into account the voltage and current ripple in these elements (without the assumption of a limitation of their smallness).

The power losses in the R_{LV} load can be found as follows:

$$P_{LV} = f \int_{t_2}^{T+t_1} \frac{[u_{LV}(t)]^2}{R_{LV}} dt + f \int_{t_1}^{t_2} \frac{[u_{LV}(t)]^2}{R_{LV}} dt, \quad (16)$$

where $u_{LV}(t) = U_0 + I_0 r + \Delta u_1(t)$ for time interval $t_2 \leq t \leq T+t_1$, and $u_{LV}(t) = U_0 + I_0 r + \Delta u_2(t)$ for time interval $t_1 \leq t \leq t_2$.

Then let us transform (16) to the following form:

$$\begin{aligned} \frac{R_{LV} P_{LV}}{f} &= \left(\frac{R_{LV} P_{LV}}{f}\right)^{(1)} + \left(\frac{R_{LV} P_{LV}}{f}\right)^{(2)} = \\ &= \int_{t_2}^{T+t_1} [V_0 + \Delta u_1(t)]^2 dt + \int_{t_1}^{t_2} [V_0 + \Delta u_2(t)]^2 dt, \end{aligned} \quad (17)$$

where $V_0 = U_0 + I_0 r$.

Let us rewrite formula (17), integrating each component and assuming $V_0^{(1)} = V_0 + \Delta u_s$, then one can obtain the following expressions, that allow computing the power losses of P_{LV} taking into account the voltage and current ripple on the load R_{LV} :

$$\begin{aligned} \left(\frac{R_{LV} P_{LV}}{f}\right)^{(1)} &= \left(V_0^{(1)}\right)^2 (T + t_1 - t_2) + \frac{A_1^2}{2 p_1} \times \\ &\times \left[e^{2 p_1 (T+t_1-t_2)} - 1\right] + \frac{A_2^2}{2 p_2} \left[e^{2 p_2 (T+t_1-t_2)} - 1\right] + \\ &+ \frac{2 V_0^{(1)} A_1}{p_1} \left[e^{p_1 (T+t_1-t_2)} - 1\right] + \frac{2 V_0^{(1)} A_2}{p_2} \times \\ &\times \left[e^{p_2 (T+t_1-t_2)} - 1\right] + \frac{2 A_1 A_2}{p_1 + p_2} \left[e^{(p_1 + p_2)(T+t_1-t_2)} - 1\right]; \end{aligned} \quad (18)$$

$$\begin{aligned} \left(\frac{R_{LV} P_{LV}}{f}\right)^{(2)} &= \left(V_0^{(1)}\right)^2 (t_2 - t_1) + A_3^2 \times \\ &\times \left[\frac{t_2 - t_1}{2} + \frac{1}{4 \omega} [\sin(2 \psi) - \sin(2(\omega(t_2 - t_1) + \psi))]\right] + \\ &+ \frac{A_4^2}{2 p_3} \left[e^{2 p_3 (t_2-t_1)} - 1\right] + \frac{A_5^2}{2 p_4} \left[e^{2 p_4 (t_2-t_1)} - 1\right] + \\ &+ \frac{2 V_0^{(1)} A_3}{\omega} [\cos(\psi) - \cos(\omega(t_2 - t_1) + \psi)] + \frac{2 V_0^{(1)} A_4}{p_3} \times \\ &\times \left[e^{p_3 (t_2-t_1)} - 1\right] + \frac{2 V_0^{(1)} A_5}{p_4} \left[e^{p_4 (t_2-t_1)} - 1\right] + \\ &+ \frac{2 A_3 A_4}{\omega \left[\left(\frac{p_3}{\omega}\right)^2 + 1\right]} \left[e^{p_3 (t_2-t_1)} \left(\frac{p_3}{\omega} \sin[\omega(t_2 - t_1) + \psi] - \right.\right. \\ &\left.\left. - \cos[\omega(t_2 - t_1) + \psi] - \frac{p_3}{\omega} \sin(\psi) + \cos(\psi)\right) + \right. \\ &\left. + \frac{2 A_3 A_5}{\omega \left[\left(\frac{p_4}{\omega}\right)^2 + 1\right]} \left[e^{p_4 (t_2-t_1)} \times \right. \right. \\ &\left.\left. \times \left(\frac{p_4}{\omega} \sin[\omega(t_2 - t_1) + \psi] - \cos[\omega(t_2 - t_1) + \psi] - \right.\right. \right. \\ &\left.\left. - \frac{p_4}{\omega} \sin(\psi) + \cos(\psi)\right) + \frac{2 A_4 A_5}{p_3 + p_4} \left[e^{(p_3 + p_4)(t_2-t_1)} - 1\right]. \end{aligned} \quad (19)$$

The expression for the power losses in the group of elements $ZD_1 \dots ZD_n, r$, taking into account the previous consideration, will look like:

$$\begin{aligned} P_i &= f \int_{t_2}^{T+t_1} \left[V_0 + \Delta u_1(t) \right] \cdot \left[\frac{\Delta u_1(t)}{R_d + r} + I_0 \right] dt + \\ &+ f \int_{t_1}^{t_2} \left[V_0 + \Delta u_2(t) \right] \cdot \left[\frac{\Delta u_2(t)}{R_d + r} + I_0 \right] dt. \end{aligned} \quad (20)$$

Next, let us transform expression (20) to the form:

$$\begin{aligned} \frac{P_i}{f} &= \left(\frac{P_i}{f}\right)^{(1)} + \left(\frac{P_i}{f}\right)^{(2)} = \\ &= \int_{t_2}^{T+t_1} \left[V_0 I_0 + \Delta u_1(t) \left(I_0 + \frac{V_0}{R_d + r} \right) + \frac{(\Delta u_1(t))^2}{R_d + r} \right] dt + \\ &+ \int_{t_1}^{t_2} \left[V_0 I_0 + \Delta u_2(t) \left(I_0 + \frac{V_0}{R_d + r} \right) + \frac{(\Delta u_2(t))^2}{R_d + r} \right] dt. \end{aligned} \quad (21)$$

After integrating each component, the following expressions can be obtained, that allow calculating power losses in the group of elements $ZD_1 \dots ZD_n, r$:

$$\begin{aligned}
 \left(\frac{P_i}{f}\right)^{(1)} &= V_0 I_0 (T + t_1 - t_2) + \frac{I_0^{(1)} A_1}{p_1} [e^{p_1(T+t_1-t_2)} - 1] + \\
 &+ \frac{I_0^{(1)} A_2}{p_2} [e^{p_2(T+t_1-t_2)} - 1] + I_0^{(1)} \Delta u_s (T + t_1 - t_2) + \\
 &+ \frac{V_0^{(2)} A_1^2}{2 p_1} [e^{2 p_1(T+t_1-t_2)} - 1] + \frac{V_0^{(2)} A_2^2}{2 p_2} \times \\
 &\times [e^{2 p_2(T+t_1-t_2)} - 1] + V_0^{(2)} (\Delta u_s)^2 (T + t_1 - t_2) + \\
 &+ \frac{2 V_0^{(2)} A_1 A_2}{p_1 + p_2} [e^{(p_1+p_2)(T+t_1-t_2)} - 1] + \frac{2 V_0^{(2)} \Delta u_s A_1}{p_1} \times \\
 &\times [e^{p_1(T+t_1-t_2)} - 1] + \frac{2 V_0^{(2)} \Delta u_s A_2}{p_2} [e^{p_2(T+t_1-t_2)} - 1]; \\
 \left(\frac{P_i}{f}\right)^{(2)} &= V_0 I_0 (t_2 - t_1) + \frac{I_0^{(1)} A_3}{\omega} [\cos(\psi) - \\
 &- \cos[\omega(t_2 - t_1) + \psi]] + \frac{I_0^{(1)} A_4}{p_3} [e^{p_3(t_2-t_1)} - 1] + \\
 &+ \frac{I_0^{(1)} A_5}{p_4} [e^{p_4(t_2-t_1)} - 1] + I_0^{(1)} \Delta u_s (t_2 - t_1) + V_0^{(2)} A_3^2 \times \\
 &\times \left[\frac{1}{2} (t_2 - t_1) + \frac{1}{4 \omega} [\sin(2\psi) - \sin(2(\omega(t_2 - t_1) + \psi))] \right] + \\
 &+ \frac{V_0^{(2)} A_4^2}{2 p_3} [e^{2 p_3(t_2-t_1)} - 1] + \frac{V_0^{(2)} A_5^2}{2 p_4} [e^{2 p_4(t_2-t_1)} - 1] + \\
 &+ V_0^{(2)} (\Delta u_s)^2 (t_2 - t_1) + \frac{2 V_0^{(2)} A_3 A_4}{\omega \left[\left(\frac{p_3}{\omega} \right)^2 + 1 \right]} [e^{p_3(t_2-t_1)} \times \\
 &\times \left(\frac{p_3}{\omega} \sin[\omega(t_2 - t_1) + \psi] - \cos[\omega(t_2 - t_1) + \psi] \right) - \\
 &- \frac{p_3}{\omega} \sin(\psi) + \cos(\psi)] + \frac{2 V_0^{(2)} A_3 A_5}{\omega \left[\left(\frac{p_4}{\omega} \right)^2 + 1 \right]} [e^{p_4(t_2-t_1)} \times \\
 &\times \left(\frac{p_4}{\omega} \sin[\omega(t_2 - t_1) + \psi] - \cos[\omega(t_2 - t_1) + \psi] \right) - \\
 &- \frac{p_4}{\omega} \sin(\psi) + \cos(\psi)] + \frac{2 V_0^{(2)} \Delta u_s A_3}{\omega} [\cos(\psi) - \\
 &- \cos[\omega(t_2 - t_1) + \psi]] + \frac{2 V_0^{(2)} A_4 A_5}{p_3 + p_4} [e^{(p_3+p_4)(t_2-t_1)} - 1] + \\
 &+ \frac{2 V_0^{(2)} \Delta u_s A_4}{p_3} [e^{p_3(t_2-t_1)} - 1] + \\
 &+ \frac{2 V_0^{(2)} \Delta u_s A_5}{p_4} [e^{p_4(t_2-t_1)} - 1], \quad (22)
 \end{aligned}$$

where $I_0^{(1)} = I_0 + V_0 / (R_d + r)$, $V_0^{(2)} = 1 / (R_d + r)$.

The power losses in the active resistance of the filter R_f can be determined by the formula:

$$P_f = f \int_{t_2}^{T+t_1} [(i_{f1})^2 R_f] dt + f \int_{t_1}^{t_2} [(i_{f2})^2 R_f] dt, \quad (24)$$

where the values of i_{f1} , i_{f2} have the following form:

$$\begin{aligned}
 i_{f1} &= I_0 + \frac{U_0 + I_0 r}{R_{LV}} + \Delta u_1(t) \left(\frac{1}{R_{LV}} + \frac{1}{R_d + r} \right) + \\
 &+ C_3 \frac{d\Delta u_1(t)}{dt}, \\
 i_{f2} &= I_0 + \frac{U_0 + I_0 r}{R_{LV}} + \Delta u_2(t) \left(\frac{1}{R_{LV}} + \frac{1}{R_d + r} \right) + \\
 &+ C_3 \frac{d\Delta u_2(t)}{dt}.
 \end{aligned}$$

Then let us transform expression (24) to the form:

$$\begin{aligned}
 \frac{P_f}{R_f f} &= \left(\frac{P_f}{R_f f} \right)^{(1)} + \left(\frac{P_f}{R_f f} \right)^{(2)} = \\
 &= \int_{t_2}^{T+t_1} \left(I_0^{(2)} + \Delta u_1(t) \left(\frac{1}{R_{LV}} + \frac{1}{R_d + r} \right) + C_3 \frac{d\Delta u_1(t)}{dt} \right)^2 dt + \\
 &+ \int_{t_1}^{t_2} \left(I_0^{(2)} + \Delta u_2(t) \left(\frac{1}{R_{LV}} + \frac{1}{R_d + r} \right) + C_3 \frac{d\Delta u_2(t)}{dt} \right)^2 dt,
 \end{aligned}$$

where $I_0^{(2)} = I_0 + (U_0 + I_0 r) / R_{LV}$.

After integrating each component, one can obtain the following expressions that allow calculating the power losses in the active filter resistance of the installation:

$$\begin{aligned}
 \left(\frac{P_f}{R_f f} \right)^{(1)} &= (I_0^{(3)})^2 (T + t_1 - t_2) + \frac{X_4^2}{2 p_1} [e^{2 p_1(T+t_1-t_2)} - 1] + \\
 &+ \frac{X_5^2}{2 p_2} [e^{2 p_2(T+t_1-t_2)} - 1] + \frac{2 I_0^{(3)} X_4}{p_1} [e^{p_1(T+t_1-t_2)} - 1] + \\
 &+ \frac{2 I_0^{(3)} X_5}{p_2} [e^{p_2(T+t_1-t_2)} - 1] + \frac{2 X_4 X_5}{p_1 + p_2} \times \\
 &\times [e^{(p_1+p_2)(T+t_1-t_2)} - 1], \quad (25) \\
 \left(\frac{P_f}{R_f f} \right)^{(2)} &= (I_0^{(3)})^2 (t_2 - t_1) + X_1^2 \left[\frac{1}{2} (t_2 - t_1) + \right. \\
 &+ \frac{1}{4 \omega} [\sin(2\psi) - \sin(2[\omega(t_2 - t_1) + \psi])] + (A_3 \omega C_3)^2 \times \\
 &\times \left[\frac{1}{2} (t_2 - t_1) + \frac{1}{4 \omega} [\sin(2[\omega(t_2 - t_1) + \psi]) - \sin(2\psi)] \right] + \\
 &+ \frac{X_2^2}{2 p_3} [e^{2 p_3(t_2-t_1)} - 1] + \frac{X_3^2}{2 p_4} [e^{2 p_4(t_2-t_1)} - 1] + \\
 &+ \frac{2 I_0^{(3)} X_1}{\omega} [\cos(\psi) - \cos[\omega(t_2 - t_1) + \psi]] + \\
 &+ 2 I_0^{(3)} A_3 C_3 [\sin[\omega(t_2 - t_1) + \psi] - \sin(\psi)] + \frac{2 I_0^{(3)} X_2}{p_3} \times
 \end{aligned}$$

$$\begin{aligned}
& \times \left[e^{p_3(t_2-t_1)} - 1 \right] + \frac{2I_0^{(3)} X_3}{p_4} \left[e^{p_4(t_2-t_1)} - 1 \right] + \frac{X_1 A_3 C_3}{2} \times \\
& \times [\cos(2\psi) - \cos(2[\omega(t_2-t_1) + \psi])] + \\
& + \frac{2X_1 X_2}{\omega \left[\left(\frac{p_3}{\omega} \right)^2 + 1 \right]} \left[e^{p_3(t_2-t_1)} \times \right. \\
& \times \left(\frac{p_3}{\omega} \sin[\omega(t_2-t_1) + \psi] - \cos[\omega(t_2-t_1) + \psi] \right) - \\
& - \frac{p_3}{\omega} \sin(\psi) + \cos(\psi) \left. \right] + \frac{2X_1 X_3}{\omega \left[\left(\frac{p_4}{\omega} \right)^2 + 1 \right]} \left[e^{p_4(t_2-t_1)} \times \right. \\
& \times \left(\frac{p_4}{\omega} \sin[\omega(t_2-t_1) + \psi] - \cos[\omega(t_2-t_1) + \psi] \right) - \\
& - \frac{p_4}{\omega} \sin \psi + \cos \psi \left. \right] + \frac{2X_2 A_3 C_3}{\left(\frac{p_3}{\omega} \right)^2 + 1} \left[e^{p_3(t_2-t_1)} \times \right. \\
& \times \left(\frac{p_3}{\omega} \cos[\omega(t_2-t_1) + \psi] + \sin[\omega(t_2-t_1) + \psi] \right) - \\
& - \frac{p_3}{\omega} \cos(\psi) - \sin(\psi) \left. \right] + \frac{2X_3 A_3 C_3}{\left(\frac{p_4}{\omega} \right)^2 + 1} \left[e^{p_4(t_2-t_1)} \times \right. \\
& \times \left(\frac{p_4}{\omega} \cos[\omega(t_2-t_1) + \psi] + \sin[\omega(t_2-t_1) + \psi] \right) - \\
& - \frac{p_4}{\omega} \cos(\psi) - \sin(\psi) \left. \right] + \frac{2X_2 X_3}{p_3 + p_4} \times \\
& \times \left[e^{(p_3+p_4)(t_2-t_1)} - 1 \right], \quad (26)
\end{aligned}$$

where

$$I_0^{(3)} = I_0^{(2)} + \Delta u_s \left(\frac{1}{R_{LV}} + \frac{1}{R_d + r} \right);$$

$$X_1 = A_3 \left(\frac{1}{R_{LV}} + \frac{1}{R_d + r} \right);$$

$$X_2 = A_4 \left(p_3 C_3 + \frac{1}{R_{LV}} + \frac{1}{R_d + r} \right);$$

$$X_3 = A_5 \left(p_4 C_3 + \frac{1}{R_{LV}} + \frac{1}{R_d + r} \right);$$

$$X_4 = A_1 \left(p_1 C_3 + \frac{1}{R_{LV}} + \frac{1}{R_d + r} \right);$$

$$X_5 = A_2 \left(p_2 C_3 + \frac{1}{R_{LV}} + \frac{1}{R_d + r} \right).$$

Approbation of the obtained theoretical results
was performed using the calculations of the parameters of the standard installation DETU 08-04-99, that is used in the State verification scheme for means of measuring the direct current electric voltage in the range 1...180 kV [14].

To the high voltage direct current power supply circuit

shown in Fig. 1 were assigned the following parameters that correspond to the installation of DETU 08-04-99 in the modes of rated voltages V_0 from 1 to 180 kV: C_1 – charging capacitor (0.1 μ F); C_2 , C_3 – filter capacitors (0.072 μ F); R_f – filter resistance (1.78 M Ω); $ZD_1, \dots, ZD_i, \dots, ZD_n$ are Zener diodes of the D818D type; R_{LV} is the resistance of the resistive voltage divider.

For the D818D Zener diodes, the value of stabilized current $I_0 = 5$ mA was selected for 27 different values of the rated voltages V_0 on the load, according to Table 1. The voltage divider has four values of input rated voltages V_0 : 180 kV; 90 kV; 60 kV; 30 kV for which the current of the divider voltage is $I_{LV} = 2.5$ mA. For the other 23 input voltages of the voltage divider V_0 , its current decreases in proportion to the input voltage.

Table 1

Calculation results for 27 power modes
of the DETU 08-04-99 installation

V_0 , kV	U_m , kV	Δ_1 , V	Δ_2 , V	Δ_p , %	$I_0 + I_{LV}$, mA
1	5.97	3.54	-4.08	0.381	5.083
2	6.61	3.81	-4.88	0.217	5.167
3	7.25	4.45	-5.69	0.169	5.250
4	7.89	5.04	-6.49	0.144	5.333
5	8.52	5.57	-7.27	0.128	5.417
6	9.16	6.04	-8.04	0.117	5.500
7	9.80	6.44	-8.81	0.109	5.583
8	10.44	6.78	-9.54	0.102	5.667
9	11.08	7.07	-10.26	0.096	5.750
10	11.72	7.31	-10.97	0.091	5.833
20	18.27	11.41	-20.65	0.080	6.667
30	24.66	13.09	-24.15	0.062	7.500
40	29.27	11.71	-22.07	0.042	6.667
50	35.22	12.46	-23.82	0.036	7.083
60	41.17	13.18	-25.51	0.032	7.500
70	46.09	12.18	-23.86	0.025	6.944
80	51.90	12.63	-24.97	0.023	7.222
90	57.71	13.09	-26.05	0.021	7.500
100	62.04	11.11	-22.32	0.017	6.389
110	67.70	11.39	-22.88	0.016	6.528
120	73.36	11.67	-23.43	0.015	6.667
130	79.02	11.95	-23.97	0.014	6.806
140	84.68	12.22	-24.51	0.013	6.944
150	90.34	12.49	-25.03	0.012	7.083
160	96.00	12.76	-25.55	0.012	7.222
170	101.66	13.02	-26.07	0.012	7.361
180	107.32	13.29	-26.59	0.011	7.500

Calculations were performed to solve the system of equations (9) – (15) for the parameters $r = 10$ k Ω for the modes $V_0 = 1 \dots 10$ kV and $r = 60$ k Ω for the $V_0 = 20 \dots 180$ kV modes. The value of r_d was assumed according to [4] equal to 22 Ω for each Zener diode, and $R_d = nr_d$, where n is the number of Zener diodes corresponding to each mode V_0 . This quantity is determined based on the average value of the D818D stabilization voltage $u_0 = 9$ V.

Based on the calculation results, the maximum positive pulsation values $\Delta u(t) = \Delta_1$ and minimum negative pulsation values $\Delta u(t) = \Delta_2$ were determined, as well as the pulsation amplitude coefficient:

$$\Delta_p = \frac{\Delta_1 - \Delta_2}{2V_0} 100, \%. \quad (27)$$

The obtained results of calculations are shown in Table 1. Table 1 also shows the value of the total average

load current $I_0 + I_{LV}$ (mA) for each DETU 08-04-99 installation operating mode.

From the data in Table 1 it follows that with increase in load voltage V_0 , the pulsation amplitude coefficient Δ_p decreases accordingly. In the $V_0 = 1$ kV mode, the pulsation amplitude coefficient $\Delta_p = 0.381\%$, and in the $V_0 = 180$ kV mode the pulsation amplitude coefficient is $\Delta_p = 0.011\%$. The above values of ripple in different operating modes of the installation differ by a factor of 35.

Using the values of P_{LV} , P_i , P_f obtained above, one can determine the energy efficiency coefficient of the DETU 08-04-99 installation with nonlinear load:

$$EFF = \frac{P_{LV} + P_i}{P_{LV} + P_i + P_f} 100 = \frac{1}{1 + P_f / (P_{LV} + P_i)} 100, \% \quad (28)$$

Table 2 shows the calculated values of EFF (28) for the DETU 08-04-99 installation for V_0 modes from 1 to 30 kV. For the $V_0 = 180$ kV mode, the EFF value is 93.1 %.

The calculated results for the DETU 08-04-99 installation, given in Table 1 and Table 2 are confirmed by the data of installation experimental study.

Table 2

The values of the energy efficiency coefficient of the DETU 08-04-99 installation for the V_0 values from 1 kV to 30 kV

V_0 , kV	P_{LV} , W	P_i , W	P_f , W	EFF , %
1.0	0.09	5.25	46.15	10.38
2.0	0.35	10.25	47.68	18.19
3.0	0.78	15.25	49.20	24.57
4.0	1.37	20.25	50.77	29.86
5.0	2.13	25.25	52.37	34.33
6.0	3.05	30.25	53.99	38.15
7.0	4.14	35.25	55.63	41.45
8.0	5.40	40.25	57.30	44.34
9.0	6.83	45.25	59.00	46.88
10.0	8.42	50.25	60.72	49.14
20.0	34.34	101.50	79.85	62.98
30.0	76.51	151.50	100.97	69.31

The discussion of the results. When determining the energy efficiency coefficient of the high-voltage installation, let us consider the power $P_{out} = P_{LV} + P_i$ as a net power, while the power P_f represents the additional power losses in the filter resistance. At the same time, an increase in the resistance of the filter R_f is a means of decreasing the amplitude of the voltage ripple in the installation load when increasing voltage U_m at the input of the circuit [5].

The peculiarity of developing a mathematical model for the typical high-voltage installation modes (Fig. 1) is that it determines the necessary parameters of the installation in the opposite direction – given average voltage drop across the group of Zener diodes U_0 for a given average current I_0 through it. The proposed solution sets the numerical value of the time instant t_1 – the start of the charging of the installation capacitor C_2 and the time instant t_2 – the «disconnection» of the right part of the installation from the capacitance C_1 , and also determines the parameters $A_1, A_2, A_3, A_4, A_5, p_1, p_2, p_3, p_4, \psi, \Delta u_s, U_m$ depending on the values of $U_0, I_0, C_1, C_2, C_3, R_{LV}, T, r, R_d, R_f$ by the analytical method, and is new.

The use of Zener diodes in the measuring group of a high-voltage direct current installation allows significantly reducing the pulsation amplitude (up to 3 and more times) and improve the voltage quality on the load [8].

It should also be noted that nowadays professional and demonstration versions of various circuit simulation programs are widely used to simulate voltage multiplication schemes, as well as processes in electrical equipment insulation. To simulate, for example, the phenomenon of partial discharges in the insulation of high-voltage equipment, demonstration versions of the programs are sufficient enough [15, 16]. However, the number of Zener diodes in the operating DETU 08-04-99 installation is tens of thousands of pieces. In this regard, on the one hand, a complete simulation of such a scheme requires expensive professional circuit simulation programs. On the other hand, as shown in this article, there is no need for a detailed circuit simulation of such a complex scheme. Taking these factors into account, the group of authors made a choice in favor of a generalized analytical solution of the problem posed in this article.

Conclusion.

1. An analytical method for solving equations for a complex system of a typical high voltage direct current installation based on a voltage doubler rectifier with an integrated R, C – filter, and a measuring group has been developed.

2. The solution obtained is generalized for the case of insertion of Zener diodes into the measuring group, while it is valid within the linearized domain of their current-voltage characteristic.

3. The use of Zener diodes in the load circuits of the installation makes it possible to significantly reduce the amplitude of voltage ripple, and also to improve the quality of the output voltage of direct current voltage multiplier.

4. A theoretical basis is developed not only for voltages and currents, but also for the electrical power of the elements of a typical high-voltage direct current installation with allowance for nonlinear voltage pulsations.

REFERENCES

1. Dwivedi C.K., Daigavane M.B. Multi-purpose low cost DC high voltage generator (60 kV output), using Cockcroft-Walton voltage multiplier circuit. *International Journal of Science and Technology Education Research*, 2011, vol.2(7), pp. 109-119.
2. Cortez D.F., Barbi I. A Family of High Voltage Gain Single-Phase Hybrid Switched-Capacitor PFC Rectifiers. *IEEE Transactions On Power Electronics*, 2015, vol.30, no.8, pp. 4189-4198. doi: 10.1109/TPEL.2014.2360173.
3. Cockcroft J.D., Walton E.T.S. Experiments with high velocity positive ions. (I) Further developments in the method of obtaining high velocity positive ions. *Proceedings of the Royal Society A. Mathematical, physical and engineering sciences*, 1932, vol.136, no.830, pp. 619-630. doi: 10.1098/rspa.1932.0107.
4. Golomedov A.V. *Poluprovodnikovye pribory. Diody vypriamitel'nye, stabiliziruyemye, tiristory: spravochnik* [Semiconductors. Rectifier diodes, Zener diodes, thyristors. Directory]. Moscow, Radio and communication Publ., 1988. 347-350. (Rus).
5. Brzhezytskiy V.O., Vendychanskiy R.V., Desiatov O.M., Haran I.A. Rationale diodes and modes of supply of standard units of high voltage direct current. *Science news of NTUU «KPI»*, 2014, no.1, pp. 7-13. (Ukr).
6. Brzhezytskiy V., Desiatov O., Suleimanov V., Khominich V. Analysis of high-voltage cascade generator pulsations of a direct current. *Technology audit and production reserves*, 2015, vol.1, no.1(21), pp. 56-61. doi:10.15587/2312-8372.2015.37219. (Ukr).

7. Brzhezitsky V., Desiatov O., Maslychenko I., Anokhin Y. Analytical research mode the voltage of high-voltage cascade generator with nonlinear loads. *Scientific Works of National University of Food Technologies*, 2015, vol.21, no.3, pp. 183-191. (Ukr).
8. Brzhezitsky V., Desyatov O., Garan J., Babicheva A. Analysis of the current ripple of cascade generator high DC voltage. *Scientific Herald of NULES of Ukraine. Series: Technique and energy of APK*, 2015, no.209-2, pp. 30-38. (Ukr).
9. Merev A., Hällström J.K. A Reference System for Measuring High-DC Voltage Based on Voltage References. *IEEE Transactions On Instrumentation And Measurement*, 2015, vol.64, no.1, pp. 184-189. doi: 10.1109/TIM.2014.2338673.
10. Anokhin Y.L., Brzhezitskyi V.O., Haran Ya.O., Masliuchenko I.M., Protsenko O.P., Trotsenko Ye.O. Application of high voltage dividers for power quality indices measurement. *Electrical engineering & electromechanics*, 2017, no.6, pp. 53-59. doi: 10.20998/2074-272X.2017.6.08.
11. Kravchenko V.I., Petkov A.A. Parametrical synthesis of high-voltage pulse test devices with capacitive energy storage. *Electrical engineering & electromechanics*, 2007. no.6, pp. 70-75. (Rus).
12. Shcherba A.A., Suprunovska N.I., Ivashchenko D.S. Modeling of nonlinear resistance of electro-spark load for synthesis of discharge circuit of capacitor by time parameters. *Technical electrodynamics*, 2014, no.3, pp. 12-18. (Rus).
13. Suprunovska N.I., Shcherba A.A. Processes of energy redistribution between parallel connected capacitors. *Technical electrodynamics*, 2015, no.4, pp. 3-11. (Rus).
14. DSTU 3863-99 *Derzhavnyi standart Ukrainy. Metrolohiia. Derzhavna povirochna skhema dlia zasobiv vymiriuvan elektrychnoi napruhy postiinoho strumu v diapazoni vid 1 do 800 kV* [DSTU 3863-99. State standard of Ukraine. Metrology. State verification schedule for means measuring of direct current electric voltage in the range from 1 to 800 kV]. Kyiv, Derzhstandart of Ukraine Publ., 1999. 10p. (Ukr).

15. Trotsenko Ye., Brzhezitsky V., Protsenko O., Chumack V., Haran Ya. Simulation of partial discharges under influence of impulse voltage. *Technology audit and production reserves*, 2018, vol.1, no.1(39), pp. 36-41. doi: 10.15587/2312-8372.2018.123309.
16. Trotsenko Ye., Brzhezitsky V., Protsenko O., Chumack V., Haran Ya. Effect of voltage harmonics on pulse repetition rate of partial discharges. *Technology audit and production reserves*, 2018, vol.2, no.1(40), pp. 37-44. doi: 10.15587/2312-8372.2018.126626.

Received 30.08.2018

V.O. Brzhezitskyi¹, Doctor of Technical Science, Professor,
 R.V. Vendychanskyi², Deputy Chief of the Research Department
 of Measurements of Electrical Values,
 Ye.O. Trotsenko¹, Candidate of Technical Science, Associate
 Professor,
 Ya.O. Haran¹, Assistant,
 O.M. Desyatov¹, Engineer,
 V.I. Khominich¹, Candidate of Technical Science, Senior
 Researcher,
¹ National Technical University of Ukraine «Igor Sikorsky Kyiv
 Polytechnic Institute»,
 37, Prosp. Peremohy, Kyiv, 03056, Ukraine,
 phone +380 44 2367989,
 e-mail: v.brzhezitskiy@ukr.net
² State Enterprise «All-Ukrainian State Research and Production
 Center For Standardization, Metrology, Certification and
 Consumers Rights Protection» (SE «Ukrmetrteststandard»),
 4, Metrolohichna Str., Kyiv, 03168, Ukraine,
 phone +380 44 5263485
 e-mail: hivolt@ukrcsm.kiev.ua

How to cite this article:

Brzhezitskyi V.O., Vendychanskyi R.V., Trotsenko Ye.O., Haran Ya.O., Desyatov O.M., Khominich V.I. Characteristics of specialized single-phase high voltage doubler rectifier. *Electrical engineering & electromechanics*, 2018, no.5, pp. 54-61. doi: 10.20998/2074-272X.2018.5.09.

M. Dehghani, Z. Montazeri, A. Ehsanifar, A.R. Seifi, M.J. Ebadi, O.M. Grechko

PLANNING OF ENERGY CARRIERS BASED ON FINAL ENERGY CONSUMPTION USING DYNAMIC PROGRAMMING AND PARTICLE SWARM OPTIMIZATION

Purpose. In the present article, a new approach of the energy grid studies is introduced to program energy carriers. In this view, a proper plan is designed on the use of energy carriers considering the energy optimum use. Indeed, the proper energy grid is designed by applying Iran energy balance sheet information. It is proper to mention that, the energy grid modelling is done in a matrix form. The electrical energy distribution among power stations is achieved by using the particle swarm optimization algorithm. In the present paper, concerning the dynamic programming method, it is tried to determine a suitable combination of energy carriers. References 16, tables 17, figures 1.

Key words: particle swarm optimization, final energy consumption, energy planning, energy carriers, dynamic programming.

Цель. В настоящей статье предлагается новый подход к исследованию энергетических сетей для планирования энергоносителей. С этой целью разработан корректный план использования энергоносителей с учетом оптимального потребления энергии. Разработана соответствующая энергосистема с использованием информации о энергетическом балансе Ирана. Необходимо отметить, что моделирование энергосистемы выполняется в матричной форме. Распределение электрической энергии между электростанциями достигается за счет использования алгоритма оптимизации методом роя частиц. В настоящей работе, посвященной методу динамического программирования, предпринята попытка определить подходящую комбинацию энергоносителей. Библ. 16, табл. 17, рис. 1.

Ключевые слова: оптимизация методом роя частиц, конечное потребление энергии, планирование в энергетике, энергоносители, динамическое программирование.

Introduction. One of the suitable criterions in determining the development level and the life quality of a typical country is the energy application. Both the duration of energy presentation and the long term access ability to sources require energy comprehensive planning. One of the key issues of energy planning is energy carriers.

Despite the present applied method, the energy planning program needs the initial comprehensive study of the energy system. It is possible to offer a general framework to model different systems holding different energy carriers like electrical, thermal, gas, etc. energies. The mentioned modelling framework is based on the energy-based approach. The energy-based main idea is defining a converter matrix having the ability of describing the generation, delivery and consumption within systems carrying some types of energies [1]. Based on the energy current optimization model, Cormio has proposed a linear-based planning optimization model in a region in south of Italy. This plan includes energy optimization details of the energy initial sources, thermal and electrical energies generation, transition and the consumption section. The energy system optimization model is introduced in [2] from the final energy consumption level to the initial energy carriers that is from down to up.

The global energy system is mainly based on applying fossil fuels like coal, oil and natural gas. Although renewable energy sources are under focused, their reliable ability is low. Considering the lack of fossil sources, transition to renewable energy sources by applying hydrogen as the energy carrier is introduced [3]. This economic transition includes uncertainty and it is simultaneously introduced by the greenhouse gases effects. By applying long-term planning, this energy substitution is investigated and it is highly tried to supply proper hydrogen or the energy carrier assessment in the future [4].

While renewable energies are introduced as the energy initial carriers, the transportation industry is highly dependent to oil energy carrier. Indeed, there is no simple renewable solution to answer the transition section demand. Today, biofuels along with electricity is introduced as a main planning choice in replacing the transportation fossil fuels [5].

Concerning the micro grid concept, the random energy planning is introduced by taking the renewable energy sources uncertainty and its oscillation entity. Renewable energy sources which are known as initial energy carriers are integral parts of a micro grid. The oscillatory entity of these sources makes a micro grid exploiting complex [6].

The common initial energy sources (the fossil fuels) are limited and they need to be programmed considering the renewable initial energy carriers. Considering the planning present limitations, four dimensions known as system, application, generation and technology terms can be discussed. Indeed, the generation and exploiting initial energy sources can be studied by considering the new energy industry properties [7]. Accordingly, different energy carriers are studied regarding their application efficiency and abilities. Thus, energy carriers exploiting is optimally done [8].

Different studies have been proposed by researchers within the field of energy planning and management. Therefore, in none of these studies, an hourly exploiting of these energy carriers to supply the final energy consumption is not investigated. In the present article, the ultimate effort is done to exploit energy carriers by neglecting energy carriers' independency. To implement this planning, the proper energy grid is designed.

In the following, in section two, the present problem is introduced. Then, in section three, the energy grid modelling is analyzed. The particle swarm algorithm is introduced in section four. Designing the proper energy

grid to be used in energy studies is done in section five. Section six simulates planning. Finally, discussion and conclusion are studied in section seven.

Problem presentation. In planning energy initial carriers, the lowest energy level that is the final energy application is considered as the first level; then, different energy losses and their converting are analyzed step by step to determine the quantity of initial energy carriers in order to supply the final energy consumption.

An important portion of the final energy use is related to the electrical energy. In each hour of planning, different modes of power stations can supply the consumption of electrical energy. For each mode, the best economic distribution among power stations must be determined. Therefore, in each hour considering different modes of power stations' combination, there are different modes of energy carriers. Indeed, we are facing the power station commitment problem. The only difference is that instead of having different combinations of power stations, we face with energy carriers different combinations. Considering the study period and the grid information, the proper combination is chosen by taking the study period length into account.

The energy grid modelling. After compiling and expanding the notion of the referent energy system in the Brochain national laboratory, the energy system simulator is developed. The matrix formulation main concept is to cut the energy system vertically [9].

The energy grid matrix model starts from the lowest energy level or the final energy consumption. Then, it reaches the highest energy level or the initial energy carriers.

At first, the final energy consumption matrix is defined as V_1 matrix based on different sections. In this case, there is

$$V_2 = T_{1,2} \times V_1, \quad (1)$$

where V_2 is the final energy consumption based on different carriers and $T_{1,2}$ is the consumption part to carriers converter part.

Considering the energy consumption, distribution and transition losses, the final energy consumption is defined as

$$V_3 = T_{2,3} \times V_2, \quad (2)$$

where V_3 is the final energy consumption based on different carriers considering losses, $T_{2,3}$, is the transition, distribution and consumption efficiency matrix.

To model the final electrical energy consumption, the electrical supply shares of different power stations are calculated by applying (3); then, the power stations input fuels are measured by (4)

$$V_{e2} = T_{e1,2} \times V_{e1}, \quad (3)$$

$$V_{e3} = T_{e2,3} \times V_{e2}, \quad (4)$$

where V_{e1} is the total generated electrical energy, $T_{e1,2}$ stands for the separation matrix of the electrical energy generation at different power stations, V_{e2} is the electrical energy generation of different power stations, V_{e3} is different power stations input fuel and $T_{e2,3}$ is the power stations efficiency matrix.

Besides, to compute the electrical energy generator carriers (5) is used

$$V_{e4} = T_{e3,4} \times V_{e3}, \quad (5)$$

where V_{e4} is the electrical energy generator vectors and $T_{e3,4}$ is the power stations' input fuel separated from different vectors input fuel matrix.

After simulating the electrical energy generation process, the need for different vectors is computed by considering the electrical energy generation

$$V_4 = V_3 + V_{e4} - V_e, \quad (6)$$

where V_4 stands for the need for different vectors considering the consumption, distribution and transition losses of electrical energy generation, and V_e is the generated electrical energy.

Some of these carriers are derived from refining process. Therefore, it is necessary to simulate the petroleum refinery; thus, (7) is used

$$V_{p2} = T_p \times V_{p1}, \quad (7)$$

where V_{p1} is the refineries maximum capacity, T_p is the share of each generated products of the petroleum refinement, and V_{p2} shows the carriers generated by refinement.

By using (8), the need for carriers can be computed considering refinement

$$V_5 = V_4 - V_{p2} + V_p, \quad (8)$$

where V_p is the refined petroleum and V_5 shows the need for carriers after considering the electrical energy generation losses and refinement.

Finally, the quantities of carriers' import and export are determined by applying

$$V_6 = V_5 - P, \quad (9)$$

where P is the national generation quantity of the initial energy carriers; V_6 is the initial energy carriers' import and export. Noticeably, the positive sign represents import and the negative sign shows the export.

In (3), in order to determine different power stations shares of the electrical energy generation, it is necessary to establish the economic distribution. To fulfill this aim, the particle swarm optimization is used.

The particle swarm optimization. The particle swarm optimization (PSO) was first introduced by Candy and Aberheart [10]. After then, it was used in different scientific and applied fields. PSO is a population based optimization algorithm in which each person is considered as a particle. These particles positions within the search space determine the problem solution. Particles can search the best position in cooperation with each other. Particles' movements can be determined by applying (10) and (11)

$$x_i(t+1) = x_i(t) + v_i(t), \quad (10)$$

$$v_i(t+1) = wv_i + c_1r_1(pbest_i(t) - x_i(t)) + c_2r_2(gbest(t) - x_i(t)), \quad (11)$$

where $x_i(t)$ is the position, $v_i(t)$ is the i -th particle velocity at t moment, $pbest_i(t)$ is the best position found by the i -th particle, and $gbest(t)$ is the best found position by the whole population till t moment, w is the inertial coefficient, c_1 and c_2 are the controlling parameters of each particle and the whole population best effect on the particles velocity and r_1 and r_2 are random numbers within (1-0).

Designing the energy grid suitable for studies.

Since the present study is novel, information related to the proper energy grid is not accessible. Indeed, in this study, the energy grid comprising the 24-hour final energy consumption information is needed. Both Iran energy balance sheet information [11] and the standard electrical grid used in the power station commitment problem studies are used.

The idea of designing the proper energy grid is proposed based on the concept of the electrical energy vital role. Indeed, some part of the final energy consumption is related to the final electrical energy consumption. In the energy balance sheet, there is no information of the final energy use. However, it is clear that the final energy consumption of different energies is not independent of one another and the final energy consumption of different energies is symmetric.

Considering the energy balance sheet, the final energy consumption for a year is in Table 1.

Table 1
Different sections of the final energy consumption [11]

Row	Sectors of energy	
1	E1 Residential, commercial, general	399.9 mboe
2	E2 Industrial	188.2 mboe
3	E3 Transportation	254.3 mboe
4	E4 Agriculture	33.4 mboe
5	E5 Other	2.5 mboe
6	E6 Non-energy	85.3 mboe
7	E_{ff} Total of final energy consumption	9636.6 mboe
8	E_{ef} Final electrical energy consumption	79.7 mboe

The final electrical energy consumption in the above table is shown by E_{ef} . It is known that considering the electrical energy losses from generation till consumption (consumption, distribution and transition losses) of power stations must generate more electrical energies in order to supply this quantity.

Concerning the final energy consumption, the electrical final energy consumption in different power stations is calculated as below

$$E_{ef} = \sum_{i=1}^n a_i E_i, \quad (12)$$

$$E_{ef} = a_1 E_1 + a_2 E_2 + a_3 E_3 + a_4 E_4 + a_5 E_5 + a_6 E_6, \quad (13)$$

where E_{ef} is the final electrical energy consumption, n is the number of different energy consumption power stations, a_i is the electrical final energy consumption coefficient in the relation which is related to i -th final energy consumption, and E_i is the i -th section final energy consumption.

Considering losses of consumption, distribution and transition of electrical energy, its consumption is calculated by applying

$$E_e = \frac{1}{\eta_e} E_{ef}, \quad (14)$$

where E_e is the electrical energy consumption; η_e is the energy grid efficiency concerning losses of consumption, distribution and transition of electrical energy.

In the next phase of designing, it is possible to approximately compute the final energy per hour by applying information related to the power station commitment problem

$$V_1^h = \frac{load^n}{E_e} V, \quad (15)$$

where V_1^h is the designed final energy consumption, $load^n$ is the grid electrical energy quantity in h hour and V is the balance sheet based final energy consumption for the E_e electrical consumption quantity or E_{ef} electrical final energy consumption quantity.

Therefore, the 24-hour information of the final energy consumption is computed. Although, this final characteristic is approximately calculated and it might differ from the real value, this information answers our energy study.

The energy grid information and designing by applying ten power stations. In order to plan energies of initial energy carriers, a ten power station system is proposed. The electrical grid is derived from [12] reference. Information related to the mentioned system is designed based on the afore-said process. These data are attached to the same paper. The maximum power station capacities equals to 3721.1 boe. It is necessary to mention that quantities related to the power station capacity are chosen approximately and in accordance with the energy balance sheet.

Simulation. Regarding the energy grid modelling, the simulation trend can be represented as the followings:

- 1) defining parameters and converting matrices;
- 2) applying 3 to 10 steps for each hour of under studied 24 hour span;
- 3) determining the final energy consumption;
- 4) determining the final energy consumption based on different carriers;
- 5) determining the final energy consumption considering the energy, distribution, transition and consumption of energies;
- 6) determining possible combinations of power station generators in order to supply the electrical energy;
- 7) the economic distribution of the electrical energy among power station generators by means of the optimization algorithm for all possible combinations;
- 8) the contribution of each carrier from the refining of crude oil;
- 9) determine the need to provide energy to the final energy consumption for each of the possible combinations;
- 10) determining the import and export of energy carriers regarding the national energy carriers presentation for each possible combination;
- 11) determining the total request, import and export values of the energy carriers in the whole under studied span (24 hours) by means of the dynamic planning method.

The objective function. One important stage in planning energy carriers is to distribute electrical energy economically. The objective function of the electrical energy economical distribution is introduced in (16). This objective function can be solved using optimization algorithms [13]

$$F_{obj} = \sum_{i=1}^{N_{FIU}} E_{FIU}^i C_{FIU}^i + \sum_{i=1}^{N_{DU}} S_{U_i} C_C^i, \quad (16)$$

$$E_{FIU}^i = \sum_{j=1}^{N_{DU}} \sum_{k=1}^{N_{U_j}^j} e_{i,j} E_{IU}^k \quad \& \quad i=1:N_{FIU}, \quad (17)$$

$$e_{i,j} \in [ETF]_{N_{FIU} \times N_{DU}}, \quad (18)$$

$$E_{IU} = \frac{1}{\eta_U} E_{OU}, \quad (19)$$

where F_{obj} is the objective function, N_{FIU} is the number of different input fuels of power station generators, E_{FIU}^i is the sum of input energy to power stations of the i -th fuel type, C_{FIU}^i is the i -th type input fuel type cost of power stations, N_{DU} is the number of different fuel generators, S_{U_i} stands for the i -th power station on or off position, C_C^i is the i -th power station constant costs, N_U^j shows the number of j -th power station generators within the under studied energy grid, e_{ij} represents the i -th fuel share coefficient from the j -th power station energy input, ETF is the power station input energy matrix converting to fuels appropriate with different power stations, E_{IU} is the power station input energy matrix, η_U shows power stations efficiency vector and E_{OU} stands for power stations output electrical energy.

In the optimization algorithm, E_{OU} is the power stations generated electrical energy which is chosen as the problem variables. Optimization limitations are defined as below:

1) the load balance

$$\sum_{i=1}^N P_i(t) = D(t), \quad (20)$$

2) the upper and lower unit generations

$$P_{\min}^i \leq P^i \leq P_{\max}^i \quad (21)$$

where N represents the number of units, $P_i(t)$ shows the i -th unit generated power at the t time, $D(t)$ is the value of electrical power request at t time, P_{\min}^i is the lower limit,

P^i manifests generation, and P_{\max}^i shows the i -th unit upper limit.

The dynamic planning application. After distributing the electrical energy in each hour of planning that is done in appropriation with each possible energy division among power stations, the planning trend continues'; thus, energy carriers combinations parallel with power stations combinations are concluded. By applying the dynamic planning method, the proper strategy of energy carriers planning is determined along with the study.

At K hour with I combination, the retrospective algorithm of computing the minimum cost is defined as

$$F_{cost}(K, I) = \min_{\{L\}} \left[P_{cost}(K, I) + S_{cost}(K-1, L : K, I) + F_{cost}(K-1, L) \right], \quad (22)$$

where $F_{cost}(K, I)$ is the minimum total cost to arrive at the (K, I) mode, $P_{cost}(K, I)$ is the (K, I) mode cost and $S_{cost}(K-1, L : K, I)$ shows the transition cost from $(K-1, L)$ to (K, I) mode. The (K, I) mode is the I combination at K hour [14].

The energy grid simulation with ten power stations. The final energy consumption based planning of energy carriers designed with ten power stations is implemented. The dynamic planning is done by saving paths equal with the number of each study hour maximum modes and its results are shown in Table 2.

Table 3 holds the need for energy carriers in order to provide final energy consumption. The need for energy carriers of the total study period is determined in Table 4. The economical distribution of electrical energy among units is represented in Table 5. The optimization algorithms access trend to the economical distribution of the electrical energy is depicted in Fig .1. Besides, considering the quantity of energy carriers national representation, the value of carriers import and export quantities are listed in Table 6.

Table 2
The output of dynamic planning in ten unit energy grids by means of PSO

Strategy						Hour
S6	S5	S4	S3	S2	S1	The initial state
2	2	2	2	2	2	1
3	3	3	3	3	3	2
3	3	3	3	3	3	3
3	3	3	3	3	3	4
3	3	3	3	3	3	5
4	4	4	4	4	4	6
4	4	4	4	4	4	7
9	9	9	9	9	9	8
9	9	9	9	9	9	9
9	9	9	9	9	9	10
10	10	10	10	10	10	11
10	10	10	10	10	10	12
10	10	10	10	10	10	13
9	9	9	9	9	9	14
9	9	9	9	9	9	15
9	9	9	9	9	9	16
9	9	9	9	9	9	17
9	9	9	9	9	9	18
9	9	9	9	9	9	19
9	9	9	9	9	9	20
9	9	4	4	4	4	21
9	6	4	4	3	3	22
7	6	4	4	3	3	23
7	6	5	4	3	2	24
8557932	8557192	8557153	8554502	8554182	8555398	Cost (dollar)

Table 3

The need for energy carriers in ten unit energy grids by means of PSO

8	7	6	5	4	3	2	1	Hour
3721.1	3721.1	3721.1	3721.1	3721.1	3721.1	3721.1	3721.1	Petroleum
51.78965	44.67028	37.55091	23.31218	16.19281	1.95407	-12.2847	-19.404	Liquid gas
-350.552	-365.265	-354.657	-429.906	-466.355	-539.254	-612.154	-647.68	Fuel oil
-11.7441	-61.1345	-123.351	-210.1	-253.46	-340.182	-426.903	-470.252	Gas oil
17.72885	1.640607	-14.4476	-46.6241	-62.7124	-94.8888	-127.065	-143.154	Kerosene
405.1893	363.9642	322.7392	240.289	199.0639	116.6137	34.16357	-7.06152	Gasoline
53.06305	50.85209	48.64113	44.2192	42.00824	37.58632	33.1644	30.95344	Plane fuel
4380.603	4190.728	3988.239	3615.204	3432.123	3065.959	2699.796	2519.415	Natural gas
26.60254	25.4941	24.38566	22.16878	21.06034	18.84346	16.62658	15.51815	Coke gas
58.79772	56.34781	53.89791	48.9981	46.54819	41.64838	36.74857	34.29867	Coal
16	15	14	13	12	11	10	9	Hour
3721.1	3721.1	3721.1	3721.1	3721.1	3721.1	3721.1	3721.1	Petroleum
30.43155	51.78965	66.02839	80.26713	94.50586	87.3865	80.26713	66.02839	Liquid gas
-459.901	-350.552	-275.868	-198.861	-135.511	-158.969	-198.861	-275.591	Fuel oil
-141.826	-11.7441	74.99814	161.7678	260.843	205.169	161.7678	75.0014	Gas oil
-30.5359	17.72885	49.90533	82.0818	114.2583	98.17004	82.0818	49.90533	Kerosene
281.5141	405.1893	487.6395	570.0897	652.5398	611.3148	570.0897	487.6395	Gasoline
46.43017	53.06305	57.48497	61.90689	66.32881	64.11785	61.90689	57.48497	Plane fuel
3831.358	4380.603	4751.988	5130.168	5531.033	5323.32	5130.168	4752.798	Natural gas
23.27722	26.60254	28.81941	31.03629	33.25317	32.14473	31.03629	28.81941	Coke gas
51.448	58.79772	63.69753	68.59734	73.49714	71.04724	68.59734	63.69753	Coal
24	23	22	21	20	19	18	17	Hour
3721.1	3721.1	3721.1	3721.1	3721.1	3721.1	3721.1	3721.1	Petroleum
-5.1653	9.073439	37.55091	66.02839	80.26713	51.78965	37.55091	23.31218	Liquid gas
-595.486	-548.095	-423.452	-275.868	-198.861	-350.552	-423.452	-496.351	Fuel oil
-370.456	-277.548	-98.4652	74.99813	161.7678	-11.7441	-98.4652	-185.186	Gas oil
-110.977	-78.8006	-14.4476	49.90533	82.0818	17.72885	-14.4476	-46.6241	Kerosene
75.38865	157.8388	322.7392	487.6395	570.0897	405.1893	322.7392	240.289	Gasoline
35.37536	39.79728	48.64113	57.48497	61.90689	53.06305	48.64113	44.2192	Plane fuel
2913.867	3278.051	4014.44	4751.988	5130.168	4380.603	4014.44	3648.277	Natural gas
17.73502	19.9519	24.38566	28.81941	31.03629	26.60254	24.38566	22.16878	Coke gas
39.19848	44.09829	53.89791	63.69753	68.59734	58.79772	53.89791	48.9981	Coal

Table 4

The need for different energy carriers within the total study period of the energy grid

Energy	Carrier	Row
89306.4	Petroleum	1
1000.893	Liquid gas	2
-9132.05	Fuel oil	3
-1916.25	Gas oil	4
-121.508	Kerosene	5
8322.891	Gasoline	6
1198.34	Plane fuel	7
98855.34	Natural gas	8
600.7739	Coke gas	9
1327.848	Coal	10

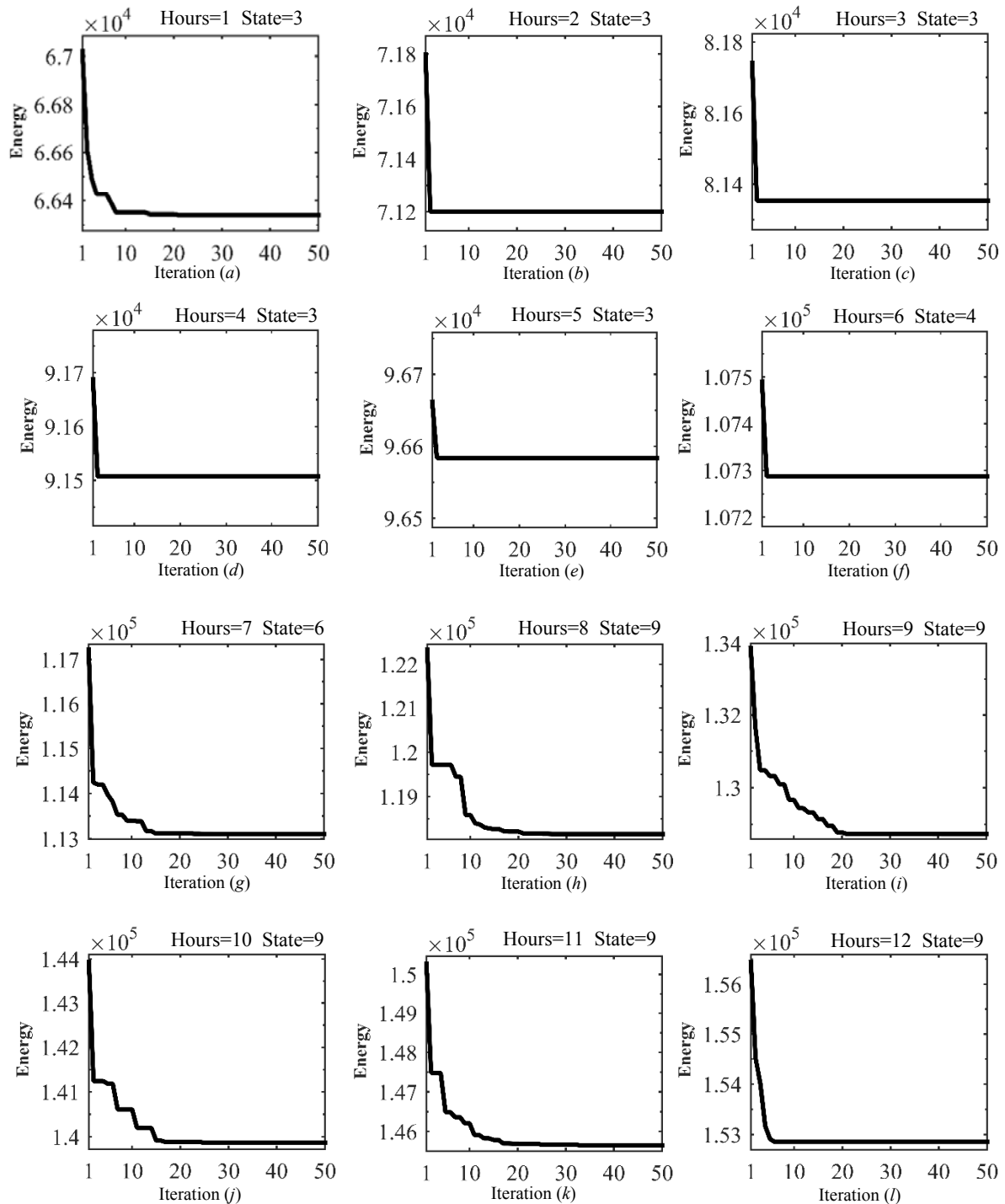
Table 5

The electrical energy economical distribution within the energy grid by utilizing PSO

OF	unit 10	unit 9	unit 8	unit 7	unit 6	unit 5	unit 4	unit 3	unit 2	unit 1	Hour
66339.36	0	0	0	0	0	0	0	129.9054	150	420.9897	1
71199.98	0	0	0	0	0	0	0	130	165.9591	455	2
81353.53	0	0	0	0	0	0	0	130	266.087	455	3
91507.08	0	0	0	0	0	0	0	130	366.2149	455	4
96583.85	0	0	0	0	0	0	0	130	416.2788	455	5
107287.4	0	0	0	0	0	0	61.40668	130	455	455	6
113108.7	0	0	0	0	0	0	111.4706	130	455	455	7
118165.9	0	54.94904	10	25	78.91501	25	20	129.9395	403.1555	454.5755	8
128802.2	0	54.92522	38.19602	25	79.91727	25	40.51524	129.8847	454.393	453.831	9
139852.8	0	54.99011	46.54565	75.69185	79.97855	25	129.9675	129.966	454.8779	454.8368	10
145735.7	55	55	55	85	80	51.98213	130	130	455	455	11
152855.1	55	55	55	85	80	157.1164	130	130	455	455	12
139852.8	31.11385	55	55	85	80	25.80435	130	130	455	455	13
128737.4	0	55	46.5999	25.09276	80	25.18803	130	130	455	454.9096	14
118165.9	0	50.46745	10	25	42.35772	25	20	129.0834	452.7482	446.8778	15
102935.5	0	54.57776	10	25	75.61226	25	20	129.572	260.4829	451.0978	16
97858.76	0	54.58248	10	25	75.74856	25	20	129.4813	209.902	451.5645	17
108012.3	0	55	10.06585	25.04071	80	25.08315	20.12963	130	401.2152	455	18
118165.9	0	55	46.61355	25.03679	80	25.13997	130	130	455	455	19
139852.8	0	53.36535	10	25	79.89353	25	70.70835	129.7906	454.3342	453.5704	20
128737.4	0	0	0	0	0	0	61.40668	130	455	455	21
108012.3	0	0	0	0	0	0	0	130	316.1509	455	22
87907.97	0	0	0	0	0	0	0	130	216.023	455	23
78494.37	0	0	0	0	0	0	0	130	216.023	455	24

Table 6

Import and export of carriers			
Import	Export	Carrier	Row
0	163006	Petroleum	1
1000.893	0	Liquid gas	2
0	9132.05	Fuel oil	3
0	1916.25	Gas oil	4
0	121.508	Kerosene	5
8322.891	0	Gasoline	6
1198.34	0	Plane fuel	7
2221.738	0	Natural gas	8
0	37.6261	Coke gas	9
367.8484	0	Coal	10



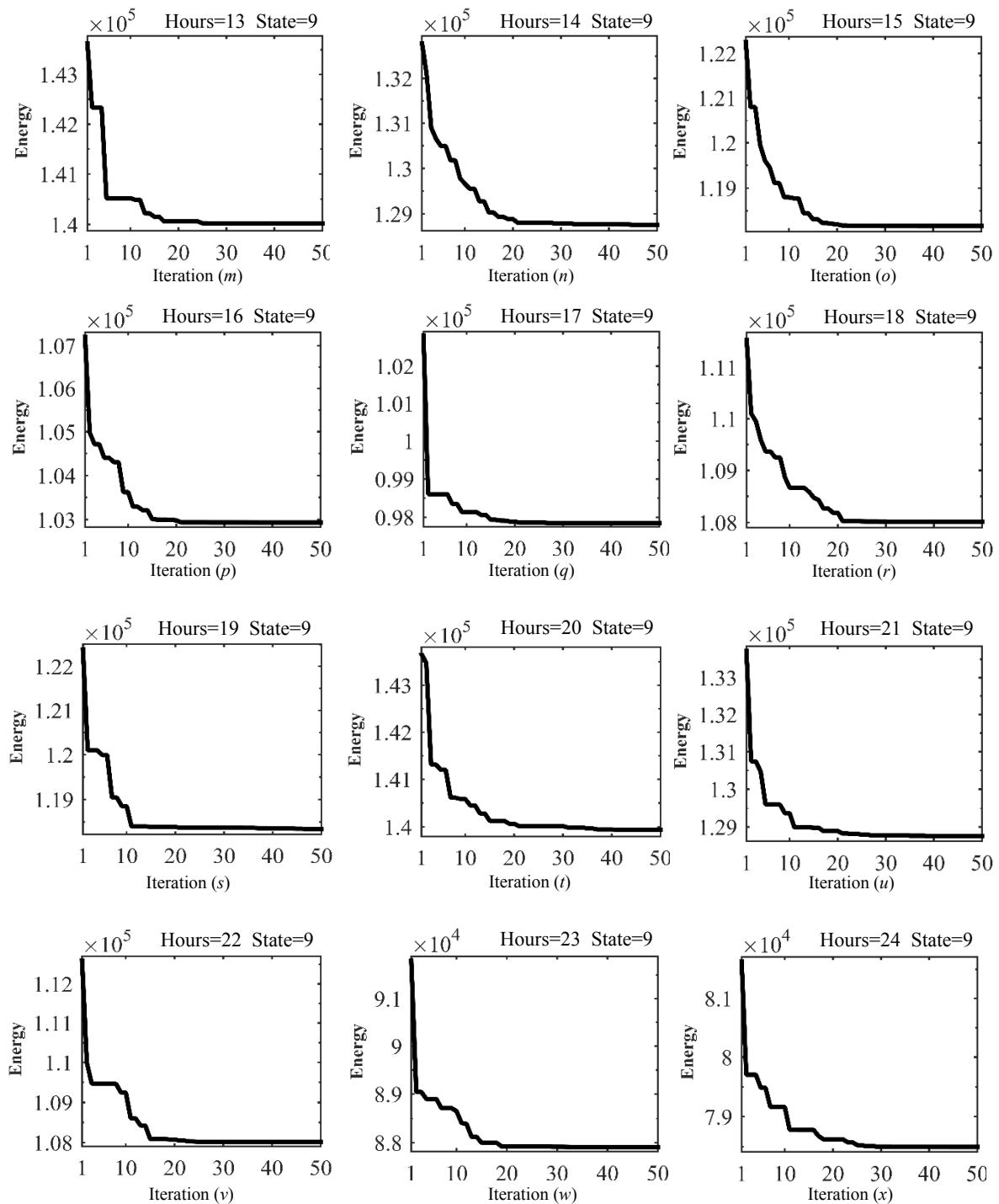


Fig. 1. The access trend to the electrical energy economical distribution\ within the energy grid by applying PSO

Discussion and conclusion. In the present article, a new approach in energy studies was introduced. In this view, the maximum effort was made to arrive at the suitable planning of energy carriers based on the final energy consumption. This planning was done such that it showed energy carriers beside each other as a system and neglected their planning independent view.

The energy grid modeling started from the lowest energy level of the final energy consumption and went to the highest level of the energy initial carriers step by step in a matrix shape. In this modelling, some factors like the

energy grid losses, the electrical energy distribution among units, and the petroleum refinement were taken into account. After a matrix form energy grid modelling, the energy grid was designed based on the 24 hour information of Iran energy balance sheet and the standard electrical grid since there was no available authentic information of energy grid.

In the proposed planning, the dynamic planning method and the particle swarm optimization algorithm were used. Indeed, particle swarm optimization algorithm was used along with the electrical energy economical

distribution; hence, the dynamic planning program was utilized in order to access the proper strategy of mixing energy carriers along with the study period.

The proposed planning done on the authentic-based designed energy grid was implemented and its results were represented.

REFERENCES

1. Krause T., Andersson G., Fröhlich K., Vaccaro A. Multiple-Energy Carriers: Modeling of Production, Delivery, and Consumption. *Proceedings of the IEEE*, 2011, vol.99, no.1, pp. 15-27. doi: 10.1109/jproc.2010.2083610.
2. Cormio C., Dicorato M., Minoia A., Trovato M. A regional energy planning methodology including renewable energy sources and environmental constraints. *Renewable and Sustainable Energy Reviews*, 2003, vol.7, no.2, pp. 99-130. doi: 10.1016/s1364-0321(03)00004-2.
3. Barbir F. Transition to renewable energy systems with hydrogen as an energy carrier. *Energy*, 2009, vol.34, no.3, pp. 308-312. doi: 10.1016/j.energy.2008.07.007.
4. Amoo L.M., Fagbenle R.L. An integrated impact assessment of hydrogen as a future energy carrier in Nigeria's transportation, energy and power sectors. *International Journal of Hydrogen Energy*, 2014, vol.39, no.24, pp. 12409-12433. doi: 10.1016/j.ijhydene.2014.06.022.
5. Ridjan I., Mathiesen B.V., Connolly D., Duić N. The feasibility of synthetic fuels in renewable energy systems. *Energy*, 2013, vol.57, pp. 76-84. doi: 10.1016/j.energy.2013.01.046.
6. Su W., Wang J., Roh J. Stochastic Energy Scheduling in Microgrids With Intermittent Renewable Energy Resources. *IEEE Transactions on Smart Grid*, 2014, vol.5, no.4, pp. 1876-1883. doi: 10.1109/tsg.2013.2280645.
7. Geng W., Ming Z., Lilin P., Ximei L., Bo L., Jinhui D. China's new energy development: Status, constraints and reforms. *Renewable and Sustainable Energy Reviews*, 2016, vol.53, pp. 885-896. doi: 10.1016/j.rser.2015.09.054.
8. Trop P., Goricanec D. Comparisons between energy carriers' productions for exploiting renewable energy sources. *Energy*, 2016, vol.108, pp. 155-161. doi: 10.1016/j.energy.2015.07.033.
9. Belier M. E.A.C.a.K.C.H. *Interfuel substitution study-the role of electrification*. Brookhaven National Laboratory informal Rept. BNL 19522 (ESAG-17), November, 1974.
10. Kennedy J., Eberhart R. Particle swarm optimization. *Proceeding of the 1995 IEEE International Conference on Neural Networks*, Perth, Australia. IEEE Service Center, Piscataway, 1995. pp. 1942-1948.
11. Available at: http://www.saba.org.ir/saba_content/media/image/2015/09/7811_orig.pdf (accessed 16 April 2016).
12. Ebrahimi J., Hosseinian S.H., Gharehpetian G.B. Unit Commitment Problem Solution Using Shuffled Frog Leaping Algorithm. *IEEE Transactions on Power Systems*, 2011, vol.26, no.2, pp. 573-581. doi: 10.1109/tpwrs.2010.2052639.
13. Dehghani M., Montazeri Z., Dehghani A., Seifi A.R. Spring search algorithm: A new meta-heuristic optimization algorithm inspired by Hooke's law. *2017 IEEE 4th International Conference on Knowledge-Based Engineering and Innovation (KBEI)*. doi: 10.1109/kbei.2017.8324975.
14. Wood A.J., Wollenberg B.F. *Power generation, operation, and control*. John Wiley & Sons, 2012.
15. IEA Publications, rue de la Fédération, 75739 Paris Cedex 15, Printed in France by STEDI, September 2004.
16. U.S. Energy Information Administration (EIA). Available at: <http://www.eia.gov> (accessed 21 July 2015).

Received 14.06.2018

M. Dehghani¹, Candidate of Power Engineering, M.Sc.,
Z. Montazeri², Candidate of Power Engineering, M.Sc. Student,
A. Ehsanifar¹, Candidate of Power Engineering, M.Sc.,
A.R. Seifi¹, Doctor of Power Engineering, Professor,
M.J. Ebadi³, Doctor of Applied Mathematics, Assistant Professor,
O.M. Grechko⁴, Candidate of Technical Science, Associate Professor,

¹ Department of Power and Control,

Shiraz University,

Shiraz, I.R. Iran,

e-mail: adanbax@gmail.com, ali.ehsanifar2020@gmail.com,

seifi@shirazu.ac.ir

² Department of Electrical Engineering,

Islamic Azad University of Marvdasht,

Marvdasht, I.R. Iran,

e-mail: Z.montazeri2002@gmail.com

³ Faculty of Marine Science,

Chabahar Maritime University,

Chabahar, Iran,

e-mail: ebadi@cmu.ac.ir

⁴ National Technical University «Kharkiv Polytechnic Institute»,

2, Kyrpychova Str., Kharkiv, 61002, Ukraine,

e-mail: a.m.grechko@gmail.com

Appendix (Tables A.1–A.11)

Table A.1. Unit Information

Row	Power plant	Capacity of unit (MW)		Efficiency	Constant cost	Priority
		Min	Max			
1	Thermal	150	455	0.368	1	1
2	Thermal	150	455	0.345	2	2
3	Combined Cycle	20	130	0.455	3	3
4	Thermal	20	130	0.317	4	4
5	Gas	25	162	0.3	5	5
6	Combined Cycle	20	80	0.47	6	6
7	Thermal	25	85	0.35	7	7
8	Thermal	10	55	0.35	8	8
9	Combined Cycle	10	55	0.5	9	9
10	Gas	10	55	0.25	10	10

Table A.2. The time information of energy networks

Row	Power plant	MUT	MDT	Cold start	Initial conditions
1	Thermal	8	8	5	8
2	Thermal	8	8	5	8
3	Combined Cycle	5	5	4	-5
4	Thermal	5	5	4	-5
5	Gas	6	6	4	-6
6	Combined Cycle	3	3	2	-3
7	Thermal	3	3	2	-3
8	Thermal	1	1	0	-1
9	Combined Cycle	1	1	0	-1
10	Gas	1	1	0	-1

Table A.3. The cost of setting up units

Row	Power plant	Hot start	Cold start
1	Thermal unit	4500	9000
2	Thermal unit	5000	10000
3	Combined Cycle unit	550	1100
4	Thermal unit	560	1120
5	Gas unit	900	1800
6	Combined Cycle unit	170	340
7	Thermal unit	260	520
8	Thermal unit	30	60
9	Combined Cycle unit	30	60
10	Gas unit	30	60

Table A.4. Matrix T_p

Petroleum	0
Liquid gas	0.032
Fuel oil	0.293
Gas oil	0.293
Kerosene	0.099
Gasoline	0.157
Plane fuel	0
Other products	0.058
Natural gas	0
Coke gas	0
Coal	0
Non-commercial fuels	0
Electricity(power)	0

Table A.5. Conversion matrix input energy to power plants

Power plant	Thermal unit	Combined Cycle unit	Gas unit
Fuel oil	0.254	0	0
Gas oil	0.003	0.082	0.166
Natural gas	0.743	0.918	0.834

Table A.6. Domestic supplies of energy carriers

Row	Energy carrier	Energy (boe)
1	Petroleum	10513
2	Liquid gas	0
3	Fuel oil	0
4	Gas oil	0
5	Kerosene	0
6	Gasoline	0
7	Plane fuel	0

8	Other products	0
9	Natural gas	4026.4
10	Coke gas	26.6
11	Coal	40
12	Non-commercial fuels	161
13	Electricity (power)	0

Table A.7. Heating value[15] and energy rates[16]

Energy carrier	Heating value	Energy rates
Petroleum	38.5 MJ/lit	48 dollar/boe
Liquid gas	46.15 MJ/kg	374 dollar/tonne
Fuel oil	42.18 MJ/kg	180 dollar/tonne
Gas oil	43.38 MJ/kg	350 dollar/tonne
Kerosene	43.32 MJ/kg	500 dollar/tonne
Gasoline	44.75 MJ/kg	450 dollar/tonne
Plane fuel	45.03 MJ/kg	555 dollar/tonne
Natural gas	39 MJ/m ³	237 dollar/1000m ³
Coke gas	16.9 MJ/kg	157 dollar/tonne
Coal	26.75 MJ/kg	61 dollar/tonne

Table A.8. Electrical load demand

Hour	1	2	3	4
Load	700	750	850	950
Hour	5	6	7	8
Load	1000	1100	1150	1200
Hour	9	10	11	12
Load	1300	1400	1450	1500
Hour	13	14	15	16
Load	1400	1300	1200	1050
Hour	17	18	19	20
Load	1000	1100	1200	1400
Hour	21	22	23	24
Load	1300	1100	900	800

Table A.9. Final energy consumption

Hour	1	2	3	4	5	6	7	8
Residential, commercial, general	1570.19	1682.347	1906.66	2130.973	2243.129	2467.442	2579.599	2691.755
Industrial	738.9593	791.7421	897.3078	1002.873	1055.656	1161.222	1214.005	1266.787
Transportation	998.4982	1069.819	1212.462	1355.105	1426.426	1569.069	1640.39	1711.711
Agriculture	131.1437	140.5111	159.2459	177.9807	187.3481	206.0829	215.4503	224.8177
Other	9.816144	10.5173	11.9196	13.32191	14.02306	15.42537	16.12652	16.82768
Non-energy	334.9268	358.8502	406.6969	454.5436	478.4669	526.3136	550.2369	574.1603
Hour	9	10	11	12	13	14	15	16
Residential, commercial, general	2916.068	3140.381	3252.537	3364.694	3140.381	2916.068	2691.755	2355.286
Industrial	1372.353	1477.919	1530.701	1583.484	1477.919	1372.353	1266.787	1108.439
Transportation	1854.354	1996.996	2068.318	2139.639	1996.996	1854.354	1711.711	1497.747
Agriculture	243.5526	262.2874	271.6548	281.0222	262.2874	243.5526	224.8177	196.7155
Other	18.22998	19.63229	20.33344	21.03459	19.63229	18.22998	16.82768	14.72422
Non-energy	622.007	669.8537	693.777	717.7004	669.8537	622.007	574.1603	502.3903
Hour	17	18	19	20	21	22	23	24
Residential, commercial, general	2243.129	2467.442	2691.755	3140.381	2916.068	2467.442	2018.816	1794.503
Industrial	1055.656	1161.222	1266.787	1477.919	1372.353	1161.222	950.0906	844.5249
Transportation	1426.426	1569.069	1711.711	1996.996	1854.354	1569.069	1283.783	1141.141
Agriculture	187.3481	206.0829	224.8177	262.2874	243.5526	206.0829	168.6133	149.8785
Other	14.02306	15.42537	16.82768	19.63229	18.22998	15.42537	12.62076	11.21845
Non-energy	478.4669	526.3136	574.1603	669.8537	622.007	526.3136	430.6202	382.7735

Table A.10. Matrix T12

	Residential and commercial	Industrial	Transportation	Agriculture	Other	Non-energy
Petroleum	0	0	0	0	0	0
Liquid gas	0.051	0.013	0.01	0	0	0
Fuel oil	0.023	0.212	0.014	0	0	0
Gas oil	0.055	0.087	0.363	0.689	0	0
Kerosene	0.141	0.002	0	0.018	0	0
Gasoline	0.002	0.002	0.573	0.003	0	0
Plane fuel	0	0	0.031	0	0	0
Other products	0	0	0	0	0	0.402
Natural gas	0.564	0.521	0.007	0	0	0.497
Coke gas	0	0.021	0	0	0	0
Coal	0.0003	0	0	0	0	0.101
Non-commercial fuels	0.064	0	0	0	0	0
Electricity(power)	0.102	0.142	0.0004	0.29	1	0

Table A.11. Matrix T23

Petroleum	1	0	0	0	0	0	0	0	0	0	0	0	0
Liquid gas	0	1	0	0	0	0	0	0	0	0	0	0	0
Fuel oil	0	0	1	0	0	0	0	0	0	0	0	0	0
Gas oil	0	0	0	1	0	0	0	0	0	0	0	0	0
Kerosene	0	0	0	0	1	0	0	0	0	0	0	0	0
Gasoline	0	0	0	0	0	1	0	0	0	0	0	0	0
Plane fuel	0	0	0	0	0	0	1	0	0	0	0	0	0
Other products	0	0	0	0	0	0	0	1	0	0	0	0	0
Natural gas	0	0	0	0	0	0	0	0	1.1601	0	0	0	0
Coke gas	0	0	0	0	0	0	0	0	0	1	0	0	0
Coal	0	0	0	0	0	0	0	0	0	0	1	0	0
Non-commercial fuels	0	0	0	0	0	0	0	0	0	0	0	1	0
Electricity(power)	0	0	0	0	0	0	0	0	0	0	0	0	1.3158

How to cite this article:

Dehghani M., Montazeri Z., Ehsanifar A., Seifi A.R., Ebadi M.J., Grechko O.M. Planning of energy carriers based on final energy consumption using dynamic programming and particle swarm optimization. *Electrical engineering & electromechanics*, 2018, no.5, pp. 62-71. doi: 10.20998/2074-272X.2018.5.10.

O.Yu. Glebov, D.G. Koliushko, G.M. Koliushko, E.P. Ereemeeva

ON THE ISSUE OF DESIGN OF GROUNDING SYSTEMS OF 330(220) KV SUBSTATIONS TO ENSURE THE ELECTROMAGNETIC COMPATIBILITY OF SECONDARY CIRCUITS

Purpose. The purpose of the work is to develop the fundamentals of the design methodology of grounding system design of substations with open switchgears 330 (220) kV, which is aimed at ensuring electromagnetic compatibility of secondary circuits of current transformers. **Methodology.** To carry out the research, the provisions of the theory of experiment planning, the theory of electrical circuits, mathematical modeling in the package Grounding 1.0 and Microsoft Excel were used. **Results.** During the one-factor experiments, the dependencies of the grounding system resistance and the voltage between the calculated points on the grounding system area, the size of the grid cell, the perimeter of the grounding system horizontal electrodes cross-section, the equivalent soil resistivity, the short-circuit current and the design factor were obtained. It is shown that the grounding system resistance and the voltage between the calculated points are practically independent of the depth of the horizontal electrodes in the depth range from 0.4 m to 1.4 m. **Originality.** The paper formulated three criteria for grounding system designing of substations 330 (220) kV, aimed at ensuring electromagnetic compatibility of secondary circuits. **Practical value.** The fundamentals of the methodology for grounding system designing are formulated according to the criterion of preventing false triggering of relay protections in emergency modes. References 10, tables 2, figures 14.

Key words: grounding system, substations, electromagnetic compatibility, secondary circuits, grounding system resistance.

Цель. Целью статьи является разработка основных положений методики проектирования конструктивного выполнения заземляющего устройства подстанций с открытыми распределительными устройствами 330(220) кВ, которая направлена на обеспечение электромагнитной совместимости вторичных цепей трансформаторов тока. **Методика.** Для проведения исследований использовались положения теории планирования экспериментов, теория электрических цепей, математическое моделирование в пакете Grounding 1.0 и Microsoft Excel. **Результаты.** В ходе проведения однофакторных экспериментов получены зависимости сопротивления заземляющего устройства и напряжения между расчётными точками от площади заземляющего устройства, размера ячейки сетки, периметра поперечного сечения заземлителей, эквивалентного удельного сопротивления грунта, тока короткого замыкания и конструктивного коэффициента. Показано, что сопротивление заземляющего устройства и напряжение между расчётными точками практически не зависят от глубины расположения горизонтальных заземлителей в диапазоне глубин от 0,4 м до 1,4 м. **Научная новизна.** В работе сформулированы три критерия проектирования заземляющих устройств подстанций 330(220) кВ, направленные на обеспечение электромагнитной совместимости вторичных цепей. **Практическое значение.** Сформулированы положения методики проектирования заземляющего устройства по критерию предотвращения ложного срабатывания релейных защит в аварийных режимах. Библ. 10, табл. 2, рис. 14.

Ключевые слова: заземляющее устройство, подстанции, электромагнитная совместимость, вторичные цепи, сопротивление заземляющего устройства.

Introduction. In paragraph 1.7.59 of the Electrical installation regulations of 2017 [1], the designation of the grounding system (GS) of the electrical installations is indicated: «...A grounding system used to ground electrical installations ... must meet all the requirements for grounding these electrical installations during the entire period of operation: protecting people from electric shock in the event of damage of insulation, conditions for network operation, protection of electrical equipment from over-voltage, electromagnetic compatibility of technical devices, which are used in these electrical installations (for example, computer and microprocessor systems, etc.). First of all, you must comply with the requirements for protective grounding...». In this paragraph it is shown that the main task of GS is to ensure electrical safety.

To solve this problem, the main criteria for the design of GS have been developed, which are set forth in the relevant paragraphs [1]:

- 1) according to the permissible GS resistance value;
- 2) according to the permissible value of the contact voltage;
- 3) according to the permissible value of the voltage on the GS.

In a number of works, for example [2], the directions of reconstruction of GS for ensuring electrical safety are considered.

However, in addition to providing electrical safety, other important tasks listed in paragraph 1.7.59 of the Electrical installation regulations of 2017, namely, ensuring electromagnetic compatibility (EMC) of technical means used in the electric power industry should be solved with the help of GS. This paragraph is the only one in [1], where requirements are set for GS to ensuring EMC of microprocessor-based technical means (MP TM), but further in the text of the document these requirements (for example, to design realization of GS) are not specified.

In the electric power industry of Ukraine, the main backbone elements are transmission lines and substations with switchgears 330(220) kV and 750(500) kV. These objects belong to electrical networks with a grounded neutral, have large ground fault currents (up to 50 kA) and pose the greatest danger for personnel and MP TM in emergency modes. The widest class of relay protection at 330(220) kV substations are those that are connected to secondary circuits of current transformers (CTs), for

example, maximum or differential current protection, directed or not directed, etc. Therefore, the provision of EMC of precisely current circuits is an urgent task for the reliable operation of substations.

The most powerful sources of electromagnetic influences in substations are short circuits on buses, direct lightning strikes or triggering of overvoltage limiters and dischargers. A common feature of these effects is the flow of large currents into the GS, although the amplitude-time parameters are significantly different. It is in these modes that the most important role for the reliable functioning of the MP TM is played by the design realization of GS. However, to date, the EMC normative documents [3] do not state the criteria for the design of GS, namely, there are no clear requirements for design realization of GS which make it possible to meet the requirements of EMC of primary and secondary circuits.

The goal of the work is development of design methodology for the design realization of a GS for substations with switchgear 330(220) kV, which is aimed at ensuring electromagnetic compatibility of current circuits.

Materials of the study. To solve this problem, it is necessary first of all to evaluate the significance of the factors affecting the main normalized parameters of the GS. To do this, we have to determine the dependence of the resistance of the GS (R_G) and voltage (UC) between the termination points of the cables of the secondary CT circuits on the GS parameters. Resistance of the GS also determines one more normalized value – the voltage on the GS (U_G) which is a danger for insulation of the outgoing cables in emergency modes.

In [4], the authors showed that the interference voltages in the secondary CT circuits are determined by the voltage between two points of the GS in which the termination of the secondary circuit cable is performed. This voltage is determined by the acting current (short circuit or lightning). By limiting this voltage, it is possible to prevent both a breakdown of the insulation of the cables and a false actuation of the relay protections. Therefore, the existing criteria for designing the GS must be supplemented with the following [5]:

- 1) prevention of breakdown of secondary cable insulation by high-frequency (pulsed) voltages when large high-frequency (pulsed) currents flow to the GS;
- 2) prevention of the breakdown of the secondary circuits' cable insulation by industrial frequency voltages when the short-circuit currents flow to the GS;
- 3) prevention of false triggering of relay protections at short-circuit from low-frequency voltages, if the secondary circuits' cable insulation is still damaged.

The first criterion is reduced to a decrease in the pulsed voltage on the GS to a value not exceeding the insulation strength of the cables. Further, when designing GS, it is necessary to provide such a design of the GS near the CTs and their terminal cabinets, where the resistance of the GS to pulsed current ($R_{G \text{ pulse}}$) during short-circuit on the equipment under consideration (or at a lightning strike to a lightning rod installed nearby) would not exceed the permissible value (R_{PERM}), Ω :

$$R_{G \text{ pulse}} \leq R_{PERM} = \frac{U_{PERM}}{I_{HF}}, \quad (1)$$

where U_{PERM} is the maximum value of the voltage, which determines the ultimate strength of the cable insulation to the pulsed voltages of the normalized form V; I_{HF} is the maximum value of the pulsed current during short-circuit on the buses (the design value typical for switchgear of each voltage class), A.

For the case of a lightning strike in a lightning rod installed nearby, instead of I_{HF} current, a lightning current $I_L = 100$ kA (or its part if there are several paths of lightning current flow into the ground) should be taken.

Table 1 shows the parameters (maximum value of I_{HF} , frequency of oscillations f_{HF}) of the high-frequency component of the short-circuit current on the busbars of open switchgears (OSG) of the corresponding voltage class (U_{nom}) [6]. If there is no data on the actual insulation resistance of control cables to pulsed voltages, then U_{PERM} can be taken equal to [3] 1 kV – for OSG-220 kV and below, to 2 kV – for OSG-330 kV and above.

Table 1
Parameters of the high-frequency component of the short-circuit current on the busbars of the OSG

U_{nom} , kV	110	220	330	500	750
I_{HF} , kA	1	2	6	8	12
f_{HF} , MHz	1.0	0.8	0.3	0.15	0.1
U_{PERM} , kV	1	1	2	2	2
R_{PERM} , Ω	1.0	0.5	0.33	0.25	0.17

The second criterion is reduced (at short-circuit on the buses of the substation) to the decrease of the voltage between the ground point of the terminal box of the CT and the ground point of the relay protection panel (U_C) to the test voltage ($U_{C,P}$), V:

$$U_C \leq U_{C,P} = 1000 \text{ V}. \quad (2)$$

The third criterion is aimed at reducing (in the case of short-circuits on the buses of the OSG) the voltages (U_C) up to the permissible value due to the relay protection parameters ($U_{C,relay}$), V:

$$U_C \leq U_{C,relay} = I_{relay} \cdot (Z_L + Z_{relay}), \quad (3)$$

where $U_{C,relay}$ is the permissible voltage between the ground point of the CT terminal box and the ground point of the relay protection panel, V; I_{relay} is the current of the setting of the threshold of the current relay (start-up of current protectors) at short-circuit on the busbars, A; Z_L is the resistance of the phase conductor of the secondary circuit CT cable, Ω ; Z_{relay} is the relay coil resistance at industrial frequency, Ω .

As the worst case, for each switchgear we should consider short-circuit on the CT, which has the longest cable of secondary circuits, i.e. the most remote CT from the building, in which the relay panels (RP) are installed. Therefore, when designing the GS it is necessary to choose such design parameters of the GS grid, under which the voltage U_C does not exceed the permissible value.

In [5], about 40 parameters affecting the voltage U_C and resistance of the GS of substation 330(220) kV are considered. Many of the parameters considered are

interrelated. However, there are seven independent factors:

- 1) the area of the GS (S_G);
- 2) the size of the grid cell of the GS (b_G);
- 3) the perimeter of the cross-section of horizontal grounding bars (p_H);
- 4) the equivalent resistivity of the soil (ρ_{EQ});
- 5) the short-circuit current on the busbars of OSG (I_S);
- 6) the constructive coefficient of the ratio of lengths (k_ℓ) – the ratio of the distance from the CT to the RP (ℓ_C) to the diagonal of the GS (D_G);
- 7) the depth of the horizontal grounding bars (t_H).

Analysis of the experimental data obtained during the diagnostics of the GS of eighty 330(220) kV substations made it possible to determine the real range of variation of these factors (see Table 2).

At the first stage of the research, single-factor experiments were conducted to determine the dependencies of the unknown quantities from each of the independent factors. To conduct such experiments, mathematical models of GS were compiled, which are square uniform

grids of areas of $1 \cdot 10^4 \text{ m}^2$, $3 \cdot 10^4 \text{ m}^2$, $5 \cdot 10^4 \text{ m}^2$, $7 \cdot 10^4 \text{ m}^2$ and $9 \cdot 10^4 \text{ m}^2$ with the dimensions of the grid cell of the GS of 5 m, 15 m and 25 m.

Table 2

The range of influencing factors		
Factor designation	Factor value	
	minimal	maximal
$S_G \cdot 10^4, \text{ m}^2$	0.906352	9.251508
$b_G, \text{ m}$	7.03	30.4
$p_H, \text{ mm}$	31.4	172.0
$\rho_{EQ}, \Omega \cdot \text{m}$	1.69	249.67
$I_S, \text{ kA}$	2.43	42.961
k_ℓ	0.236	0.955
$t_H, \text{ m}$	0.5	2.0

Fig. 1 shows the grids of GS with different area and grid cell size of 15 m, and also the location of the short-circuit point (ϕ_0) and calculated points ($\phi_1 - \phi_5$), which correspond to the different locations of the building of the RP.

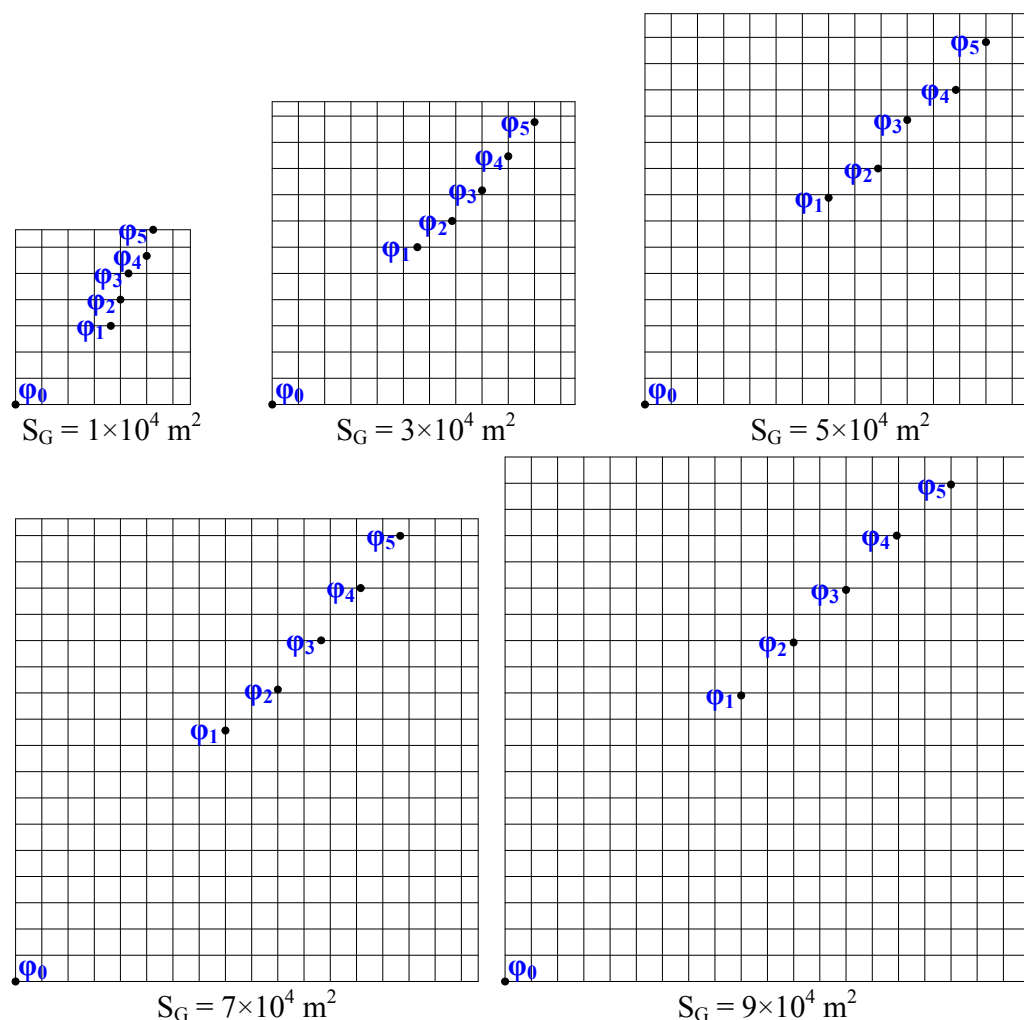


Fig. 1. Uniform grids of GS with grid cell size $b_G = 15 \text{ m}$

The location of the short-circuit point in the corner of the GS grid is the worst case, which makes it possible to perform the «upper» estimation of the required parameters, i.e. provides some margin to compensate for the aging of the insulation of the cables and the change in

the parameters of the GS in the process of operation.

Values of the factors were taken at a level close to the average of the ranges indicated in Table 2: $S_G = 5 \cdot 10^4 \text{ m}^2$; $b_G = 15 \text{ m}$; $p_H = 92 \text{ mm}$; $\rho_{EQ} = 80 \Omega \cdot \text{m}$; $I_S = 21 \text{ kA}$; $k_\ell = 0.7$; $t_H = 0.7 \text{ m}$.

During the experiment, the following parameters were determined: the resistance of the GS (R_G); the potential of the entry point of the short-circuit current φ_0 , and of the calculated points $\varphi_1, \varphi_2, \varphi_3, \varphi_4, \varphi_5$ for which the values of the constructive coefficient k_t were 0.5; 0.6; 0.7; 0.8; 0.9, respectively. The voltage $U_{C,i}$ is determined by the formula:

$$U_{C,i} = \varphi_0 - \varphi_i. \quad (4)$$

Fig. 2, 3 show graphs of the dependencies $R_G = f(S_G)$ and $U_C = f(S_G)$, respectively. Dependence $R_G = f(S_G)$ is decreasing, and the dependence $U_C = f(S_G)$ is increasing. With an increase in the GS area by a factor of 9, the resistance of the GS decreases 2.73 times, and the voltage U_C increases by 1.61 times. These dependencies are non-linear, so with the certainty $R^2 = 1$ they are approximated by polynomials of the fourth degree. Approximation of dependencies and determination of its reliability were performed in Microsoft Excel spreadsheet environment. Since the dependence $R_G = f(S_G)$ is nonlinear, to obtain linear models in conducting a multifactorial experiment, the range of S_G values should be divided into sections.

Fig. 4, 5 show graphs of the dependencies $R_G = f(b_G)$ and $U_C = f(b_G)$, respectively. Both dependencies are increasing. When the size of the GS grid cell is increased by 5 times, the resistance of the GS increases by 1.16 times, and the voltage U_C increases by 2.56 times. These dependencies are linear (or close to linear for U_C) character, so with a confidence not less than $R^2 = 0.988$ they are approximated by the equations of a straight line.

Fig. 6, 7 show graphs of the dependencies $R_G = f(p_H)$ and $U_C = f(p_H)$, respectively. Both dependencies are decreasing. With an increase in the perimeter of the cross-section of horizontal grounding bars by 4.75 times, the GS resistance decreases by 1.28 times, and the voltage U_C by 4.94 times. These dependencies are non-linear in nature, but with a confidence not less than $R^2 = 0.86$ they are approximated by the equations of a straight line.

Fig. 8, 9 depict the graphs of the dependencies $R_G = f(\rho_{EQ})$ and $U_C = f(\rho_{EQ})$, respectively. The dependence $R_G = f(\rho_{EQ})$ is increasing and is practically linear in nature, so with a confidence not lower than $R^2 = 0.998$ it is approximated by the equation of a straight line. With an increase in the equivalent resistivity of the ground by a factor of 25, the GS resistance increases by a factor of 13. The dependence $U_C = f(\rho_{EQ})$ is essentially nonlinear and has an extremum point – a maximum, so the range of ρ_{EQ} values should be divided into sections. It is advisable to take the boundary of sections division at a value of $\rho_{EQ} = 50 \Omega \cdot m$. In each section, the dependence $U_C = f(\rho_{EQ})$ can be approximated by a straight line equation with a confidence not lower than $R^2 = 0.94$.

The dependence of the GS resistance on the short-circuit current on the busbars of the OSG is caused by the nonlinear dependence of the longitudinal resistance of the

ferromagnetic (steel) grounding bars on the amplitude and frequency of the current flowing through them, which in turn is due to the magnetic permeability dependence $\mu = f(H)$ on the magnetic field strength [10]. Fig. 10, 11 show graphs of the dependencies $R_G = f(I_S)$ and $U_C = f(I_S)$, respectively. An analysis of the results obtained for grids of GS of various areas shows that the GS resistance depends on the short-circuit current on the busbars of the OSG only at currents less than 10 kA. The dependence $R_G = f(I_S)$ is decreasing, and the dependence $U_C = f(I_S)$ is increasing. With an increase in the short-circuit current on the OSG busbars by 11 times, the GS resistance decreases by 1.11 times, and the voltage U_C increases by 19.32 times. The dependence $R_G = f(I_S)$ is non-linear, so with a confidence $R^2 = 1$ it is approximated by a polynomial of the fourth degree. The dependence $U_C = f(I_S)$ is practically linear, so with a confidence not less than $R^2 = 0.999$ it is approximated by the equation of a straight line.

Fig. 12 depicts the graph of dependence $U_C = f(k_t)$, the analysis of which shows that U_C essentially depends on the constructive coefficient. The dependence $U_C = f(k_t)$ is increasing. When the coefficient k_t is increased by 1.8 times, the voltage U_C increases by 1.17 times. The dependence is practically linear, so with a confidence not lower than $R^2 = 0.98$ it is approximated by the equation of a straight line.

Fig. 13, 14 show graphs of the dependencies $R_G = f(t_H)$ and $U_C = f(t_H)$, respectively, the analysis of which shows that both parameters are practically independent of the depth of the horizontal grounding bars in the depth range from 0.4 m to 1.4 m. The dependence $R_G = f(t_H)$ is decreasing, and the dependence $U_C = f(t_H)$ is increasing. When the depth of the horizontal grounding bars is increased by a factor of 3.5, the GS resistance decreases only by 1.74 %, and the voltage U_C increases only by 3.58 %.

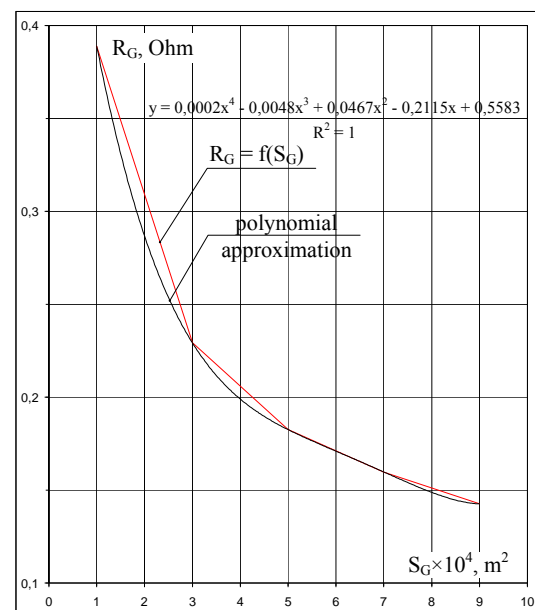
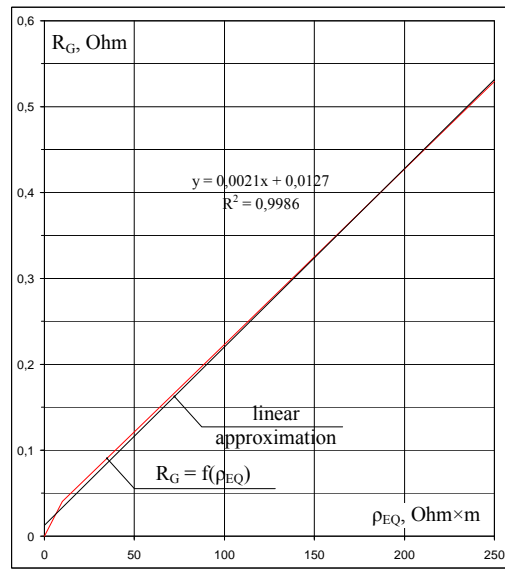
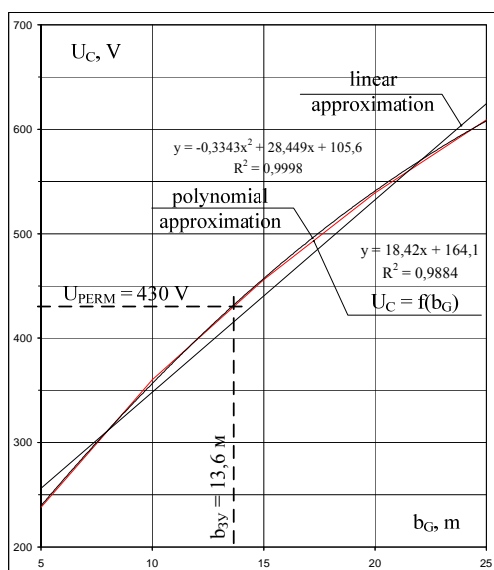
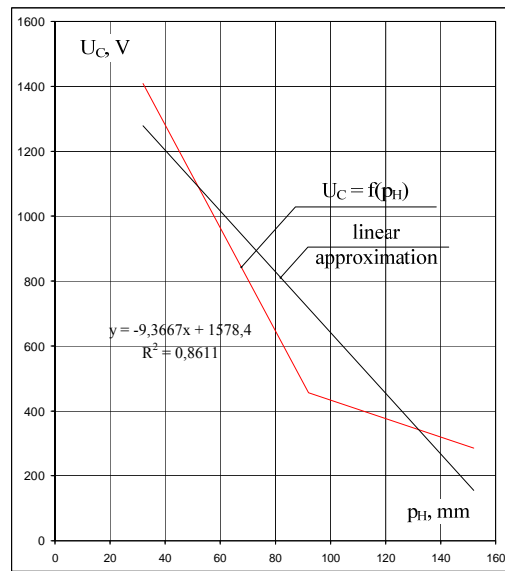
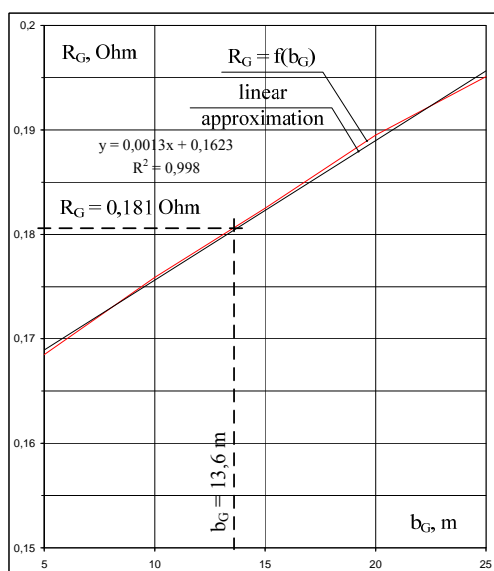
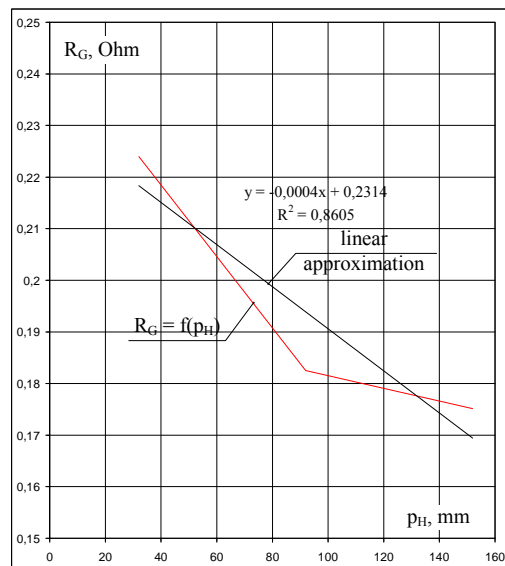
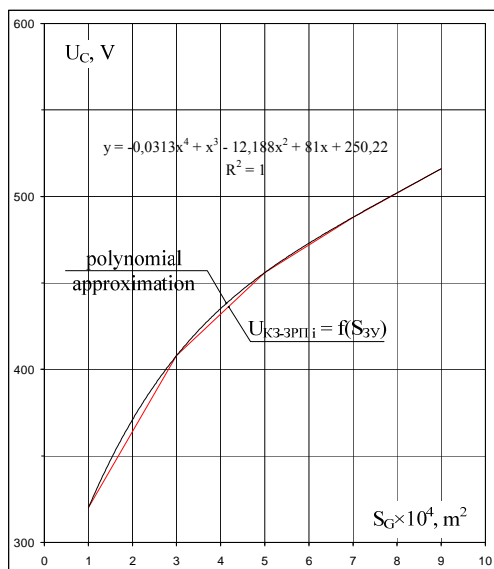


Fig. 2. Dependence $R_G = f(S_G)$



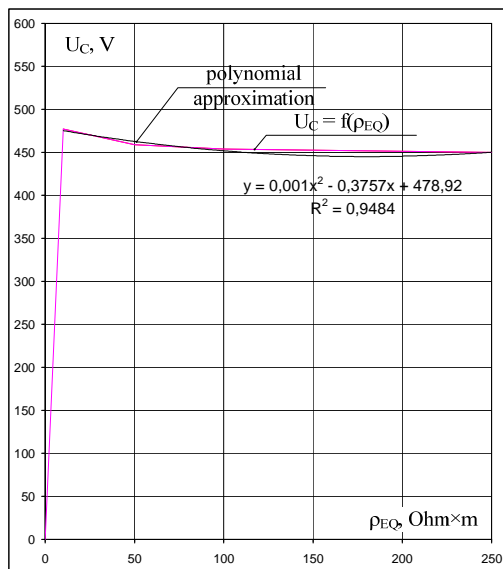


Fig. 9. Dependence $U_C = f(\rho_{EQ})$

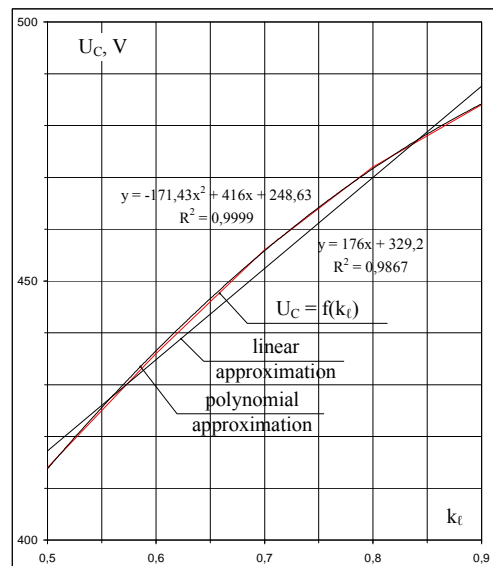


Fig. 12. Dependence $U_C = f(k_t)$

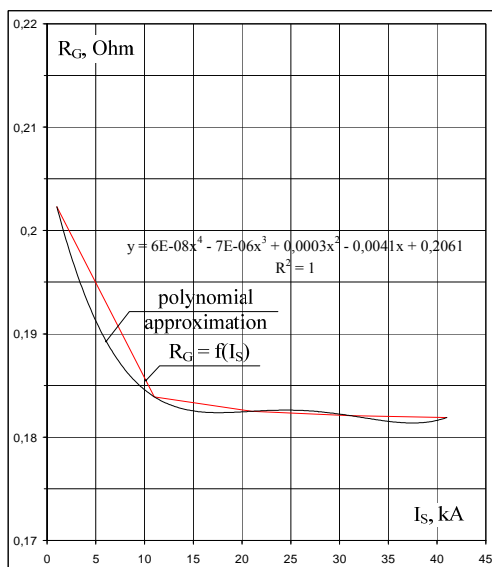


Fig. 10. Dependence $R_G = f(I_s)$

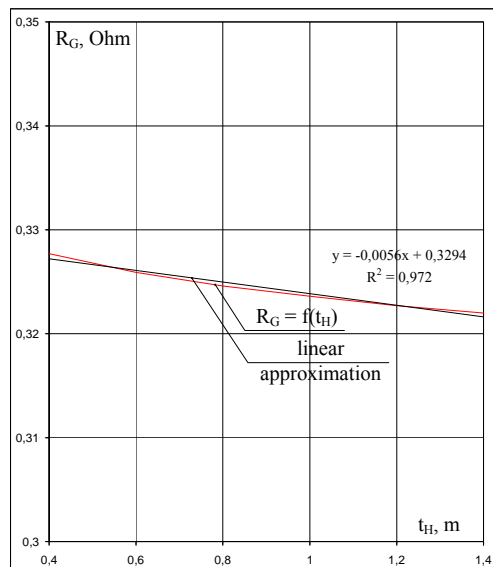


Fig. 13. Dependence $R_G = f(t_H)$

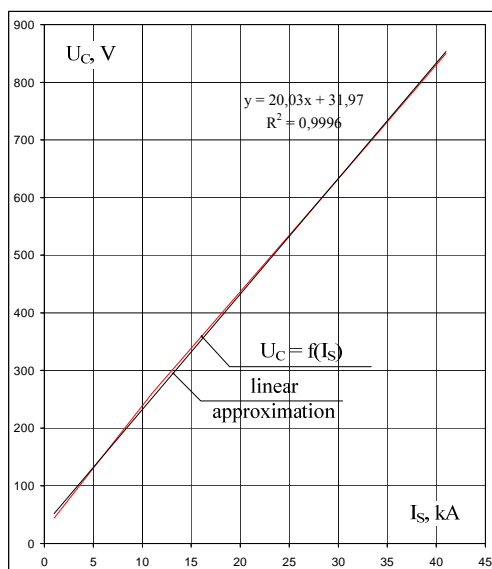


Fig. 11. Dependence $U_C = f(I_s)$

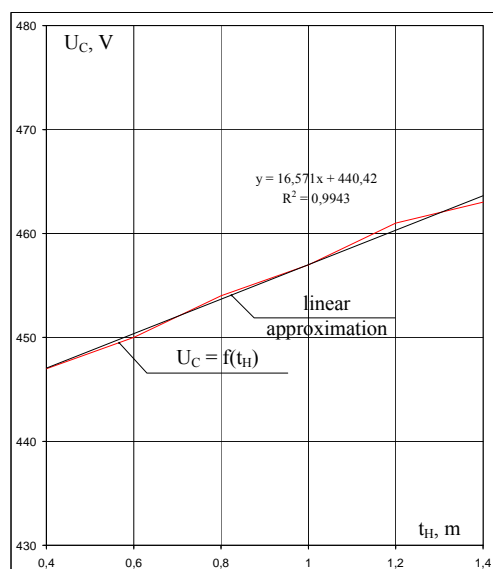


Fig. 14. Dependence $U_C = f(t_H)$

On the basis of the results of the conducted studies, it is possible to formulate the main provisions of the design methodology for the design realization of the GS of substations with switchgears 330(220) kV, which is aimed at providing EMC of current circuits:

- when designing the GS, the initial data is set with the following parameters: S_G , ρ_{EQ} , I_S , k_t , as well as $U_{C,relay}$. The SG area (S_G) is determined by the type of primary circuit scheme and the layout of the switchgears. Equivalent soil resistivity (ρ_{EQ}) is determined by the parameters of the geoelectric structure of the soil at the location of the designed GS and is determined at the stage of the pre-design surveys. The short-circuit current on the busbar of the OSG (I_S) is determined by the distance of the substation from the energy sources. The constructive coefficient (k_t) is determined by the diagonal of the GS and the distance from the CT to the building of the RP. The voltage U_{PERM} is determined by the parameters of the relay protection (the brand and length of the current cable and the type of the current relay);

- next, it is necessary to determine the size of the grid cell (b_G) and the perimeter of the cross-section of the horizontal grounding bars (p_H). To do it, it is necessary to plot the graphs of the dependence $U_C = f(S_G; b_G; p_H; \rho_{EQ}; I_S; k_t)$ for the given values of S_G , ρ_{EQ} , I_S , k_t at the variation of b_G , taking p_H from the standard series of rolled steel (for example, the strip 6×40 mm², in which $p_H = 92$ mm). After plotting the graph, we determine the size of the GS grid cell from the condition $U_C \leq U_{C,relay}$. For example, for the set of factors considered in this paper for $U_{C,relay} = 430$ V (see Fig. 5), the grid cell size should not exceed $b_G \leq 13.6$ m;

- then it is necessary to determine R_G from the given values of the parameters S_G , ρ_{EQ} , I_S and the obtained values of the parameters b_G and p_H , substituting them into the dependence $R_G = f(S_G; b_G; p_H; \rho_{EQ}; I_S)$. For example, for the set of factors considered and the obtained values $p_H = 92$ mm and $b_G = 13.6$ m, the resistance R_G will be 0.181Ω (see Fig. 4);

- next, it is necessary to determine the voltage on the GS ($U_G = I_S R_G$) according to the set I_S value and the obtained R_G value. For example, for a given short-circuit current on the busbars of OSG $I_S = 21$ kA and the obtained value $R_G = 0.181 \Omega$, the voltage U_G will be 3801 V, which does not exceed the permissible value (see paragraphs 1.7.104 and 1.7.105 of the Electrical installation regulations of 2017), equal to 5000 V;

- if the voltage on the GS is greater than the permissible value, then reduce the value of b_G and/or increase the value of p_H , and then recalculate the values of R_G and U_G ;

- the values of the parameters S_G , b_G and p_H should be used to compose the graphic part of the GS design and calculation of the cost of the horizontal grounding bars.

Conclusions.

1. In the paper it is proposed to supplement the existing technique for designing the GS of substations 330(220) kV with three more criteria aimed at ensuring electromagnetic compatibility of current circuits:

- prevention of breakdown of insulation of current circuit cables by pulsed voltages during short-circuit on busbars of OSG or lightning strikes;
- prevention of breakdown of insulation of current circuits cables by industrial frequency voltages at short-circuit on the busbars of OSG;
- prevention of false triggering of relay protections against low-frequency voltages during short-circuit on busbars of OSG.

2. In the paper, one-factor experiments were performed and the dependencies of the resistance of the GS and the voltage between the calculated points on seven factors are obtained: the area of the GS (S_G); the size of the grid cell of the GS (b_G); perimeter of the cross-section of horizontal grounding bars (p_H); equivalent soil resistivity (ρ_{EQ}); short-circuit current on the busbars of OSG (I_S); constructive coefficient (k_t); the depth of the horizontal grounding bars (t_H). The following is shown:

- the dependencies $R_G = f(S_G)$, $R_G = f(p_H)$, $U_C = f(p_H)$, $R_G = f(I_S)$, $R_G = f(t_H)$ are decreasing, and the dependencies $U_C = f(S_G)$, $R_G = f(b_G)$, $U_C = f(b_G)$, $R_G = f(\rho_{EQ})$, $U_C = f(I_S)$, $U_C = f(k_t)$, $U_C = f(t_H)$ are increasing;

- the dependencies $R_G = f(S_G)$, $U_C = f(S_G)$, $R_G = f(I_S)$ are non-linear, so they are approximated by polynomials of the fourth degree;

- the dependencies $R_G = f(b_G)$ and $U_C = f(b_G)$, $R_G = f(p_H)$, $U_C = f(p_H)$, $R_G = f(\rho_{EQ})$, $U_C = f(I_S)$, $U_C = f(k_t)$, $R_G = f(t_H)$, $U_C = f(t_H)$ are linear (or close to linear), therefore they are approximated by the equations of a straight line;

- the dependence $U_C = f(\rho_{EQ})$ is nonlinear and has an extremum point – a maximum, therefore the range of ρ_{EQ} values should be divided into sections, on each of which the dependence $U_C = f(\rho_{EQ})$ can be approximated by the equation of the straight line;

- R_G and U_C parameters are negligibly dependent on t_H in the considered depth range from 0.4 m to 1.4 m.

3. The paper formulates the main provisions of the methodology for designing a GS with a uniform grid by the criterion for preventing false triggering of relay protections with an example of its use.

4. In order to create an engineering methodology for designing a design realization of the GS that is aimed at providing EMC of current circuits, in future studies it is necessary to conduct multifactor experiments to determine the dependence of the GS resistance and the voltage U_C on the parameters S_G , b_G , p_H , ρ_{EQ} , I_S , k_t .

REFERENCES

1. *Pravila ulashtuvannya electroustanovok* [Electrical installation regulations]. Kharkiv, Fort Publ., 2017. 760 p. (Ukr).
2. Rudenko S.S., Koliushko D.G., Kashcheyev O.V. Determination of direction to reconstruction of grounding system. *Electrical engineering & electromechanics*, 2017, no.2, pp. 57-61. (Ukr). doi: 10.20998/2074-272X.2017.2.09.
3. IEC/TS 61000-6-5 Electromagnetic compatibility (EMC) – Part 6-5: Generic standards – Immunity for power station and substation environments.
4. Voronina Z.A., Glebov O.Yu., Koliushko G.M. Determination of the levels of electromagnetic interference in the cables of current transformers with short-circuit on

substation buses in order to ensure electromagnetic compatibility. *Bulletin of NTU «KhPI»*, 2011, no.16, pp. 44-59. (Rus).

5. Baranov M.I. *Zabezpechennya enerhetychnoyi bezpeky Ukrayiny shlyakhom pidvyshchennya nadiynosti roboty stratehichnykh enerhoobyektiv v normalnomu ta avariynnykh rezhymakh. Zvit pro NDR (promigny; № derzhreestratsiyi 0117U000534)* [Ukraine's energy security by increasing the reliability of the operation of strategic energy facilities in normal and emergency modes. Report on research work. State registration no.0117U000534]. Kharkiv, NTU «KhPI» Publ., 2017. (Ukr).

6. STO 56947007-29.240.044-2010. *Metodicheskie ukazaniya po obespecheniyu elektromagnitnoy sovместимости na ob'ekтах электросетевого хозяйства* [Methodical instructions on ensuring electromagnetic compatibility on objects of electronetwork economy]. Moscow, JSC FGC UES Publ., 2010. 147 p. (Rus).

7. Burgsdorf V.V., Yakobs A.I. *Zazemlyayushchie ustroystva elektroustanovok* [Grounding device of electrical installations]. Moscow, Energoatomizdat Publ., 1987. 400 p. (Rus).

8. Koliushko D.G. The interface of the program complex for Grounding system calculating of electric power objects. *Bulletin of NTU «KhPI»*, 2007, no.34, pp. 71-79. (Rus).

9. Link I.Yu., Koliushko D.G., Koliushko G.M. A mathematical model is not an equipotential ground grids

substation placed in a double layer. *Electronic modeling*, 2003, vol.25, no.2, pp. 99-111. (Rus).

10. Nayfeld N.R. *Zazemleniye, zashchitnyye mery elektrobezopasnosti*. [Earthing, protective measures of electro-safety] Moscow, Energiya Publ., 1971. 312 p. (Rus).

Received 11.07.2018

O.Yu. Glebov¹,

D.G. Koliushko², Candidate of Technical Science, Senior Research Associate,

G.M. Koliushko³, Candidate of Technical Science, Senior Research Associate,

E.P. Eremeeva⁴,

¹ Scientific-&-Research Planning-&-Design Institute «Molniya» National Technical University «Kharkiv Polytechnic Institute», 47, Shevchenko Str., Kharkiv, 61013, Ukraine, phone +380 57 7076671,

e-mail: nio5_molniya@ukr.net

² National Technical University «Kharkiv Polytechnic Institute», 2, Kyrypchova Str., Kharkiv, 61002, Ukraine, phone +380 57 7076671,

e-mail: nio5_molniya@ukr.net

How to cite this article:

Glebov O.Yu., Koliushko D.G., Koliushko G.M., Eremeeva E.P. On the issue of design of grounding systems of 330(220) kV substations to ensure the electromagnetic compatibility of secondary circuits. *Electrical engineering & electromechanics*, 2018, no.5, pp. 72-79. doi: 10.20998/2074-272X.2018.5.11.

00008

Матеріали приймаються за адресою:

Кафедра "Електричні апарати", НТУ "ХПИ", вул. Кирпичова, 21, м. Харків, 61002, Україна

Електронні варіанти матеріалів по e-mail: a.m.grechko@gmail.com

Довідки за телефонами: +38 050 653 49 82 Клименко Борис Володимирович

+38 067 359 46 96 Гречко Олександр Михайлович

